

# Sheffield Hallam University

*Modelling and state-estimation of steelmaking in an electric arc furnace.*

BOLAND, F. M.

Available from the Sheffield Hallam University Research Archive (SHURA) at:

<http://shura.shu.ac.uk/19665/>

## A Sheffield Hallam University thesis

This thesis is protected by copyright which belongs to the author.

The content must not be changed in any way or sold commercially in any format or medium without the formal permission of the author.

When referring to this work, full bibliographic details including the author, title, awarding institution and date of the thesis must be given.

Please visit <http://shura.shu.ac.uk/19665/> and <http://shura.shu.ac.uk/information.html> for further details about copyright and re-use permissions.

DAK CODE No

101 381 283 2.

699B

**SHEFFIELD POLYTECHNIC  
LIBRARY SERVICE**

MAIN LIBRARY

~~101 381 283 2~~

ProQuest Number: 10695705

All rights reserved

INFORMATION TO ALL USERS

The quality of this reproduction is dependent upon the quality of the copy submitted.

In the unlikely event that the author did not send a complete manuscript and there are missing pages, these will be noted. Also, if material had to be removed, a note will indicate the deletion.



ProQuest 10695705

Published by ProQuest LLC (2017). Copyright of the Dissertation is held by the Author.

All rights reserved.

This work is protected against unauthorized copying under Title 17, United States Code  
Microform Edition © ProQuest LLC.

ProQuest LLC.  
789 East Eisenhower Parkway  
P.O. Box 1346  
Ann Arbor, MI 48106 – 1346

MODELLING AND STATE-ESTIMATION OF STEELMAKING  
IN AN ELECTRIC ARC FURNACE

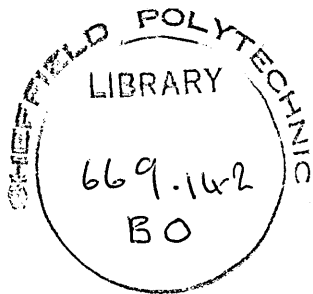
by

F. M. BOLAND

Thesis submitted to the Council for National Academic Awards  
for the degree of Doctor of Philosophy.

Research conducted in the Department of Electrical and Electronic  
Engineering, Sheffield City Polytechnic.

April 1977.



77-18958 -01 9

## ACKNOWLEDGEMENTS

The author wishes to thank Dr. S. P. Sabberwal (formerly of Sheffield City Polytechnic), Professor H. Nicholson (University of Sheffield) and Mr. J. D. Gifford (British Steel Corporation) who supervised this research, for their advice and guidance.

The author is grateful to Mr. D. Abraham for his encouragement and support of the work and the interest shown in the work by Dr. R. Smith and Dr. W. A. Barraclough is also appreciated..

Thanks are also due to the British Steel Corporation for permission to undertake plant investigations and the many valuable discussions with staff at the BSC Swinden Laboratories, Rotherham.

The financial support from the South Yorkshire Education Authority as a Research Assistant at Sheffield City Polytechnic is also gratefully acknowledged.

Finally the author would like to thank both his wife Elizabeth for her continual support and assistance in the preparation of this thesis and Mrs. C. W. Jennings for typing the thesis.

## SUMMARY

The commercial incentives to obtain improved control of the steelmaking process in the electric arc furnace are presented and progress made in applying computer control is reviewed. The development of a mathematical model of the refining process is shown to be restricted by the complex metallurgical nature of the process and the deficiency of existing plant instrumentation. The ability of a mathematical model, evolved from theoretical considerations, to simulate accurately a limited class of operating practice is demonstrated. A compromise between complexity and implied certainty of the model is obtained by a reduction in the dimension of the model state vector and by the introduction of a white Gaussian noise process to account for the effect of the ignored states and the hypotheses on which the model is developed. Techniques recently developed for obtaining noise corrupted measurements of the carbon content and temperature of the process are investigated and the statistics of the uncertainty on these measurements is determined. The implementation of the extended Kalman filter for on-line state estimation is considered and the operation of the filter under varied conditions of uncertainty is discussed. A technique for controlling divergence of the filter algorithm is presented and the results of simulations indicate that estimates of the states can be obtained to the accuracy required for the design of a refining control strategy.

## TABLE OF CONTENTS

	<u>Page No.</u>
1 INTRODUCTION	
<b>1.1 Motivation</b>	<b>1</b>
1.2 Operating Practice	2
1.3 History of Previous Work	3
1.3.1 Mathematical Models	3
1.3.2 State Estimation	5
1.3.3 Computer Control of Electric Furnace Steelmaking	7
1.4 Programme of Work	8
2 SELECTION OF A MODELLING TECHNIQUE	
2.1 Introduction	11
2.2 Theoretical Model of the Steelmaking Process in the Electric Arc Furnace	12
2.2.1 Selection of Major Reactions	12
2.2.2 Thermodynamics of Steelmaking	13
2.2.3 Kinetics of Steelmaking	17
2.3 Conclusions	22
3 A MATHEMATICAL MODEL OF THE REFINING PROCESS IN THE ELECTRIC ARC FURNACE	
3.1 Introduction	23
3.2 Process Variables	23
3.3 Oxygen Dissolved in the Bath	24
3.4 Decarburization	
3.4.1 General	24
3.4.2 Component I, the Reaction between Carbon and Gaseous Oxygen	25
3.4.3 Component II, Reaction between Dissolved Oxygen and Dissolved Carbon	27

3.5	The Oxidation of Manganese	30
3.6	Slag Basicity Ratio	31
3.7	Iron in the Slag	33
3.8	Material Balance	34
3.9	The Kmole Fraction of Iron Oxide in the Slag	34
3.10	The Oxygen Activity of the Slag	34
3.11	The Kmole Fraction of Manganese Oxide in the Slag	34
3.12	Heat Balance	35
3.13	Summary	35
4	THE DERIVATION OF EMPIRICAL RELATIONSHIPS AND PARAMETER ESTIMATES	
4.1	Introduction	37
4.2	Least Squares Fit Applied to Carbon-Oxygen Data	37
4.3	The Interaction between the Submerged Oxygen Jet and the Molten Steel	38
4.3.1	Introduction	38
4.3.2	Bubble Size	39
4.3.3	Jet Trajectory	40
4.3.4	Solution of Eqn. 4.2	41
4.3.5	Calculation of the Mass Transfer Coefficient ( $k_1$ ) for the Reaction between Gaseous Oxygen and Carbon	42
4.3.6	Estimation of the value of $a_{\text{O}}^1$ the Oxygen Activity in the Jet	42
4.4	Derivation of the Relationship for determining the Oxygen Potential of the Slag	44
4.5	Estimation of the Relationship between Slag-Metal Interfacial Area and Bath Turbulence	44
4.5.1	The Stagnant Bath Slag-Metal Interfacial Area	44
4.5.2	The Effect of Bath Turbulence on the Interface	45
4.5.3	The Slag-Metal Interface Area	45
4.6	The Rate Constant $k_2$ for the Reaction between dissolved Carbon and Oxygen	46

4.7	The Effect of Slag Composition on the Activity Coefficient Ratio $\gamma_{\text{MnO}}/\gamma_{\text{FeO}}$	46
4.8	Estimation of the Rate Constant $k_3$ for the Manganese Oxidation Reaction	47
4.9	Explanation and Selection of values of the Coefficients $H_i$ for $i = 1, 17$ occurring in the Heat Balance for the Process	47
4.9.1	Introduction	47
4.9.2	Evaluation of the Coefficients	48
4.10	Comments	48
5	RESULTS OF SIMULATION STUDIES	
5.1	Introduction	50
5.2	Calculation of Error Weights and the Tolerance for the Approximate Truncation Error	50
5.3	Solution of Model Equations	51
5.4	Model Performance	51
5.4.1	General	51
5.4.2	Oxygen Efficiency	52
5.4.3	Total Decarburization Time	52
5.5	Conclusions	53
6	DATA COLLECTION AND PARAMETER OPTIMIZATION	
6.1	Introduction	54
6.2	Further Plant Studies	54
6.2.1	General Study of the Modes of Furnace Operation	54
6.2.2	Monitoring of Furnace Operation	56
6.2.3	Slag Sampling	56
6.2.4	Further Data	56
6.3	Investigation of the thermal behaviour of the process during refining	57
6.4	Parameter Optimization	58
6.5	Discussion	59

7	ESTIMATION OF THE STATES DURING REFINING IN THE ELECTRIC ARC FURNACE	
	7.1 Introduction	61
	7.2 Reduced Dimension Model	61
	7.2.1 Stochastic Variables	61
	7.2.2 Stochastic Process Model	63
	7.3 Process Noise Model	65
	7.4 Measurements	67
	7.5 Filter Algorithm	69
	7.6 Implementation of the Filter Algorithm	70
	7.6.1 Process-Noise Decoupling	70
	7.6.2 Divergence Control	71
	7.7 Results	73
	7.7.1 General	73
	7.7.2 Simulation Studies	75
	7.8 Conclusions	83
8	CONCLUSIONS	85
	REFERENCES	90
	APPENDIX 1	A1.1
	APPENDIX 2	A2.1
	APPENDIX 3	A3.1
	APPENDIX 4	A4.1
	APPENDIX 5	A5.1
	APPENDIX 6	A6.1

## LIST OF PRINCIPAL SYMBOLS

### Chemical

$A_i$	interface area, $m^2$
$a_i$	thermodynamic activity of species, $i$ , dimensionless
$EQ_i$	chemical equilibrium constant, dimensionless
$f_i$	Henrian activity coefficient of species, $i$ , dimensionless
$k_i$	empirical rate constant for species involved in transport of element $i$
$M_i$	Molecular weight of species, $i$ , dimensionless
$m_i$	(molecular weight of species, $i$ ,) $\times 10^{-1}$ , dimensionless
$N_i$	Kg-mol fraction of species, $i$ , dimensionless
$U$	The oxygen injection rate.
$U_x$	velocity at a distance $x$
$\gamma_i$	Raoultian activity coefficient of species, $i$ , dimensionless
$\rho_i$	density of species, $i$ , $kg/m^3$
$\mu_i$	viscosity of species, $i$ , $kg/ms$

### Stochastic Process Model

$a_i$	coefficients in process model
$a^*_i$	coefficients in filter model
$E(.)$	the expected value of .
$F(.)$	the discrete-time process model
$f(.)$	continuous time process model
$G_k$	linearised-disturbance-coefficient matrix
$H$	measurement coefficient matrix
$I_{n \times n}$	identity matrix of order $n$
$K_i$	equilibrium constant
$K_k$	Kalman filter gain matrix
$k$	discrete time interval
$P_k$	covariance matrix of state estimate

$(p_{ij})_k$	element of $P_k$
$Q_k$	disturbance covariance matrix
$(q_{ij})_k$	element of $Q_k$
$R_k$	measurement noise covariance matrix
$s_i$	non-linear function
$u_k$	control vector
$v_k$	measurement noise vector
$w_k$	disturbance vector
$x_k$	state vector
$y_k$	measurement vector
$z_k$	innovations vector
$(\cdot)_{k+1}^k$	predicted estimate of $(\cdot)$
$(\cdot)_{k+1}^{k+1}$	estimate of $(\cdot)$
$x_i^0$	initial value of $x_i$

#### SUPERSCRIPTS

$x_i', y_i'$	denotes concentration of bath species in wt.%
$x_i'', y_i''$	denotes concentration of slag species as a kg-mol fraction
$a_i^*$	denotes equilibrium activity of species operator

#### SUBSCRIPTS

$Mn, 0, \dots$	denotes a property of that species
( )	denotes a species in the slag phase
_____	denotes a species in the bath phase
(g)	denotes a species in the gas phase

## Introduction

### 1.1 Motivation

The use of gaseous oxygen to accelerate the refining process in steelmaking was proposed<sup>1</sup> as early as 1924, however the technology required for the economic production and handling of bulk liquid oxygen was not available until the end of the second World War. During the war Germany developed the necessary technology for military purposes and subsequently it was acquired by Allied investigators. The Electric Arc Furnace sector of the steelmaking industry was a leader<sup>2</sup> in the use of the oxygen lance, which is now employed in most large shops both as a tool to assist refining and during the melting stage as an auxiliary energy supply.

The role of the Electric Arc Furnace in the steelmaking industry encompasses the manufacture of a wide range of steels from a cold scrap charge. The 'power-on' to 'tap' time for furnaces of capacity in excess of 100 tonnes is approximately 4 hours and the refining part of the steelmaking cycle typically takes 1.5 hours. A time saving in this period of at least 10 minutes per cast produced, due to a reduction in time taken to reach control decisions, reduction in the probability of errors in additions calculations and corresponding reduction in the time taken to obtain correct analyses, is likely to be achieved by computer aided refining control. The financial value of this time saving would depend on steel market conditions. However, it would typically allow at least one extra cast to be produced per week per furnace, which in times of heavy steel demand would be worth in the order of £100,000 per annum per furnace. There would also be savings in refractory costs and alloy additions cost due

to improved energy control, reduced residence time in the furnace and more effective use of alloy additions. An accurate model of the refining process would also allow a much more effective application of the 'least-cost-mix' technique to furnace charge weight calculations by allowing the 'least-process-cost mix' to be determined.

## 1.2 Operating Practice

The energy requirement for the refining of medium and low alloy steels in the Electric Arc Furnace is supplied almost wholly by electric power through the electrodes. Control of the level of power input must take into account the state of the bath, the effect of the arcs on refractory erosion, the desired end-point temperature and in some works the maximum demand constraints imposed by the Electricity Supply Authority. Although some advances have been made towards solving part of this complex problem by on-line computer control, particularly in electrical power demand control, in general the level of power input is controlled by the furnace operators. Medium and low alloy steels are refined to meet an end-point state determined typically by eleven chemical specifications and one temperature specification. Chemical specifications are normally given as bounded intervals, for example the final carbon may be required to be between 0.35% and 0.4%.

Concentrations of specific alloying elements may be changed by making alloy additions and impurities are removed by the injection of gaseous oxygen and by the establishment of a suitable slag. The temperature is primarily increased by the use of electric power, but the heat liberated by exothermic reactions must also be considered. The temperature can be decreased by the addition of a coolant, usually lime, but the need to make this adjustment can normally be taken as an indication of bad steelmaking technique. Independent

control of individual variables is not possible. For example blowing longer to decrease carbon also affects the temperature of the process and the iron oxide concentration of the slag, hence, control of the process is complex and requires great skill from the operator.

Continuous measurement techniques are not available, at present, for most of the process variables and the high temperature, in excess of 1600°C, and highly corrosive nature of the system are but two of the many difficulties encountered when obtaining what information there is available from the process. It is desirable that all the target specifications are met simultaneously so that no time, oxygen or electricity are expended on end-point corrections. So even if continuous measurements were available, some predictive algorithm would still be necessary so that the process could be controlled to meet simultaneously the end-point constraints.

### 1.3 History of Previous Work

#### 1.3.1 Mathematical Models

During recent years, much research effort has been devoted to the problem of identifying steelmaking processes for control purposes. The major part of this effort has concerned steelmaking in the basic oxygen converter. Although the results of this work are not directly applicable to the arc furnace process, the common chemical principles of steel refining under basic slags and similarity in engineering environment of all steelmaking processes ensure the suitability of a review of this work as a prelude to the present investigation.

A survey of the literature exposes a variety of mathematical models but they reduce to two basic types since division between those evolved using analytical and those evolved using empirical or statistical techniques is possible. The

requirements of an exact mathematical model for an equilibrium oxygen refining process are presented in Philbrook<sup>3</sup> and the limitations of both thermodynamic data and theoretical evaluation of some of the variables are pointed out. To model the kinetics of the nonequilibrium basic oxygen process Philbrook makes suggestions concerning the forms of semi-empirical equations that are most likely to be fruitful. Subsequently research groups throughout the world have studied the problem and many of the evolved models have been reported in the literature. Typical of this work in the United Kingdom are the dynamic models developed in U.M.I.S.T. by Middleton and Rolls<sup>4</sup> and for the British Steel Corporation by Weeks<sup>5</sup>. In Japan, Asai and Muchi<sup>6</sup> have made a theoretical analysis of the oxygen converter by the use of a mathematical model and in Belgium, Nilles and Denis<sup>7</sup> established a model which describes the transfer of oxygen from the lance to the metal and slag. Wells<sup>3</sup> report of work on the feasibility of applying state estimation techniques to oxygen steelmaking contains a mathematical model of the process. Wells also refers to two other studies, not reported in the open literature, which have been conducted in the U.S.A. A feature common to all of these models is their complexity, the U.M.I.S.T. model consists of 40 first order, nonlinear, ordinary differential equations and a similar number of algebraic equations. Although close simulation of the full-scale plant has been attributed to most of these models their practical limitations, for use in the on-line control of the process, arise not only from complexity but also because many of the variables required to characterize the state are nonmeasurable. This latter problem will be given further consideration when the use of on-line state estimation is reviewed.

Greenfield<sup>9</sup> has argued a case for employing regression analysis to develop a linear multivariable model of the basic oxygen process. In particular it was found that the model parameters could be readily updated in the course of refining and that a feedback control system could be employed since a suitable quadratic cost function was available. Mayer et al<sup>10</sup> have shown that the dynamics of the decarburization process in the oxygen converter can be modelled by an exponential function which describes the end-point refining curve. By making use of material and thermal balances it is possible to develop static models of some oxygen steelmaking processes in which some of the coefficients used are theoretically determined while the remainder are obtained from a statistical analysis. This technique has been used to model the refining of stainless steels in the Electric Arc Furnace<sup>11,12</sup>. Such combinational models have also been used in the control of basic oxygen steelmaking<sup>13,14</sup> and the view has been expressed<sup>15</sup> that it would be difficult to effect much improvement on a static basis.

### 1.3.2 State Estimation

Although the aerospace and aircraft industries were quick to apply the filtering theory of Kalman<sup>16</sup> and Kalman and Bucy<sup>17</sup> to control problems, only recently have these techniques been applied in the steel industry. Wells<sup>8</sup> reports on a study of the feasibility of applying the extended Kalman filter to a basic oxygen converter. This study made use of a complex twenty-four equation model of the process to generate synthetic data and a reduced dimensional model in the filter algorithm. From the results of this investigation Wells concluded that the reduced model is not accurate enough for use with only continuous measurement of the carbon monoxide

content of the waste gases. In particular the filter failed to track satisfactorily the true carbon and temperature states. This failure might, at least in part, have been anticipated since an examination of the transition matrix of the filter model shows that when only carbon monoxide is measured the filter is decoupled from the uncertainty in the thermal dynamics and possibly also the carbon dynamics. This decoupling, which is not mentioned by Wells, explains why the states tend to follow the filter model and to ignore the observations. This problem of divergence is considered in Chapter 7. Wagner<sup>18</sup> also considers the application of an extended Kalman filter to steel production in the oxygen converter. His filter model is similar to that described in Kawasaki<sup>12</sup> but no results are presented and the study serves only to indicate possible problems which might arise in a subsequent attempt to implement this work. Kornblum and Tribus<sup>19</sup> make use of Bayesian inference to design an end-point control system for the oxygen converter. The process model in this system is similar to that of Mayer et al<sup>10</sup> but here the model parameters are assumed to be random with statistics known a priori from data obtained from previous heats. They conclude that this approach, wherein decision theory is used to account for the uncertainty associated with the model and observations, should give even more accurate control than that at present achieved by the Jones and Laughlin Steel Company<sup>20</sup> who make use of Mayer's model in a deterministic fashion. Soliman et al<sup>21</sup> present results of a first feasibility study of the application of the extended Kalman filter to the estimation of the temperature and bath composition in the argon-oxygen blown stainless-steel process.

The results of this study indicate that reliable estimates of the metal bath composition can be obtained even when only bath temperature can be measured.

### 1.3.3 Computer Control of Electric Furnace Steelmaking

Until recently the role of the computer in the control of the production of steel in the Electric Arc Furnace has largely concerned decisions for optimum plant and scrap usage with few applications to the control of batch production in individual furnaces. Gosiewski and Wierzbicki<sup>22</sup> present a dynamic control system for optimizing electric power input during the melting stage of the steelmaking process. Their preliminary results show a 5% reduction in energy consumption for the melting stage, the duration of which was reduced by 11%. They describe in detail how the theoretical problems of process optimization and of control system synthesis are solved by means of the Maximum Principle. Wheeler et al<sup>23</sup> describe how control of the power level during the refining period of the process may be effected. The model of the energy transfer in the furnace, which is the basis of the control system, was the result of several years of research performed on production Electric Arc Furnaces. The complexity of the model is such that a large process-control digital computer would be required to implement the control system. So Wheeler and his co-workers also present a simplified regression model that enables an inexpensive analogue controller to be used on plant which cannot justify the cost of the sophisticated system. Static optimization of the stainless steelmaking process in the Electric Arc Furnace has been studied by Lipszyc<sup>12</sup> and by Calanog and

Geiger<sup>11</sup>. A computer control system based on a static model has been used to control stainless refining at the Detroit plant of Jones and Laughlin<sup>24</sup>. Optimal control of arc furnace steelmaking has been investigated by Woodside et al<sup>25</sup>. They present a highly simplified model of chemical and thermal dynamics of the process and the existence of a singular arc on the optimal power input trajectory is investigated.

#### 1.4 Programme of Work

To appreciate some of the practical problems associated with the proposed investigation, a study of plant operating practice was conducted. Subsequent to this study and a consideration of the general requirements of the model a theoretical basis for model development was adopted. The formulation of a function describing the change in Free Energy associated with the refining reactions was shown to resolve the problem of determining the equilibrium trajectory of the process to the solution of a constrained optimization problem. However, due to the inadequacy in range and accuracy of the available fundamental thermochemical data it was found that it is not at present possible to calculate the equilibrium bounds of the process. A lumped parameter representation of the diffusion mechanisms describing the primary refining reactions was investigated in the light of current metallurgical theory. It was concluded from these studies that the process could not be identified solely from analytic studies but that combined theoretical and empirical investigation was a worthwhile approach to the development of a practical model of the process. The major refining reactions were determined by analysis of collected plant data, taking into consideration the available metallurgical theory. The mechanisms of these reactions were investigated and a system of equations describing the rates of reaction was formulated. To

overcome the limitations of both thermodynamic data and theoretical evaluation of some parameters it was necessary to apply intuitive judgement to an indepth study of the literature on the metallurgy of steelmaking and statistical analysis to the available plant data. Consequently empirical and semiempirical relationships were derived, techniques for parameter estimation developed and a multi-variable model of the process evolved. This model was then tested using typical plant data and the results indicated that the model provided a reasonable representation of the refining process. A further period of plant studies was then conducted and data from monitored casts were collected. During this study samples of slag were taken along with the standard bath analyses. It was proposed that these data be used in conjunction with a non-linear parameter estimation procedure to improve the performance of the model. However, a critical assessment of the range and accuracy of these data and of the magnitude of the discontinuities inherent in the operating practice resulted in a rejection of this proposal. Instead the model in its original form was used to simulate the monitored casts. These studies showed that with only minor adjustments, the original model could simulate very accurately those casts during which no major abrupt changes in operation occurred. From the practical viewpoint the model was, however, limited by its dependence on process data which are not easily obtained. Hence, from an investigation of plant data it was found that the dimension of the model could be reduced by treating some of the state variables as random parameters whose statistics are known apriori. This reduction in dimension of the model was compatible with the conclusion that because of the problems associated with modelling abrupt changes in process behaviour an accurate deterministic model of <sup>the</sup> process was unobtainable. A study of the theory of

stochastic processes and the practical problems of implementing filter procedures was conducted. Subsequently a computer code for the Extended Kalman Filter was written. The accuracies of available techniques for indirect measurement of process variables were obtained and the filter was implemented. Its performance under a variety of levels of uncertainty was studied and the possibilities of using simple techniques to control divergence were investigated.

## Selection of a modelling technique

### 2.1 Introduction

The problem of identifying a system has been defined by Zadeh<sup>26</sup> as follows:

'Identification is the determination, on the basis of input and output, of a system within a specified class of systems, to which the system under test is equivalent.'

To specify a suitable class of systems for a given problem the purpose of the identification must receive primary consideration. The ultimate objective of the present investigation is the design of a control program for the batch refining process. Such a control program must determine the inputs required for optimal transition from one state to another. If this program is to effect control using the existing inputs, the bounded nature of the power and oxygen control variables and the impulse effect of bulk furnace additions deny the use of a feedback controller. Hence on the assumption that the proposed control program must be capable of operation in an open-loop manner it follows that a fairly accurate model of the system dynamics is required. The furnace is shown schematically in Fig. 2.1 and a description of a standard operating practice is presented in Appendix 1. The control problem can be given a simplified representation if only the dominant system variables, these are the process temperature and the carbon concentration of the bath, are considered. The refining process starts with liquid metal at a temperature of about 1580°C with a carbon content of about 0.5% greater than that required by the order specification. The process ends when the carbon content has been reduced to the desired level and the process temperature has been raised to a level necessary for satisfactory pouring into ingot moulds.

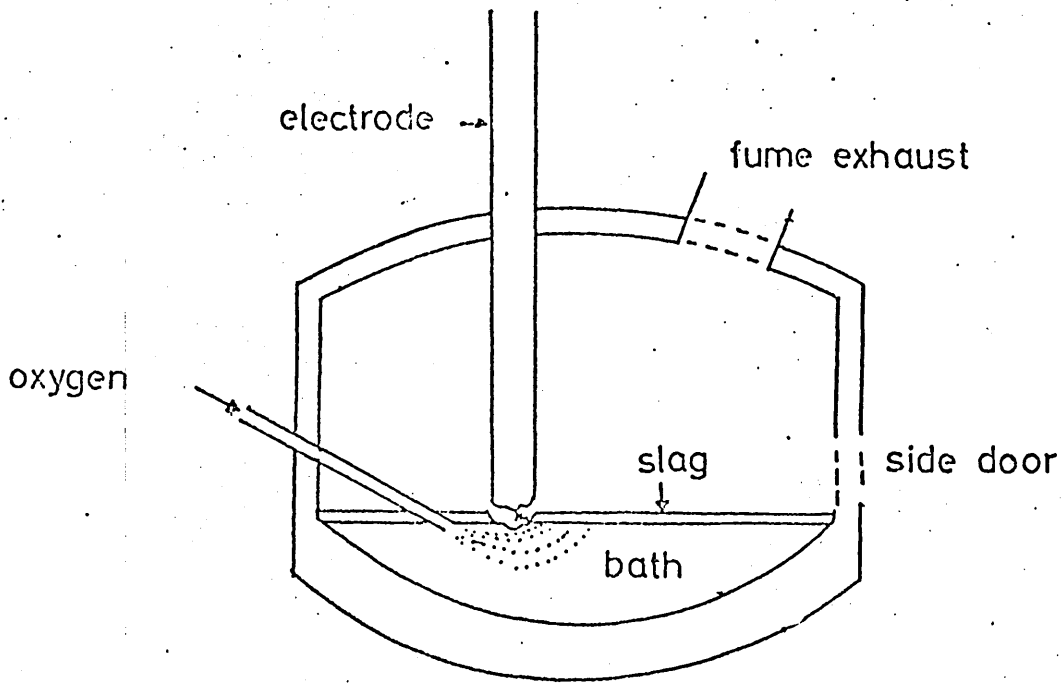


FIG 2.1 Schematic of Electric Arc Furnace

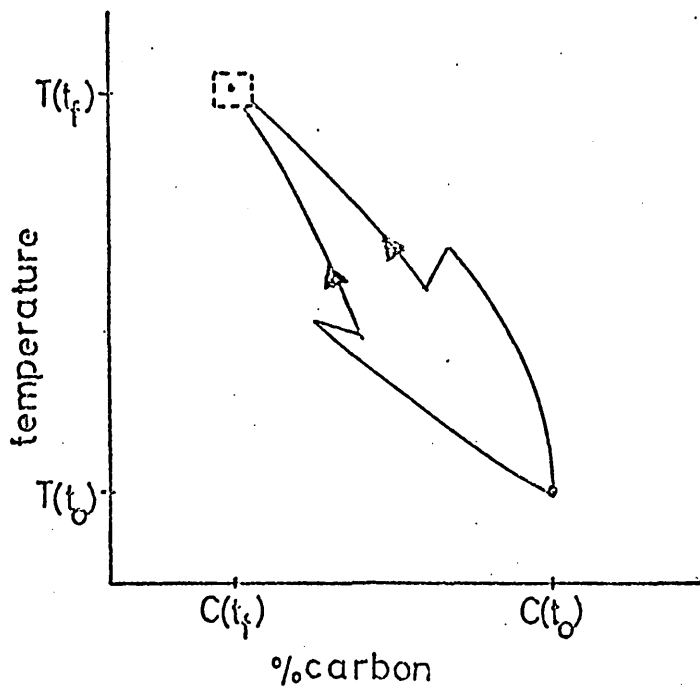


FIG 2.2 Carbon - Temperature Trajectories

The course of refining may therefore be illustrated as a trajectory on the carbon-temperature phase plane. Typical trajectories are shown in Fig. 2.2 and the end-point specifications are indicated by an area of the space. The effects of bulk furnace additions are shown to cause discontinuities in the phase-trajectory.

Two classes of models might be considered to present possible solutions to the identification problem; multivariable statistical models and explicit mechanistic models. The former approach was rejected for the following reasons.

- (a) The limitations in the existing instrumentation and the wide range of steels produced are such that the time and effort required to obtain sufficient well monitored plant data for significant statistical studies to be made would be prohibitive.
- (b) The model would not provide a good basis for either on-plant or off-plant control studies since significant extrapolation outside of the data range would be meaningless.

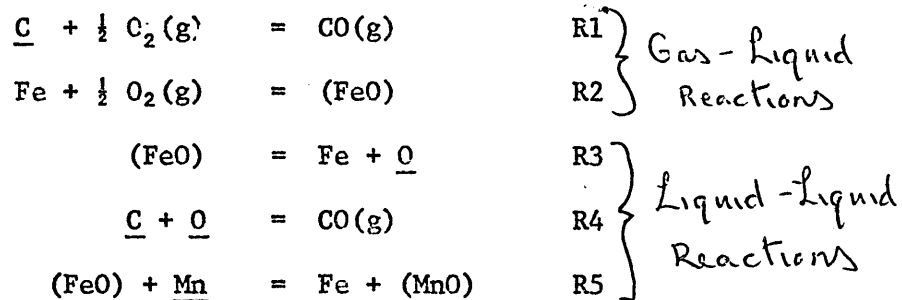
To develop a mathematical model of the process on a theoretical basis its fundamental chemistry must be examined. To this end a simple model of the possible reaction mechanism within the gas entrainment zone was developed (see Appendix 2). This model was, however, rejected on both practical and theoretical grounds and it was then decided that the process should be examined in depth.

## 2.2 Theoretical model of the steelmaking process in the electric arc furnace

### 2.2.1 Selection of major reactions

The problem of selection of reactions, and their mechanisms, occurring during the refining of steel is not confined to the electric arc furnace process. None of the processes at

present in use is fully understood. Hypotheses of reactions and reaction mechanisms must be based on critical investigations of plant data and taking into consideration the available metallurgical theory. Subsequently Table 2.1 was derived from collected plant data and data published in the literature<sup>2,33,40</sup>. In theory, reaction between all the system species occurs but an analysis of the changes in Gibbs Free Energy associated with the possible reactions justifies limiting the investigation to a small subset. The following were selected:



A formal representation of the refining reactions requires that the thermodynamics and the kinetics of the process be considered. The literature contains much descriptive and graphical results of research into these aspects of steelmaking but little has been presented which relates these general results to an underlying mathematical structure. It is therefore expedient that the extent to which the fundamental chemistry of the process can be mathematically modelled should be determined.

### 2.2.2 Thermodynamics of steelmaking

A criterion for spontaneous change within an isolated system is included in the Second Law of Thermodynamics - within an isolated system entropy must tend towards a maximum. The interrelationship of other state functions, such as internal energy, with entropy allow for the establishment of a whole set of criteria for spontaneous change within systems subject

SPECIES	LOCATION	MAJOR SOURCE	MAX. CONC. AT MELTOUT
C	BATH	Scrap + Charged Graphite	1.0 %
O	"	Atmospheric Air Charged Flux O Infiltration	No Analysis Available
Si	"	Scrap	0.05%
Mn	"	Scrap	0.4 %
P	"	Scrap	0.04%
S	"	Scrap + Impurities e.g. Rubber	0.04%
Cr	"	Scrap	0.3 %
Mo	"	Scrap	0.06%
Ni	"	Scrap	0.3 %
Al	"	Only Significant when added to the Ladle at Tapping	
Cu	"	Scrap	0.3 %
Sn	"	Scrap	0.03%
MnO	SLAG	Scrap	10.0 %
MgO	"	Refractories	7.0 %
CaO	"	Charged Lime + Fluospar	55.0 %
SiO <sub>2</sub>	"	Scrap + Limestone	17.0 %
Al <sub>2</sub> O <sub>3</sub>	"	Refractories	7.0 %
P <sub>2</sub> O <sub>5</sub>	"	Scrap	2.0 %
(Fe) <sub>T</sub>	"	Charged Mill scale + (Fe <sub>2</sub> O <sub>2</sub> ) Oxidized Bath (Fe O <sub>3</sub> )	25.0 %

TABLE 2.1 The System Species and Meltout Concentrations

to constraints. Now over a short time increment the steel-making process can be treated as a closed system, constant in pressure and temperature and subject to mass balances. Such a system is not necessarily isolated and may exchange heat and work with its surroundings. Under these conditions the criterion for direction of change and condition of equilibrium is obtained by considering the Gibbs Free Energy of the system.

The Gibbs Free Energy,  $G$ , is defined as

$$G = E - TS + PV \quad 2.1$$

where

- $E$  = the internal energy
- $T$  = the absolute temperature
- $S$  = the entropy
- $P$  = the pressure
- $V$  = the volume

are system variables.

Now for a reaction at constant pressure

$$dG = dE - TdS + PdV \quad 2.2$$

If only pressure-volume work is possible, then

$$dE = q_p - PdV \quad 2.3$$

where  $q_p$  = heat transferred.

It follows from the definition of entropy and the second law that

$$dS \geq \frac{q_p}{T} \quad 2.4$$

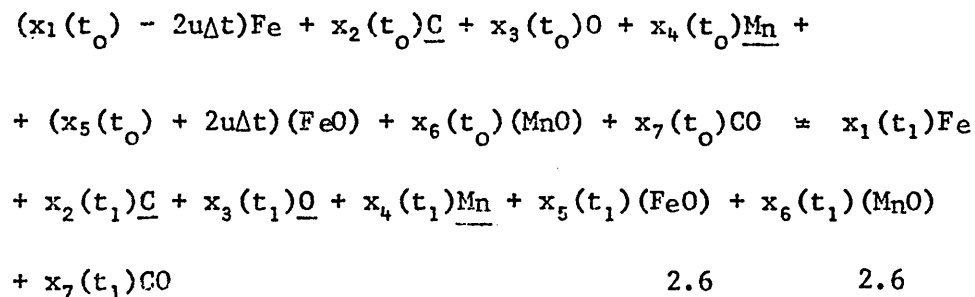
Substituting 2.3 and 2.4 into 2.2

$$dG = q_p - TdS \leq 0 \quad 2.5$$

Therefore for any spontaneous change which does not result in a change in pressure and temperature the associated change in the Gibbs Free Energy must be negative. The system is in equilibrium when no further decrease is possible.

If the furnace is assumed to be in equilibrium at time  $t = 0$ , the change in state due to the injection of a quantity,  $u\Delta t$ , of gaseous oxygen,  $O_2$ , can be considered in terms of the resulting change in Free Energy, provided that the time increment,  $\Delta t$ , is such that the heat flow from endothermic and exothermic reactions is insufficient to significantly change the temperature of the system. It is well known that the steelmaking process will consume all the injected oxygen, that is no oxygen escapes with the waste gases. This assumption is implicit in the present formulation wherein it is assumed that no surplus oxygen is available for reaction to form carbon dioxide, (carbon dioxide may of course be formed in the furnace atmosphere due to reaction with infiltrated air). The quantity of injected oxygen may be considered in terms of an equivalent amount,  $2u\Delta t$ , of iron oxide and the change in distribution of the system's chemical species can be formulated as follows;

Let the concentrations of  $Fe$ ,  $C$ ,  $O$ ,  $Mn$ ,  $(FeO)$ ,  $(MnO)$ ,  $CO$  at time  $t = t_0$  be  $x_1(t_0)$ ,  $x_2(t_0)$ , etc. Now if a quantity  $u\Delta t$  of gaseous oxygen is injected the bulk reaction can be written



Subject to

$$x_i(t) \geq 0 \quad \text{all } i \qquad 2.7 \qquad 2.7$$

and element balances

$$A X(t_1) = AX(t_0) + a 2u\Delta t \qquad 2.8$$

where

$$A = \begin{pmatrix} 1 & 0 & 0 & 0 & 1 & 0 & 0 \\ & & & & & & \\ 0 & 1 & 0 & 0 & 0 & 0 & 1 \\ & & & & & & \\ 0 & 0 & 1 & 0 & 1 & 1 & 1 \\ & & & & & & \\ 0 & 0 & 0 & 1 & 0 & 1 & 0 \end{pmatrix} \quad \text{and } a = \begin{pmatrix} -1 \\ 0 \\ 0 \\ 0 \\ 1 \\ 0 \\ 0 \end{pmatrix}$$

Determination of the equilibrium state at  $t = t_1$  may therefore be expressed as the following optimization problem

$$\begin{aligned} & \text{minimize } G(X(t_1)) \\ & \text{subject to } AX(t_1) - b = 0 \quad 2.9 \\ & \quad \quad \quad X(t_1) \geq 0 \end{aligned}$$

where  $G(X(t_1)) = \sum_{i=1}^7 \mu_i x_i(t_1)$

$\mu_i$  = the partial molar Free Energy of  $i$

$$b = AX(t_0) + a_2 u \Delta t$$

Now if  $\mu_{Tsi}^0$  is the molar Free Energy of  $i$  in its standard state at a temperature,  $T$ , then  $\mu_i$  is related to  $\mu_{Tsi}^0$  by the equation

$$\mu_i = \mu_{Tsi}^0 + RT \ln a_i$$

where  $R$  = Gas Constant

$a_i$  = the activity of species  $i$  relative to its standard state

The standard state for species in solution in iron is the infinitely dilute solution and the standard state for species in the slag is assumed to be the pure substance. Henry's and Raoult's laws may therefore be used to give

$$a_i = M_i f_i x_i / \sum_{j=1}^4 M_j x_j \quad i = 2, 3, 4$$

$$a_k = \frac{e_k x_k}{x_5 + x_6 + n_{ex}} \quad k = 5, 6$$

where  $M_i$  is the molecular weight of species  $i$  and  $f_i$  and  $e_k$  are Henrian and Raoultian activity coefficients respectively. The constant  $n_{ex}$  accounts for the non-variable slag species such as calcium oxide. The activities of iron,  $a_1$ , and carbon monoxide  $a_7$  may be assumed to be unity.

The problem of determining the equilibrium trajectory of the refining process is therefore equivalent to the constrained optimization problem 2.9. The simpler problem of determining the equilibrium state in a mixture of gases has been shown to be convex<sup>27</sup> and Bracken and McCormick<sup>28</sup> have reported its solution by use of the sequential unconstrained minimization technique, SUMT. It is not, however, the problem of determining a solution technique that makes this approach impractical at present, it is the availability of thermodynamic data. Values of the Henrian activity coefficients,  $f_i$ , for species in the bath are available<sup>29</sup>. Determination of the activities of species in slags has had no comparable success. Approaches to the subject based on the treatment of the species as ionic solutions<sup>30</sup> do allow for some interactive effects, but to date no generally accepted interaction coefficients have been evaluated. Molar Free Energies for species in standard states,  $\mu_{Tsi}^0$ , are available<sup>31</sup> but values differing by in excess of 10% can be found in the literature.

### 2.2.3 Kinetics of Steelmaking

From the control viewpoint knowledge of the endpoint or equilibrium state is only of secondary importance. The rate at which the reactions proceed is of primary concern, since it is generally accepted that during refining in the arc furnace the major process species are not in equilibrium. To determine the rate of reaction it is necessary to conduct

a step-by-step analysis of the underlying chemical and diffusion processes which are contributory to the bulk reaction. The rate of the bulk reaction is determined by the rate of the slowest contributory step. As has been demonstrated in the previous section it is the injection of gaseous oxygen that perturbs the system from the equilibrium state, the partitioning of this oxygen between the various phases is shown schematically in Fig. 3.1. To illustrate this step-by-step analysis the reaction between dissolved oxygen and carbon may be considered. This reaction requires a nucleation site. Studies of ore-fed systems<sup>32</sup> have confirmed the theory that these sites are located on the bottom of the furnace. The sequence of steps in transferring oxygen from the slag to the carbon monoxide bubble on the hearth of the furnace are:

1. Transport of  $(\text{FeO})$  in the slag to the slag-metal interface
2. The reaction  $(\text{FeO}) = \text{Fe} + \underline{\text{O}}$  at the interface
3. Transport of oxygen in the metal, away from the slag-metal interface
4. Transport of (a) Oxygen and (b) Carbon, in the metal, from the bulk metal to the phase boundary between the metal and the CO bubbles
5. The reaction  $\underline{\text{C}} + \underline{\text{O}} = \text{CO}(\text{g})$  at the gas-metal interface
6. Rise of CO bubbles out of the metal and slag into the furnace atmosphere

At the temperatures typical of steelmaking the rates of chemical reactions, steps 2 and 5, are several orders of magnitude greater than the observed bulk reaction rate hence these steps are eliminated from further consideration. It may also

be assumed that step 6 cannot be rate controlling. Since the oxygen concentration of the slag is high only the diffusion of iron need be considered when determining the rate of step 1. The rate of diffusion of iron in the slag is sufficiently large for the steelmaking practice under consideration for this step to be eliminated. This being so since well fluxed slags of high fluidity are obtainable by use of good slag control and also because the use of gaseous oxygen ensures that pure FeO is available. The determination of the rate controlling step from steps 3 and 4 is not easily resolved. In the present study it is shown that step 3 is probably rate limiting for carbon concentrations greater than some critical value. Step 3 may be described mathematically by the following lumped parameter form of Fick's first diffusion law

$$\frac{dO}{dt} = A_s \frac{D_o}{\delta_o} (a_o^* - a_o) \quad 2.10$$

where  $A_s$  = the metal-slag interfacial area  
 $D_o$  = the oxygen diffusion coefficient  
 $\delta_o$  = the thickness of the boundary layer  
 $a_o^*, a_o$  = the chemical activity of the oxygen in equilibrium with the slag and the activity of the bulk oxygen concentration respectively.

Values for the parameters  $D_o$  and  $\delta_o$  are available, but the use of laboratory determined values in the description of the industrial process must be viewed with caution. In particular it is quite certain that  $\delta_o$  will decrease with increasing reaction rate since the boundary layer thickness is a decreasing function of the Reynold's number for the bulk flow. The area of the slag-metal interface,  $A_s$ , may be determined,

for the stagnant bath, from the dimensions of the furnace.

However, during a vigorous carbon boil the turbulence of the bath will increase the area. An exact determination of equilibrium oxygen activity,  $a_o^*$ , would require the solution of the nonlinear programming problem presented in the previous section but an approximate solution can be obtained by considering the equilibrium of the reaction  $(FeO) = Fe + \underline{O}$  in terms of the activity of the iron oxide concentration of the slag. The activity of the bulk oxygen concentration,  $a_o$ , may be replaced by the bulk oxygen concentration as a weight percent which may be considered a system variable. Since 2.10 also determines the rate of the bulk carbon oxidation reaction the general form of the rate of carbon oxidation in  $wt.\% \cdot s^{-1}$  is as follows

$$\frac{d\%C}{dt} = f_1 \left( \frac{d\%C}{dt} \right) (f_2 (a_{FeO}) - \%O) \quad 2.11$$

where  $f_1$  is a function relating  $A_s$ ,  $D_o$  and  $\delta_o$  to the boil rate

$f_2$  is a function relating the equilibrium activity of the oxygen in the metal at the metal slag interface to the iron oxide activity of the slag.

This implicit formulation of the reaction kinetics shows how even a preliminary analysis of underlying metallurgy of the process leads to a model structure far too complex for control purposes. Similar formulations may be obtained to describe the rates of the other major reactions. If the chemical variables are denoted by a vector  $X(t)$  and their equilibrium values by  $X^*(t)$  the dynamics of the refining process may be described in the following general form

$$\dot{X}(t) = f(X(t))(g(X(t)) - h(X^*(t), U)) \quad 2.12$$

where  $U$ , the oxygen injection rate, has been included in the arguments of  $X^*$  since, as has been shown in the previous

section, the equilibrium trajectory is a function of the injection rate.

To complete this theoretical formulation of a process model the thermal dynamics must be considered. The major influence on the temperature of the system is the power input by the electric arcs, but a complete thermal balance for the process requires that the heat generated and absorbed by the chemical reactions should be considered, also the heat losses due to convection and radiation must be evaluated. The general formulation of this heat balance is of the form

$$\frac{dT(t)}{dt} = a_1 (T(t) - T_0)^4 + a_2 (T(t) - T_0) + C_B^{-1} \{ P(t) + WHM \sum_{i=1}^n h_i \dot{X}_i(t) \} \quad 2.13$$

where  $a_1$ ,  $a_2$  are constants

$T(t)$ ,  $T_0$  are the system and ambient temperatures respectively

$C_B$  is the heat capacity of the system

$P(t)$  is the electric power input

$WHM$  is the weight of hot metal

$h_i$  is the heat liberated (or absorbed) by the reaction of  $X_i$ .

If the assumption is made that a discrete time model of the process can be obtained from the system equations 2.12 and 2.13 wherein the time increment  $\Delta t$  is such that the variation in the process temperature is sufficiently small that the conditions required in 2.2.2 are satisfied then the theoretical model can be described by the flow chart in Fig 2.3.

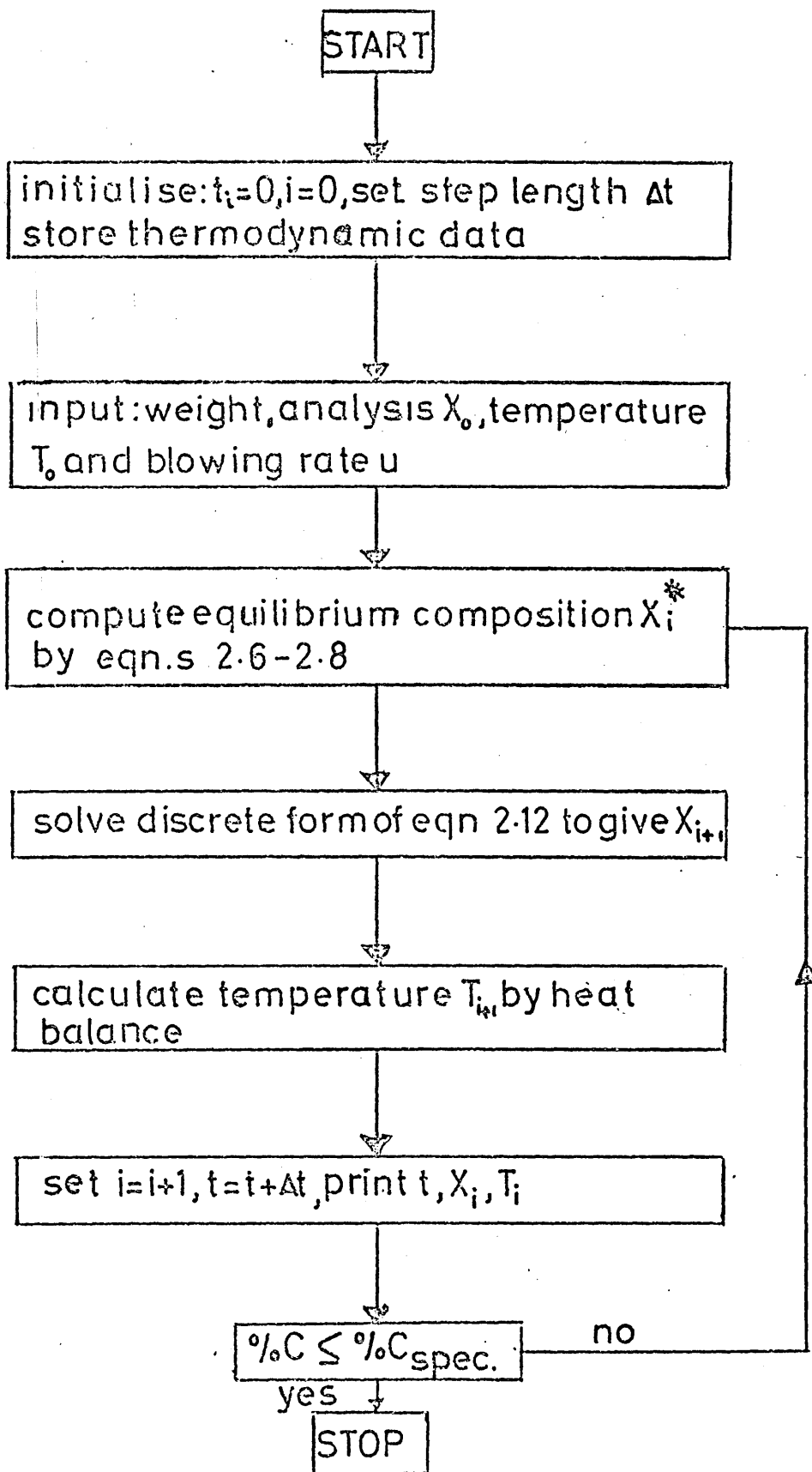


FIG 2.3 Flow Chart for Theoretical Model

### 2.3 Conclusions

The terms of reference of the investigation are shown to be best satisfied by the development of a model on a theoretical basis.

The formulation of an exact mathematical model has demonstrated that the limitations of available thermodynamic data are such that calculation of the equilibrium trajectory of the process is not possible. Moreover, as no established knowledge of the reaction mechanisms exists a wholly analytic study of the kinetics is not feasible.

In consideration of these conclusions, it seems inevitable that a practical process model must incorporate many features which are dependent on the individual furnace and the particular practice. These features may best be understood by developing the model on a theoretical basis. Furthermore this should permit the basic model to be applicable to any furnace and the use of adaptive techniques to up-date empirical coefficients, thus improving its accuracy.

A mathematical model of the refining process  
in the electric arc furnace

### 3.1 Introduction

It has been shown in Chapters 1 and 2 that to formulate a mathematical model of the refining of steel in the arc furnace that not only must the complex chemistry of the process be understood but also, that engineering judgement is required to overcome the many inadequacies in the available data and theory. A solution to this problem is presented here and the process is described by a set of differential and algebraic equations. Treatment of the techniques employed in estimating parameters has been left until Chapter 4 and only the structure of the equations is presented. Where necessary additional studies on the chemistry of the process are provided. It should be noted that when required the following is the conversion from kmol per tonne to weight percent.

$$\%i = C_i \times M_i \times 10^{-1}$$

where  $C_i$  = the concentration of  $i$  in kmol tonne<sup>-1</sup>

$M_i$  = the molecular weight of the  $i$  species

### 3.2 Process Variables

For preliminary studies the following were determined as being the necessary variables to give adequate description to the interactive nature of the process.

O : the bulk oxygen concentration in the bath  
(kmol, tonne<sup>-1</sup>)

C ; the carbon concentration of the bath  
(kmol tonne<sup>-1</sup>)

Mn: the manganese concentration of the bath  
(kmole tonne<sup>-1</sup>)

$\beta$	;	the slag basicity ratio
(FeO)	;	the iron oxide concentration of the slag (kmol tonne <sup>-1</sup> )
WSL	;	weight of slag (tonnes)
WHM	;	weight of bath (tonnes) ( $\rho = \text{WSL}/\text{WHM}$ )
$N_{\text{FeO}}$	;	kmol fraction of FeO in the slag
$a_{\text{FeO}}$	;	Chemical activity of FeO in the slag
$N_{\text{MnO}}$	;	kmol fraction of MnO in the slag
T	;	the temperature of the bath ( <sup>o</sup> K)
(MnO)	;	the concentration of MnO in the slag (kmol tonne <sup>-1</sup> )

### 3.3 Oxygen dissolved in the bath

Studies of carbon/oxygen concentrations in oxygen steelmaking processes<sup>33,34,35</sup> show that although equilibrium is not attained a definite correlation exists between their respective concentrations. If carbon and oxygen are in equilibrium at 1600<sup>o</sup>C the following relationship has been shown to exist between their concentrations<sup>41</sup>

$$\%C \times \%O = \frac{2.02 \times 10^{-3} \times P}{1. + 0.85 \times \%O} \quad 3.1$$

where P = total pressure (atms)

Only limited data are available for the carbon/oxygen concentrations in the electric arc furnace and that presented by Hills and Knaggs<sup>36</sup> were correlated to give a relationship of the form (see Chapter 4)

$$\underline{O} = a(\underline{C})^b \quad 3.2$$

where a and b are constants

### 3.4 Decarburization

#### 3.4.1 General

The reaction between carbon and oxygen is the most important one occurring during refining. Its importance lies not only

in the necessity of taking the carbon down to some specification or range, but also in the vigorous stirring action of the 'carbon boil'. This agitation assists in the promotion of slag-metal reactions by increasing the interfacial area and generally cleans and gives homogeneity in the bath.

The metallurgical theory for this reaction has been described briefly in Chapter 2 and the dynamical equation for the reaction is developed on the assumption that it has two components.

#### 3.4.2 Component 1, the reaction between carbon and gaseous oxygen.

Since it is not generally accepted that this reaction occurs, a justification for its selection is necessary. Until the mid-sixties, investigations of the mechanism of the carbon-oxygen reaction mostly considered the classical open-hearth process, that is, oxygen for decarburisation is supplied through the slag layer. These investigations supported the theory that since homogeneous nucleation of carbon monoxide bubbles is improbable, nucleation must be heterogeneous occurring either at the slag-metal interface or on the furnace hearth. Nucleation at imperfections on the furnace hearth is now the accepted mechanism for carbon oxidation in processes where the oxygen is introduced through the slag<sup>32</sup>. However, results of recent research<sup>37,38,39</sup> show that the decarburization mechanism, when gaseous oxygen contacts directly with molten steel, must be different from that which had been accepted for classical open-hearth steelmaking. In particular this research has demonstrated that when Fe-C melts are decarburized under an oxidizing atmosphere the reaction mainly takes place at the gas-metal interface. It is therefore reasonable to conclude that reaction between

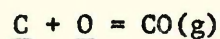
oxygen and carbon will occur in electric arc furnace steel-making where an oxygen entrainment zone exists below the slag. The rate of this reaction may be expected to be determined by the diffusion of oxygen, down to some critical carbon concentration<sup>38,39</sup>. However, it is not reasonable to expect this to be the sole reaction occurring, since the effect of carbon shortage has been estimated to manifest at concentrations as high as 1% . For this reason, a partitioning of the oxygen has been developed as displayed in Fig. 3.1. It is accepted that below some critical concentration it is the transfer of carbon that is rate limiting. Therefore, the rate of the first component of the decarburization reaction (i.e. the Free Surface Reaction) can be expressed in the following form, for carbon concentrations greater than this critical value

( $C_{kr}$ )

$$\frac{dC}{dt} = k_1 A_1 (a_o^1 - a_o^{eq}) \quad 3.3$$

where  $a_o^{eq}$  = the oxygen activity for equilibrium with the carbon in the bath ( $a_o^{eq} = EQ_1 / \%C$ )

$EQ_1$  = the equilibrium constant for the reaction



$a_o^1$  = the oxygen activity in the entrainment zone

(see Chapter 4)

When  $\underline{C} < C_{kr}$  the rate of this component of the reaction is controlled by the mass transfer of carbon to the reaction site. Thus, the change-over to carbon control can be determined as follows:

$$\text{Let } \xi_1 = D_c (\%C - EQ_1 / a_o^1)$$

$$\xi_2 = D_o (a_o^1 - EQ_1 / \%C)$$

where  $D_c$  = the diffusivity of carbon in liquid steel

$D_o$  = the diffusivity of oxygen in liquid steel.

For  $\xi_1 > \xi_2$  the rate of the reaction is controlled by the transport of oxygen

$\xi_1 < \xi_2$  the rate of the reaction is controlled by the transport of carbon

$\xi_1 = \xi_2$  Neither transport is dominantly controlling.

In the present study this transition is not considered significant and the first inequality ( $\xi_1 > \xi_2$ ) is replaced by  $\xi_1 \geq \xi_2$ .

### 3.4.3 Component II - Reaction between dissolved oxygen and dissolved carbon

For this reaction the rate may be limited either by the transport of oxygen from the slag to the metal, or by the transport of oxygen through the bath to the gas metal interface. A critical survey of the literature revealed that the degree of approach to equilibrium between the carbon and oxygen in the bath was related to the furnace shape.

Shallower types of furnaces, for example the open hearth, have a carbon/oxygen relationship a lot closer to equilibrium than that of the deeper B.O.F. It is admittedly somewhat unreasonable to compare two processes so different in refining speeds. But it is reasonable to deduce from a comparison of the electric arc furnace and the B.O.F. which have similar slag (FeO) contents, but different bath oxygen contents at the same carbon concentration, that the electric arc furnace is closer to equilibrium because;

- (i) it has a greater hearth surface area/unit volume,
- (ii) its mean slag-hearth path is shorter, and
- (iii) it has a greater slag metal interfacial area/unit volume.

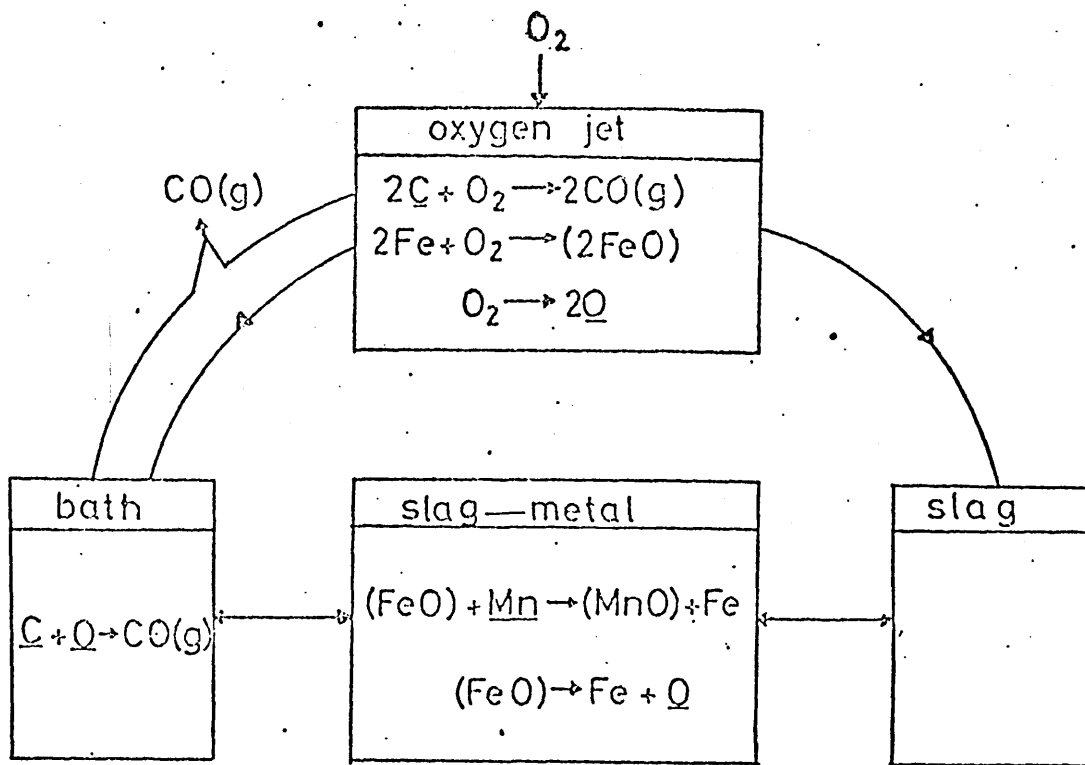


FIG 3.1 Oxygen Distribution and Process Reactions

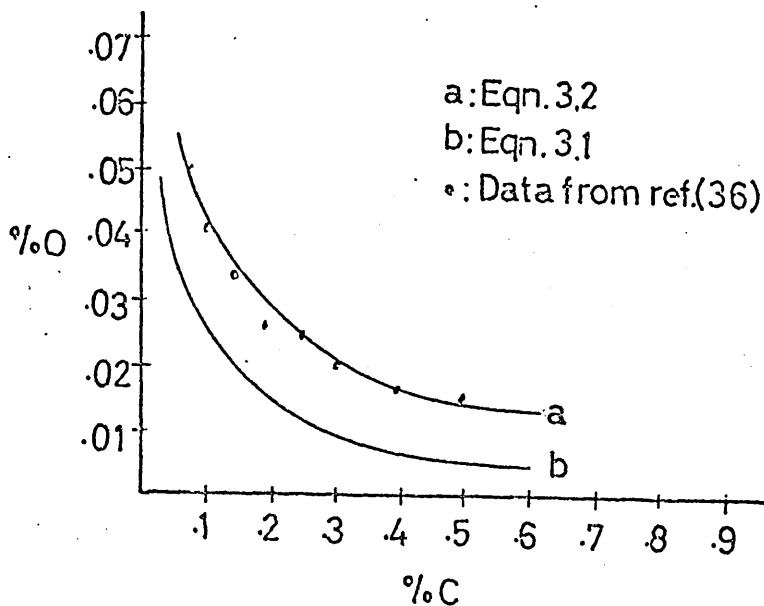


FIG 3.2 Effect of Carbon on Oxygen Concentration

Fig. 3.2 shows that the departure from equilibrium is carbon dependent and increases more noticeably when the carbon concentration drops below about 0.3%. Since concentrations greater than this coincide with the most vigorous period of the 'carbon boil' it was concluded that the increased slag-metal surface area accounts for the reduced departure to a significant extent. The problem may be illustrated in terms of three separate oxygen activities, as shown in Fig. 3.3. If oxygen diffusion from the bulk metal to the carbonmonoxide-metal interface is rate controlling then the chemical potential for the reaction would be given by

$$\Delta O_1 = a_{\underline{O}} - a_{\underline{O}}^{eq}$$

Substituting 3.2 and the equilibrium constant  $EQ_1$  of the reaction  $\underline{C} + \underline{O} = Co$  gives

$$\Delta O_1 = a(\underline{C})^b - EQ_1/\underline{C}$$

It is shown in Fig. 3.2 that this relationship is an accurate description of  $\Delta O_1$  for a wide range of carbon content and different operating practices. Hence if the hypothesis, that the rate of reaction is determined by  $\Delta O_1$ , is accepted then it would be reasonable to conclude that the rate of reaction would be only weakly related to the turbulence of the bath. This however is not so, Barnsely and Thornton<sup>42</sup> have found that the rate of injection,  $q^0$ , for optimum efficiency of decarburization (here efficiency is a measure of the quantity of oxygen required to oxidize 0.01% of carbon per ton of metal) is related to the furnace capacity and lance diameter by

$$q^0 = 50d(6 + \sqrt{Wt})$$

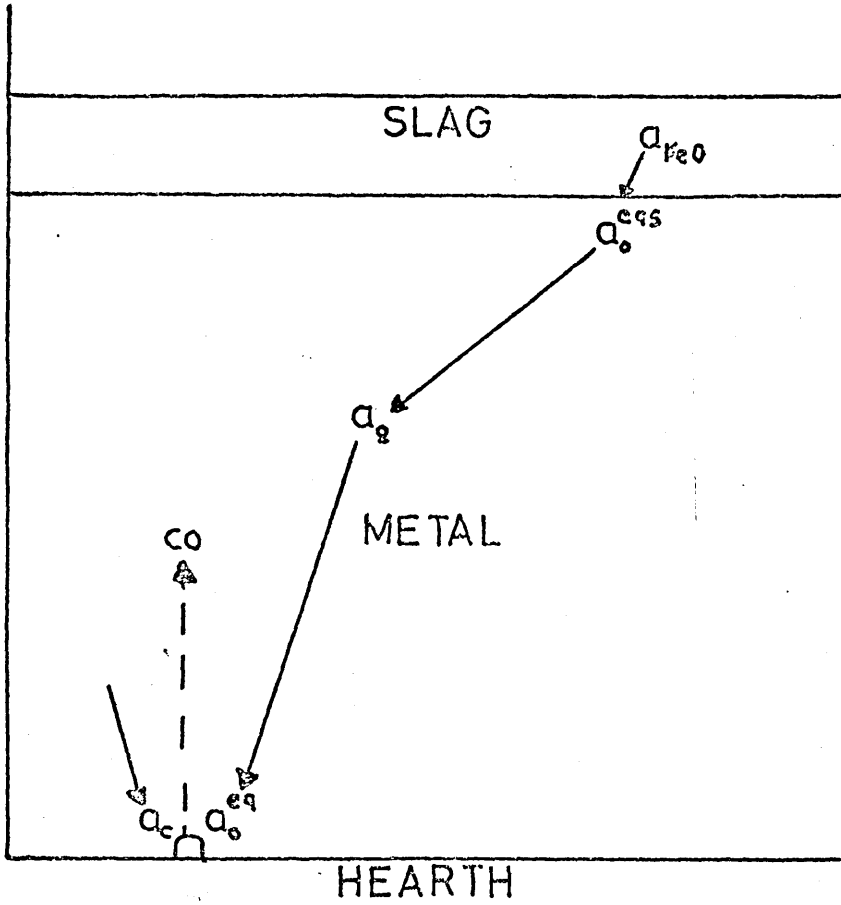


FIG 3.3 Localized Oxygen Activities

where  $q^o =$  rate of oxygen injection ( $\text{ft}^3\text{min}^{-1}$ )

$d =$  lance diameter (in)

$Wt =$  bath weight (tons)

An examination of this equation reveals that the optimum oxygen input is a function of the furnace diameter,  $D$ , since  $\sqrt{\text{tons}} \propto D$ . Also at constant gas momentum, the following linear relationship exists between two different lance diameters and oxygen flow rates:

$$\frac{d_1}{d_2} = \frac{q_1}{q_2}$$

It is significant that this relationship is satisfied by the equation for optimum oxygen input rate. Hence it seems reasonable to conclude that the stirring effect derived from the momentum imparted to the bath by the oxygen stream is a major factor in determining the rate of oxygen transfer.

The rate controlling step was therefore decided to be the transport of oxygen from the slag to the metal. The rate of this reaction can be expressed as:

$$\frac{dC}{dt} = -k_2 A_2 (a_o^{\text{eqs}} - a_o) \quad 3.4$$

During the 'carbon boil' vigorous stirring of the bath occurs and this turbulence increases the slag-metal interfacial area.  $A_2$  is therefore written as a function of the boil rate and of the mechanical energy of the oxygen jet.

$$A_2 = A_{\text{Min}} (f_1(u) + e(|\dot{C}|)^f) \quad 3.5$$

where  $A_{\text{Min}}$  is the area of the slag-metal interface for a stagnant bath

For the conditions  $\xi_1 > \xi_2$  the rate of decarburisation for the process is given by:

$$\frac{dC}{dt} \text{ total} = -k_1 A_1 (a_o^1 - a_o^{eq}) - k_2 A_2 (a_o^{eqs} - a_o)$$

3.6

where  $a_o^{eqs}$  is the oxygen activity for equilibrium with the oxide content of the slag. Substitution for the various parameters gives:

$$\frac{dC}{dt} = -k_1 A_1 (a_o^1 - EQ_1 / \%C) - k_2 A_2 (a_{FeO} / EQ_2 - \%O)$$

3.7

Assumptions made in Chapter 4 reduce this equation to the following:

$$\frac{dC}{dt} = - \{ k_1 A_1 (a_o^1 - EQ_1 / \%C) + k_2 A_{Min} f(u) (a_{FeO} / EQ_2 - \%C) \} / \{ 1 - ek_2 A_{Min} (a_{FeO} / EQ_2 - \%C) \}$$

3.8(a)

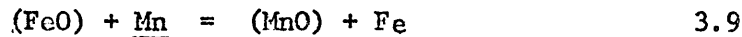
For the condition  $\xi_1 < \xi_2$  this equation becomes:

$$\frac{dC}{dt} = - \{ k_1 A_1 (\%C - EQ_1 / a_o^1) + k_2 A_{Min} f(u) (a_{FeO} / EQ_2 - \%C) \} / \{ 1 - ek_2 A_{Min} (a_{FeO} / EQ_2 - \%O) \}$$

3.8(b)

### 3.5 The oxidation of Manganese

The partitioning of manganese between the slag and the metal is described by the reaction



Though this reaction has received little attention in the literature, comparison studies between steel making processes and virtual maximum rate studies<sup>34, 35</sup> for the reaction conclude that equilibrium is closely approached towards the end of the oxygen refining period. The rate of the reaction during the injection period is considered to be controlled by the mass transport of manganese to the slag-metal interface. The rate of this transport process can be written as:

$$\frac{d \underline{MN}}{dt} = -k_3 A_3 (a_{\underline{Mn}} - a_{Mneq})$$

the reaction as:

$$EQ_3 = \frac{a_{MnO}}{a_{FeO} \cdot a_{Mneq}} \quad 3.10$$

If the concentration of MnO and FeO in the slag are expressed as kmol fractions, assigning Raoultian activity coefficients gives:

$$EQ_3 = \frac{\gamma_{MnO} N_{MnO}}{\gamma_{FeO} N_{FeO} a_{Mneq}} \quad 3.11$$

The relationship between  $\frac{\gamma_{MnO}}{\gamma_{FeO}}$  and the basicity of the slag is studied in Chapter 4.

Since this reaction, like the rate controlling reaction for the second component of decarburisation takes place at the slag-metal interface  $A_3$  must be the same as  $A_2$ . The performance equation describing the oxidation of manganese is therefore:

$$\frac{d Mn}{dt} = -k A_3 \min(f_1(u) - e(|C|)^f) (\%Mn - f_2(\beta)) \quad 3.12$$

$$N_{MnO}/EQ_3 N_{FeO}$$

### 3.6 Slag Basicity Ratio

Steelmaking slags have a large number of component oxides. These complex systems may be either acidic, neutral or basic. The present study is confined to practices using basic slags. The basicity of a slag is expressed as the ratio between the concentrations of the basic and acidic components.

The form adopted here is as suggested by Pearson et al<sup>35</sup>:

$$\beta = \frac{N_{CaO} + N_{MnO} + N_{MgO}}{N_{SiO_2} + N_{Al_2O_3} + N_{P_2O_5}} \quad 3.13$$

where  $N_i$  = Number of kmol of  $i$  species

The concentration of  $MgO$ , dissolved from the hearth can be expected to be near saturation<sup>43</sup>. The influence of iron oxide and basicity on the solubility of  $MgO$  has been investigated<sup>43</sup>. A comparison between the results of this study and the limited plant data available justifies treating  $N_{MgO}$  as being constant, as an initial assumption.

(ii)  $CaO$

The dissolution of lime in slag proceeds at a rate controlled by the diffusion of  $CaO$  across the solid-liquid interface<sup>44</sup>. The area of this interface cannot be estimated because bulk lime tends to disintegrate at random. Moreover, the practice of using powdered lime does not remove the difficulty of considering what part of the area may be blocked by a film of dicalcium silicate. The rate of precipitation of this film is dependent on the viscosity of the slag<sup>45</sup> and hence on the composition and temperature of the slag. The problem of describing this process can be avoided if it is assumed that all the charged lime is dissolved shortly after the start of the oxygen blow. This assumption is valid for the arc furnace because the use of arc power permits the slag to be controlled to meet almost any desired characteristic, a fact that is the real basis of the flexibility of steelmaking in the arc furnace.  $N_{CaO}$  is therefore treated as a constant but the problem of describing the lime dissolution rate may present itself again when lime additions must be considered as control variables.

(iii)  $SiO_2$  and  $P_2O_5$

As shown in Table 2.1 the melt-out bath analysis indicates a low concentration for silicon. It is therefore reasonable to expect little change in the slag silica thus permitting

SiO<sub>2</sub>  
 treating  $N_{P_2O_5}$  as being constant.

(iv) Al<sub>2</sub>O<sub>3</sub>

An investigation of the limited published work<sup>4,6</sup> concerning the solubility of Al<sub>2</sub>O<sub>3</sub> in slag, concluded that for the concentrations occurring in the present study, see Table 2.1, the slag must be near saturated with Al<sub>2</sub>O<sub>3</sub>,  $N_{Al_2O_3}$  was therefore considered as constant.

(v) MnO

The oxidation reaction for manganese has been described in 3.5. The product of this reaction is considered to be the sole variable in the basicity ratio.

The performance equation for  $\beta$  is given by

$$\frac{d\beta}{dt} = \frac{1}{N_{SiO_2} + N_{P_2O_5} + N_{Al_2O_3}} \times \frac{d N_{MnO}}{dt} \quad 3.14$$

3.7 Iron in the slag

The distribution of iron between its ferrous and ferric states is not easily resolved. This problem has been studied<sup>4,3</sup> in terms of the j-ratio =  $\frac{Fe^{+++}}{(Fe^{++} + Fe^{+++})}$  and it has been shown that this ratio is sensitive to slag composition in the range of commercial slags. The present study does not take into account this distribution and all the iron oxidised is assumed to exist as FeO. Although this assumption cannot be wholly justifiable, the fact that practically all of the carbon reacts to form carbon monoxide can be taken as an indication of little surplus oxygen being available. Hence the occurrence of Fe<sub>2</sub>O<sub>3</sub> is probably not all that significant.

From the oxygen partitioning given in Fig. 3.1, it follows that the rate of reaction for iron oxide is obtainable from an oxygen balance,

giving:

$$\frac{d \text{FeO}}{dt} = (1/\rho) (2u + \frac{dC}{dt} + \frac{d \text{Mn}}{dt} - \frac{dO}{dt} ) \quad 3.15$$

### 3.8 Material balance

To determine the slag and bath weights a dynamic material balance is used. The ratio of slag to bath weight is given by:

$$\rho = \frac{\text{WSL}^0 + \int_0^t (\text{FeO} \times \text{WHM} \times M_{\text{FeO}} \times \rho) dt}{\text{WHM}^0 - \int_0^t (\text{FeO} \times \text{WHM} \times M_{\text{Fe}} \times \rho) dt} \quad 3.16$$

where  $\text{WSL}^0$  and  $\text{WHM}^0$  are the initial slag and bath weights respectively.

It should be noted that in deriving this balance only the oxidation of iron was considered to have a significant effect on the slag and bath weights.

### 3.9 The kmol fraction of iron oxide in the slag

The kmol fraction of iron oxide is given by:

$$N_{\text{FeO}} = \frac{N_{\text{FeO}}^0 + \int_0^t \left( \frac{d \text{FeO}}{dt} \right) dt}{\Sigma + \int_0^t \left( \frac{d \text{FeO}}{dt} - \frac{1}{\rho} \frac{d \text{Mn}}{dt} \right) dt} \quad 3.17$$

where  $\Sigma = N_{\text{SiO}_2} + N_{\text{P}_2\text{O}_5} + N_{\text{CaO}} + N_{\text{Al}_2\text{O}_3} + N_{\text{MgO}} + N_{\text{FeO}}^0 + N_{\text{MnO}}^0$

### 3.10 The oxygen activity of the slag

The activity of iron oxide in a complex basic slag is not readily calculable. The problem of deriving a relationship to give a continuous estimate of this variable is considered in Chapter 4. There a regression analysis is performed on published data and an expression of the following form is obtained.

$$a_{\text{FeO}} = \alpha_0 + \alpha_1 N_{\text{FeO}} + \alpha_2 \beta \quad 3.18$$

### 3.11 The kmol fraction of manganese oxide in the slag

The kmol fraction of manganese is given by

$$N_{\text{MnO}} = \frac{N_{\text{MnO}}^0 + \int_0^t \left( \frac{-1}{\rho} \frac{d \text{Mn}}{dt} \right) dt}{\Sigma + \int_0^t \left( \frac{d \text{FeO}}{dt} - \frac{1}{\rho} \frac{d \text{Mn}}{dt} \right) dt} \quad 3.19$$

### 3.12 Heat balance

The rate of change of temperature of the bath is calculable from an enthalpy balance for the process. Heat of reaction and heat contents are available in the literature<sup>47</sup>. Heat losses due to radiation, convection and conduction are taken as being constant. Cooling due to infiltrating air is accounted for and a fraction of this is assumed to react with carbon monoxide to form carbon dioxide. A certain proportion of the heat from this reaction is considered to be radiated back to the bath.

$$\begin{aligned} \frac{dT}{dt} = & (WHM \left( \frac{dO}{dt} H_1 + \frac{dC^1}{dt} (H_2 + H_3 T) + \frac{dC^2}{dt} \right. \\ & \left. (H_4 + H_3 T) + \frac{d \text{Mn}}{dt} (H_5 + H_6 T) + \frac{d \text{FeO}}{dt} \right. \\ & \left. \rho (H_7 + H_8 T) + H_{11} \frac{dC}{dt} (H_{12} + H_{13} T) \right. \\ & \left. + U(H_{16} + H_{17} T) + E) / (H_9 WHM + H_{10} WSL) \end{aligned} \quad 3.18$$

Where  $\frac{dC^1}{dt}$  and  $\frac{dC^2}{dt}$  refer to the first and second components of the decarburisation reaction respectively and E is electric power input. Estimated values for  $H_i$  and what they represent will be given in Chapter 4.

### 3.13 Summary

The structure of a set of equations required to simulate the process has been described. Since the structure is subject to the

validity of many hypotheses the set may require expansion or modification when more accurate plant data or experimental evidence becomes available. In Appendix 4 the current parameter estimates are only assumed to be accurate to  $\pm 10\%$ .

The derivation of empirical relationships and  
parameter estimates

4.1 Introduction

In the previous chapter the development of a mathematical model of the refining process has demonstrated the necessity for both the derivation of relationships to describe phenomena and the estimation of parameters not theoretically evaluated. In this chapter a solution to these problems is obtained by analyses of the results of both plant investigations and a wide range of work reported in the literature.

4.2 Least squares fit applied to carbon-oxygen data.

Despite the recent progress <sup>33,36,48,49,50</sup> in the field of oxygen determination in steel, a study of the literature reveals that for the electric arc furnace only limited data are available.

The following data were obtained from the work<sup>36</sup> of Hill and Knaggs:

%O	.04	.032	.026	.0225
%C	.1	.15	.2	.25

Two functions were considered:

(1) A power curve

$$\%O = \alpha_o (\%C)^{\alpha_1} \quad 4.1(a)$$

Results

$$\alpha_o = 9.4 \times 10^{-3}$$

$$\alpha_1 = -0.63$$

$$\text{Correlation coefficient} = -0.99$$

$$\%O = \alpha_0^1 \text{ EXP.}(\alpha_1^1 \%C) \quad 4.1(b)$$

## Results

$$\alpha_0^1 = 6.0 \times 10^{-2}$$

$$\alpha_1^1 = -3.87$$

$$\text{Correlation coefficient} = -0.986$$

The correlation coefficients, being a measure of that degree of association between the data points, indicate that the power curve is the more probable relationship. This is in agreement with the result of similar studies conducted by Coheur and Nilles<sup>34</sup> on the carbon/oxygen relationship in four other steelmaking processes.

The data used in the present study do not include any carbon concentrations representative of the earlier part of the refining period. The two functions 4.1(a), 4.1(b) were therefore tested with melt-out data from the literature<sup>33</sup>.

### %O Evaluated by

%C	%Oact	Power curve	Exponential function
.3	0.019	0.020	0.019
.4	0.016	0.0160	0.013

These tests endorse the adoption of equation 4.1(a) to relate the concentrations of dissolved carbon and oxygen.

## 4.3 The interaction between the submerged oxygen jet and the molten steel

### 4.3.1 Introduction

The oxygen jet affects a number of the chemical and physical processes occurring in the furnace:

#### (i) The decarburisation rate

Against a decreasing oxygen efficiency, the rate of decarburisation increases with the oxygen flow,

subject to the limitations imposed by splashing and pressure drop considerations.

(ii) Oxygen efficiency

A range of input rates which give optimum efficiency, for each lance diameter and furnace size, have been reported<sup>42</sup>.

(iii) Mixing

The transfer of momentum between the jet and the liquid imparts a stirring effect to the bath.

(iv) Refractory Wear

Direct contact between the jet and the refractories results in serious refractory erosion.

(v) Splashing

The bath is only capable of dissipating a limited amount of jet energy before liquid spouts are formed which result in excessive fume loss and refractory wear.

Despite the apparently important role of the oxygen jet no theoretical studies of its fluid dynamics could be found in the literature. Some more general studies of gas-liquid systems<sup>51-56</sup> provide the basis of the present investigation.

#### 4.3.2 Bubble size

Bubble size has been shown to be dependent on the dimensions of the orifice and its Reynolds number<sup>57</sup>. This study concluded that for Reynolds numbers exceeding 40,000 the bubble size is virtually constant and has an average diameter of about 0.4 cm.

The Reynolds number,  $N_{Re}$ , is given by:

where

$q$  = gas flow rate ( $\text{m}^3/\text{s}$ )

$d_o$  = lance diameter (m)

$\lambda_g$  = kinematic viscosity ( $\text{m}^2/\text{s}$ )

For the present study the gas kinematic viscosity  $\lambda_g$  is less than  $10^{-4}$   $\text{m}^2/\text{s}$  at the process temperature. The flow rate is  $0.71 \text{ m}^3/\text{s}$  and the lance diameter  $0.038\text{m}$ . These values give an orifice Reynolds number greater than  $40,000$ . It may also be noted that for optimum oxygen efficiency (see 3.43) Barnsley and Thornton have shown that the ratio  $q/d_o$  is related to furnace capacity and for a  $140$  tonne capacity furnace (as considered here) this gives a Reynolds number of  $7 \times 10^5$ .

#### 4.3.3 Jet trajectory

Themelis et al<sup>51</sup> derived the following equation to describe the trajectory of a gas jet in a liquid:

$$\frac{d^2 Y_r}{dX_r^2} = 4N_{fr}'^{-1} \left( \frac{\tan^2(\theta_c/2)}{\cos \theta_o} \right) \left( 1 - \frac{dY_r}{dX_r} \right)^{\frac{1}{2}} X_r^2 C \quad 4.3$$

Where  $Y_r = y/d_o$  = dimensionless vertical distance  
from jet pole

$X_r = x/d_o$  = dimensionless horizontal distance  
from jet pole

$$N_{fr}' = \frac{\rho_g U_o^2}{g(\rho_l - \rho_g)d_o}$$

$d_o$  = orifice diameter

$\rho_l, \rho_g$  = liquid and gas densities respectively

$\theta_c$  = jet cone angle

$\theta_o$  = angle of inclination of axis of orifice to  
horizontal

$C$  = volume of fraction of gas in jet at a distance  
 $x$  from jet pole given by

$$C = \frac{d_o}{d} \left( C + \frac{\rho_1}{\rho_g} (1 - C) \right)^{\frac{1}{2}}$$

$d$  = jet diameter at a distance  $x$  from the orifice.

From the geometry of the jet,  $d = 2x \tan (\theta_o/2)$ .

The following values were estimated from data obtained in the course of plant studies.

$$N'_{fr} = 210$$

$$d_o = 0.038\text{m}$$

$$\rho_1, \rho_g = 7.16 \times 10^3 \text{ and } 1.43 \text{ kg/m}^3$$

$$\theta_o = -30^\circ$$

From the literature<sup>51</sup>  $\theta_c \doteq 20^\circ$

#### 4.3.4 Solution of Equation 4.2

The equation was solved numerically subject to the following initial conditions

$$\text{at } X_r = \frac{1}{2 \tan(\theta_c/2)}, \quad Y_r = 0, \quad \frac{dY_r}{dX_r} = \tan \theta_o$$

The resulting jet trajectory is presented in Fig. 4.1.

The average jet velocity at a distance  $x$  from the orifice is given by

$$U_x = U_o \left( C + \frac{\rho_1}{\rho_g} (1 - C) \right)^{-1} \quad 4.4$$

From the jet trajectory the approximate distance ( $\bar{x}$ ) travelled can be measured.

$$\bar{x} = 1\text{m.}$$

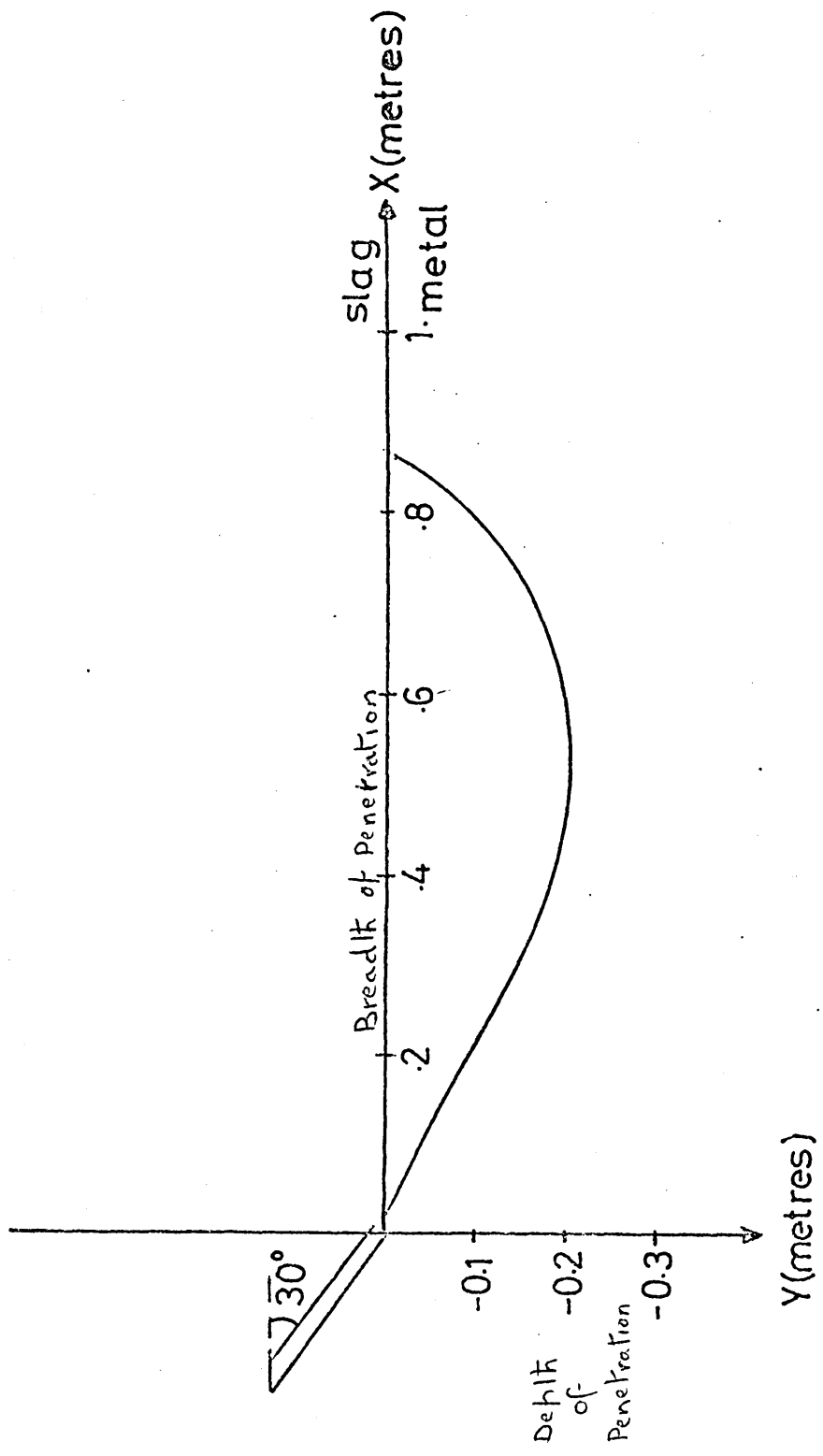


FIG 4.1 Trajectory of Oxygen Jet in Molten Steel

$$\text{tr} = \int_0^{\bar{\ell}} \frac{1}{U_x} dx \quad 4.5$$

Equation 4.5 was solved numerically using Simpson's Rule and an average residence time of 0.25 secs obtained. The volume of gas in the bath is, after correction for temperature and pressure, approximately  $1\text{m}^3$ .

From 4.3.2 the average bubble diameter before correction is  $4 \times 10^{-3}\text{m}$ . Correcting for temperature and pressure gives an approximate diameter of  $7.5 \times 10^{-3}\text{m}$ . The gas-metal interfacial area can be estimated as follows

$$\begin{aligned} A_1 &= \frac{\text{Vol. of gas}}{\text{Vol. of bubble}} \times \text{surface area of bubble} \\ &= 74.0 \text{ m}^2. \end{aligned}$$

#### 4.3.5 Calculation of the mass-transfer coefficient ( $k_1$ ) for the reaction between gaseous oxygen and carbon

If direct proportionality is assumed between mass transport and diffusivity, the mass transport coefficient can be expressed as

$$k_1 = \frac{A_1 D_o \rho_\ell}{\delta \cdot (\text{wt. bath})} \quad 4.6$$

From the literature  $D_o = 5 \times 10^{-9} (\text{m}^2/\text{s})$ ,  $\delta = 3 \times 10^{-5} (\text{m})$ .

Substitution of these values into Equation 4.6, assuming the initial bath weight to be  $140 \times 10^3 \text{ kg}$  gives

$$k_1 = 7 \times 10^{-3} \text{ s}^{-1}$$

#### 4.3.6 Estimation of the value of $a_o^1$ the oxygen activity in the jet

For an oxygen injection rate of  $1500 \text{ cu.ft/min}$  the rate of decarburisation of the bath is approximately  $6 \times 10^{-4}$ .

0.17 kmol.tonne<sup>-1</sup>. For ore-fed processes, which have similar slag oxygen potentials the rate of decarburisation is approximately  $2 \times 10^{-4}$  kmol.tonne<sup>-1</sup>.s<sup>-1</sup>. From equation 3.1 the oxygen potential of the bath for equilibrium with a carbon concentration of 0.5%  $\equiv 0.43$  kmol.tonne<sup>-1</sup>, is

$$a_{\text{oeq}} = 0.004$$

The rate of the decarburization reaction in the jet zone is given by:

$$\frac{dc}{dt} = k_1 (a_o^1 - a_{\text{oeq}})$$

Substitution of the above values of  $\frac{dc}{dt}$ ,  $k_1$  and  $a_{\text{oeq}}$  gives

$$\begin{aligned} a_o^1 &= \frac{(6 - 2) 10^{-4}}{7 \times 10^{-3}} + 0.004 \\ &= 6 \times 10^{-2} \end{aligned}$$

This value of  $a_o^1$  was taken as an initial estimate for use in equation 3.3.

It is of interest to note that the accuracy of these estimated values of  $k_1$  and  $a_o^1$  can be tested in a general sense as follows:

In 3.4.2 it was stated that changeover from oxygen transport control to carbon transport control occurred when  $\zeta_1 = \zeta_2$

Substituting the estimated value for  $a_o^1$  and 0.002 for  $E_{Q_1}$  (see 3.4.2) with  $D_o = 5 \times 10^{-5}$  and  $D_c = 7 \times 10^{-7}$  gives

$$5 \times 10^{-5} (0.06 - 0.002/\%C_{\text{kr}}) = 7 \times 10^{-5} (\%C_{\text{kr}} - 0.002/0.06)$$

$$\%C_{\text{kr}} = 0.17$$

This estimated value of  $\%C_{\text{kr}}$  is in close agreement with the value of 0.16 which has been reported<sup>42</sup> for plant practice.

## of the slag

The complexity of steelmaking slags has been discussed in Chapter 3. Turkdogan et al<sup>81</sup> studied the effects of composition by expressing slag compositions as mole fractions of oxides. The results of this investigation were drawn on a ternary diagram, Fig. 4.2, giving iso-activity curves of ferrous oxide in the system (CaO + MnO + MgO) - FeO - (SiO<sub>2</sub> + P<sub>2</sub>O<sub>5</sub>). A study of slag analyses concluded that for the present investigation, the slag composition can be constrained to an area bounded by,

$$\begin{aligned} \text{(i)} \quad & 2 \leq \beta \leq 5 \\ \text{(ii)} \quad & 0.0 \leq N_{\text{FeO}} \leq 0.25 \end{aligned} \quad \text{where } \beta = \frac{N_{\text{CaO}} + N_{\text{MnO}} + N_{\text{MgO}}}{N_{\text{SiO}_2} + N_{\text{P}_2\text{O}_5} + N_{\text{Al}_2\text{O}_3}}$$

This region is indicated in Fig. 4.2

A multiple linear regression analysis was conducted on data from the area defined above.

The resulting relationship is

$$a_{\text{FeO}} = 0.555 + 2.24 N_{\text{FeO}} - 0.1778 \quad 4.7$$

Iso-activity lines determined by equation 4.7 are shown in Fig. 4.3 data from the ternary diagram are included to display the accuracy of this relationship over the constrained region.

## 4.5 Estimation of the relationship between slag-metal interfacial area and bath turbulence

### 4.5.1 The stagnant bath slag-metal interfacial area

For an Electric Arc Furnace of 140 tonnes capacity the internal shell diameter is approximately 6.7m. The corresponding slag-metal interfacial area for a stagnant bath is,

$$A_{\text{min}} = 35.0 \text{ m}^2$$

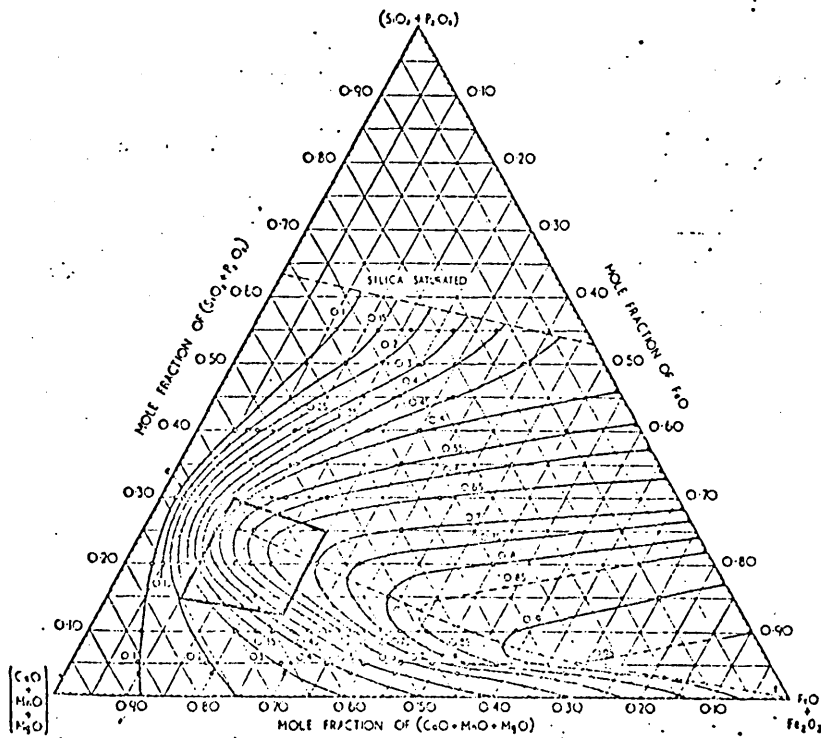


FIG 4.2 Activity of Ferrous Oxide in Complex Slags

(from Turkdogan and Pearson; J.I.S.I. pp.217-223, 1953 )

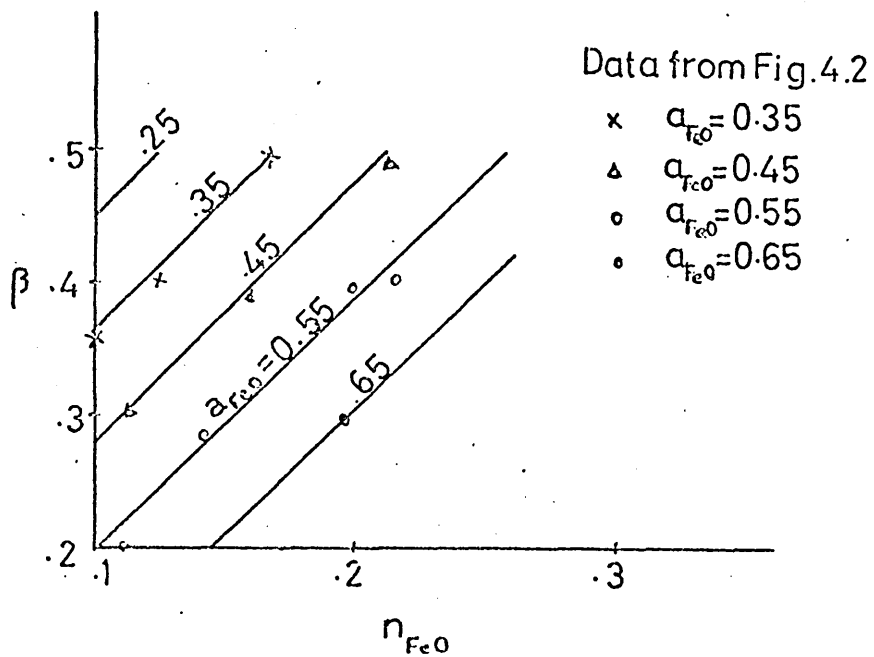


FIG 4.3 Iso-activity Lines for Ferrous Oxide

Energy is available for stirring from two sources<sup>54</sup>:

- (i) Mechanical energy of the oxygen stream
- (ii) Conversion of thermal energy, released owing to exothermic reactions, to mechanical energy.

The resulting bath turbulence increases the effective slag-metal phase boundary area. This increase in area is due to both the agitation of the actual slag-metal interface and to the dispersion of FeO formed in the vicinity of the oxygen jet.

#### 4.5.3 The slag-metal interface area

The total mechanical energy of the bath cannot be calculated since no estimate can be made of the fraction of thermal energy converted into mechanical energy. Consequently only an inexact study of the effect of stirring is possible. The following relationship is suggested to describe this effect on the interface area.

$$A_2 = A_{\min} (f_1(u) + e \left( \left| \frac{dc}{dt} \right| \right)^f) \quad 4.8$$

Where  $f_1(u)$  = the effect of the stirring action of the oxygen jet. ( $f_1(u) \geq 1$ )

$e \left( \left| \frac{dc}{dt} \right| \right)^f$  = the effect of turbulence due to the carbon boil

For preliminary studies  $f_1(u)$  and  $f$  were set equal to unity. The latter simplification allowed equation 3.8 which is implicit in  $\frac{dc}{dt}$ , to be reduced to the form described in equation 3.9. It has been reported<sup>58</sup> that at the peak of the boil the effective slag-metal area is probably about twice the stagnant bath area. For a stagnant bath area of 35 m<sup>2</sup>, assuming a boil rate of  $6 \times 10^{-3}$  (kmol.(tonne.s)<sup>-1</sup>), a value of  $1.7 \times 10^3$  for  $e$  was estimated.

and oxygen (See equation 3.4)

The rate of this component of the decarburisation reaction has been shown to be given by

$$\frac{dc}{dt} = k_2 A_2 \left( \frac{a_{\text{FeO}}}{EQ_2} - a_{\text{O}} \right)$$

As stated in 4.3.6 for a carbon content of 0.43 ( $\text{kmol.tonne}^{-1}$ ) the rate of this component is approximately  $2 \times 10^{-4}$  ( $\text{kmol. (tonne.s)}^{-1}$ ).

From equation 4.1 (a),  $a_{\text{O}} = 1.4 \times 10^{-2}$ . Assuming a value of 0.3 for  $a_{\text{FeO}}$  as being typical, it follows that

$$k_2 \doteq 1.0 \times 10^{-4} \text{ s}^{-1}$$

#### 4.7 The effect of slag composition on the activity coefficient ratio

$\gamma_{\text{MnO}}/\gamma_{\text{FeO}}$  (See equation 3.11)

The effect of slag basicity on the activity coefficient ratio has been studied<sup>35</sup>. This investigation, which included data from other similar studies, concluded that the ratio increased steeply with basicity and closely approaches unity at  $\beta = 5$ .

The data presented in this study was subjected to a regression analysis to give

$$\frac{\gamma_{\text{MnO}}}{\gamma_{\text{FeO}}} = f_2(\beta) = (1. \alpha_0 \text{EXP.}(\alpha_1 \beta)) \quad 4.9$$

$$\text{Results} \quad \alpha_0 = 3.27$$

$$\alpha_1 = -0.95$$

$$\text{correlation coefficient} = 0.99$$

reaction (See equation 3.12)

The manganese oxidation reaction proceeds at a maximum rate during the early part of the carbon boil. This was deduced from a study of plant data and is supported by the fact that the slag-metal interface  $A_2$  is at a maximum at this time. Substitution of the following data, which are typical of the process, into equation 3.12 permits  $k_3$  to be estimated.

$$\%Mn = 0.25$$

$$N_{FeO} = 0.1$$

$$N_{MnO} = 0.08$$

$$\frac{Y_{MnO}}{Y_{FeO}} = 0.24$$

$$\frac{dMn}{dt} = 1 \times 10^{-5} \text{ wt\%/s}$$

$$k_3 = 2.8 \times 10^{-4} \text{ s}^{-1}$$

#### 4.9 Explanation and selection of values of the coefficients $H_i$ for $i = 1, 17$ occurring in the heat balance for the process

##### 4.9.1 Introduction

A base temperature of  $295.15^{\circ}\text{K}$  is taken for all reactions, other than the solution of oxygen, so the additional heat required to raise the reaction products to the process temperature must be included. The generalised expression for the heat of reaction is

$$\Delta H_T = \Delta H_1 + \Delta H_2(T - 295.15)$$

kJ/(kmol of product)

A positive sign for  $\Delta H_T$  denotes a heat input and a negative sign of heat loss.

- (i)  $H_i$  ( $i = 1, \dots, 8$  and 12, 13) values for these coefficients were obtained from the literature<sup>47</sup>.
- (ii)  $H_9$  This coefficient represents the heat required to raise the temperature of 1 tonne of the bath by 1<sup>o</sup>k;  
 $H_9 = -860 \text{ kJ}/(\text{tonne } ^\circ\text{k}^{-1})$
- (iii)  $H_{10}$  The heat required to raise the temperature of 1 tonne of slag by 1<sup>o</sup>k.  
 $H_{10} = -2300 \text{ kJ}/(\text{tonne } ^\circ\text{k}^{-1})$
- (iv)  $H_{11}$  A coefficient which incorporates that fraction of the evolved CO that reacts with infiltrated air and the fraction of the heat given off, that is radiated to the bath.  
 $H_{11} = 0.3$
- (v)  $H_{14}$  Heat loss due to radiation and water cooling and convection. This was assumed constant and a value of -8400 kJ/s was estimated from the literature<sup>59</sup>.
- (vi)  $H_{15}$  Rate of infiltration of air into the furnace, assumed constant at 0.2 kg/s.
- (vii)  $H_{16}, H_{17}$  Terms in the expression for the heat content of  $O_2$  and air at T<sup>o</sup>k.  
 $H_{16} = -16,000 \text{ kJ}/\text{kmol}; H_{17} = 38.0 \text{ kJ}/(\text{kmol } ^\circ\text{k})$

#### 4.10 Comments

In this chapter combined statistical and theoretical analyses of both collected and published plant data have been employed to obtain estimates of values for the elements of the parameter set associated with the mathematical model of the refining process. It is probable that some of the parameter estimates and regression coefficients presented here have at best only order of magnitude

accuracy. However, it will be shown later that this uncertainty is tolerable when state estimation is employed to filter these stochastic features of the process model.

### 5.1 Introduction

In order to determine the accuracy with which the dynamical model, developed in the previous chapters, simulated the industrial process the equations were integrated numerically. Initial conditions typical of the process were available from the plant study reported in Appendix 1 and the system was forced by inputs similar in magnitude and duration to those employed in standard operating practice. The Runge-Kutta method with Gill's coefficients was used since it was available as a subroutine on the Polytechnic computer. The chief advantage of Gill's procedure lies in the requirement of a minimum amount of storage locations. It does, however, have the disadvantage that neither the truncation errors nor estimates of them are obtained in the calculation procedure. Therefore control of accuracy and adjustment of step size  $h$  is done by comparison of the results due to double and single step size  $2h$  and  $h$ . This control requires an input vector of error weights and a tolerance for the approximate truncation error.

### 5.2 Calculation of error weights and the tolerance for the approximate truncation error

A test value  $\delta$  for accuracy is generated in the following way:-

$$\delta = \frac{1}{15} \sum_i \lambda_i (|y_i^{(1)} - y_i^{(2)}|) \quad 5.1$$

where  $\lambda_i$  = error weight on  $i$ th estimate, also  $\sum_i \lambda_i = 1$

$y_i^{(1)}$  = estimate of  $y_i(t_0 + 2\Delta t)$  computed using step size  
 $h = \Delta t$

$y_i^{(2)}$  = estimate of  $y_i(t_0 + 2\Delta t)$  computed using step size  
 $h = 2\Delta t$ .

$\mu_i$	$\lambda_i = \frac{1/\mu_i}{\sum_{i=1}^{12} 1/\mu_i}$	$\mu_i$	$\lambda_i = \frac{1/\mu_i}{\sum_{i=1}^{12} 1/\mu_i}$
$i = 1$ $1 \times 10^{-4}$	$8.06 \times 10^{-1}$	$i = 7$ $1 \times 10^0$	$8.06 \times 10^{-5}$
$i = 2$ $1 \times 10^{-3}$	$8.06 \times 10^{-2}$	$i = 8$ $1 \times 10^{-2}$	$8.06 \times 10^{-3}$
$i = 3$ $1 \times 10^{-3}$	$3.06 \times 10^{-2}$	$i = 9$ $1 \times 10^{-2}$	$8.06 \times 10^{-3}$
$i = 4$ $1 \times 10^{-2}$	$8.06 \times 10^{-3}$	$i = 10$ $1 \times 10^{-2}$	$8.06 \times 10^{-3}$
$i = 5$ $1 \times 10^{-1}$	$8.06 \times 10^{-4}$	$i = 11$ $1 \times 10^1$	$8.06 \times 10^{-6}$
$i = 6$ $1 \times 10^0$	$8.06 \times 10^{-5}$	$i = 12$ $1 \times 10^{-1}$	$8.06 \times 10^{-4}$

TABLE 5.1 Error Weights

$$\lambda_i = \frac{\Delta}{\mu_i / (\sum_i (|y_i^{(1)} - y_i^{(2)}|))} \quad 5.2$$

where  $\mu_i = 1/(\text{maximum permissible } (|y_i^{(1)} - y_i^{(2)}|))$

The values selected for  $\mu_i$  and the corresponding values of  $\lambda_i$  are presented in Table 5.1.

The tolerance E is obtained by substitution of the maximum permissible estimation errors in Equation 5.1, to give

$$E = \frac{1}{15} \sum_i \lambda_i / \mu_i = 10^{-4}$$

for the values presented in Table 5.1.

### 5.3 Solution of model equations

The state space formulation of the process model, as was coded for use with the integration procedure, is presented in Appendix 3.

The set of initial values for the process variables, the control inputs and the set of process parameters are also presented there.

The system of equations was solved using a step size of 10.0s, which was found to satisfy the tolerance E and the variables were printed at one minute intervals. The trajectories of the major process variables are presented in Figs. 5.1-5.

### 5.4 Model Performance (refer Figs. 5.1, 2, 3, 4, 5)

#### 5.4.1 General

The initial low rate of decarburization is in agreement with observed practice where initiation of the carbon flames does not occur until a short time after the start of injection.

This low rate of decarburisation coincides with an increase in the iron oxide content of the slag. The oxidation of iron

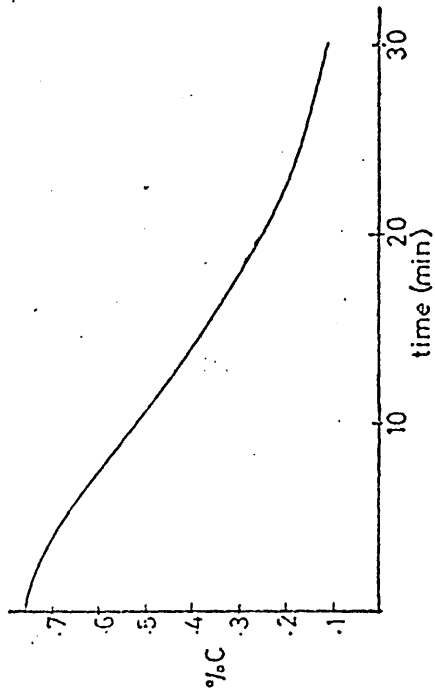


FIG 5.1 Carbon Response

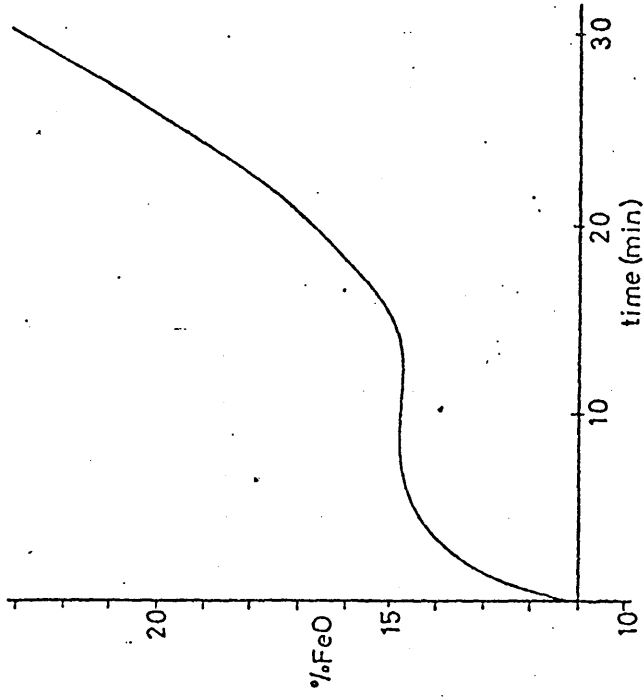


FIG 5.3 Iron Oxide Response

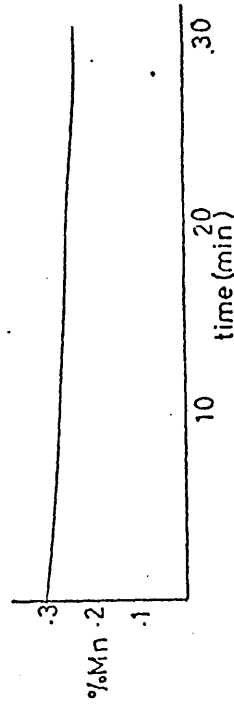


FIG 5.2 Manganese Response

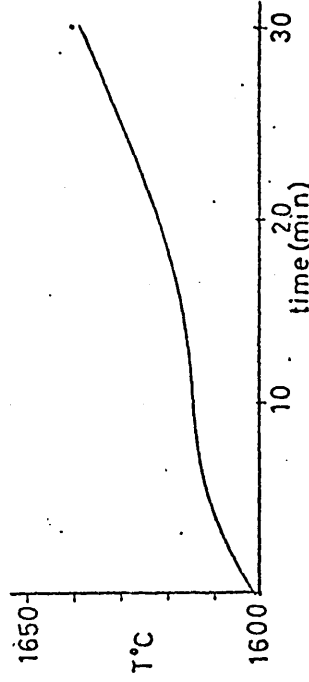


FIG 5.4 Temperature Response

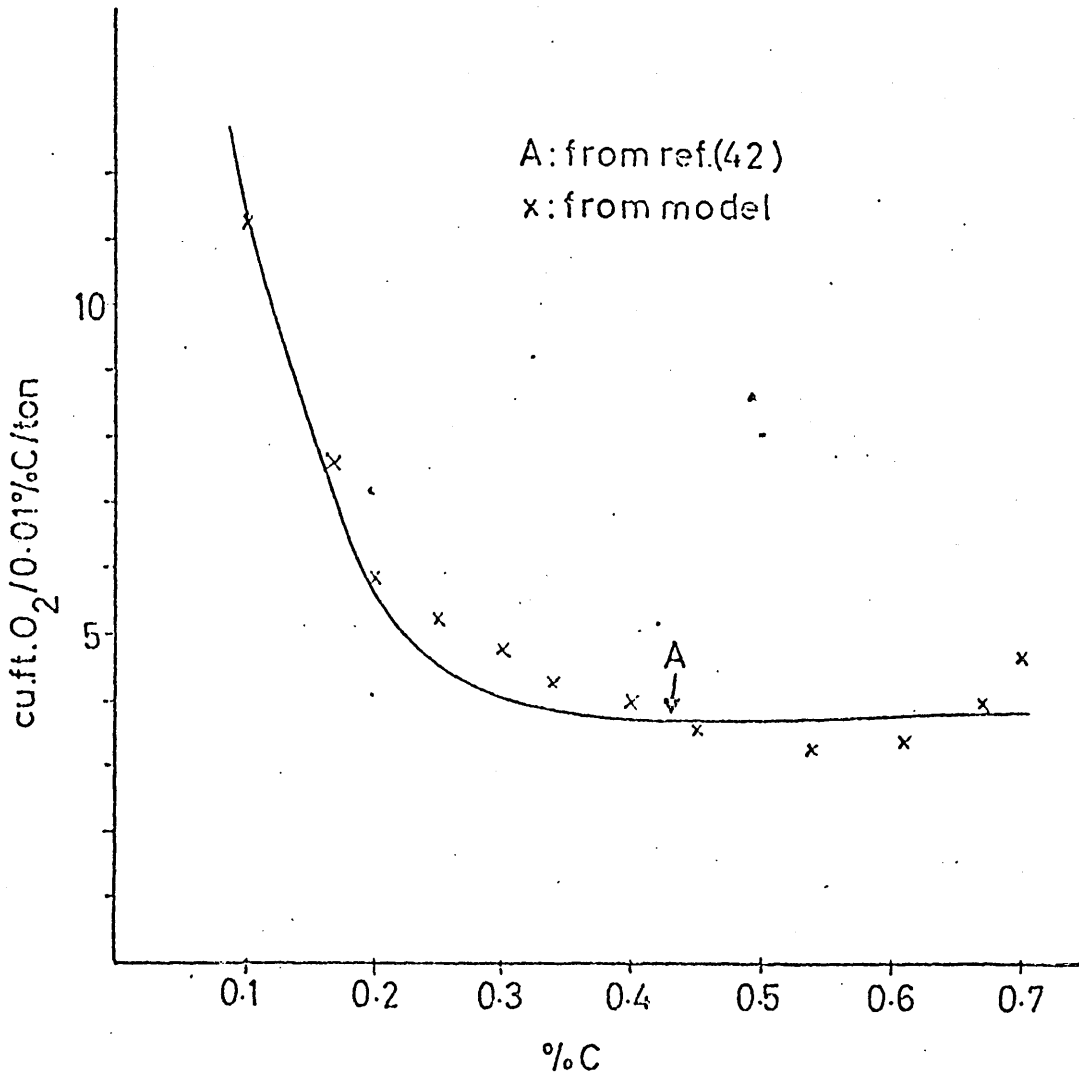


FIG 5.5 Oxygen Efficiency of Process and Model

Once the boil gets started, the temperature rise is less pronounced, this may be explained as being a result of the heat required to maintain the endothermic second component of the decarburization reaction. The influence of carbon transport control manifests at about 0.42%C. The effect of carbon shortage can also be observed where the iron oxide content of the slag increases more rapidly with decreasing carbon content.

The rate of oxidation of manganese remains almost constant over the duration of the boil. This is in agreement with practice, but in the absence of adequate plant data little can be concluded.<sup>A</sup>

#### 5.4.2 Oxygen efficiency

The efficiency of the process can be measured by calculating the oxygen required to remove 0.01%C per tonne of steel.

The efficiency predicted by the model is displayed in Fig. 5.5 along with the data from the literature. The results from the model study show a good proximity to these latter data. These extra data were obtained from studies in the refining process in an eight ton furnace and the agreement achieved may be taken as an indication of the validity of the model structure.

#### 5.4.3 Total decarburization time

The plant data available does not provide the time taken to reach the desired carbon content. The total refining time is provided, this includes periods when no oxygen is injected.

---

<sup>A</sup> It should be noted that these conclusions were limited to comparisons between the simulation results and data obtained from the literature and during the plant study reported in Appendix 1.

decarburization period can be estimated by considering the total carbon drop, the total volume injected and the blowing rate. Only an approximate value is obtained since the volume of oxygen injected during melt down is not available for subtraction from the total. Applying this technique gives a decarburisation period of 40 mins. The shorter period predicted by the model can be explained by the volume of oxygen injected during melt down and by the inefficiencies inherent in the practice of stopping and starting the injection during the refining period.

### 5.5 Conclusions

A study of the capability of the model to simulate the industrial process has been conducted. It has been shown that the model in its present form, wherein values for parameters were obtained from a physical analysis, can make predictions of the trajectories of the steelmaking process which are comparable with the observed practice. The study does, however, expose limitations in the range and accuracy of the available plant data. Hence, if a more meaningful analysis of the possible role of the model as the basis for a practical control system is to be conducted then the need for carefully monitored plant data must be satisfied.

## Data Collection and Parameter Optimization

### 6.1 Introduction

The results presented in Chapter 5 indicate that, in its present form, the model has a generally correct structure. It must, however, be extended to include the effects the power input from the electric arcs before further studies can be conducted to determine how accurately it simulates actual furnace practice. For this reason a further series of plant investigations were conducted. It was intended that sufficient chemical and thermal process data should be collected during these investigations to allow the parameters in the model to be adjusted using a non-linear parameter estimation program. Such a program had been obtained from the IBM Share Library and had been tested using simple non-linear models. However, subsequent to a thorough investigation of plant operation and an analysis of the range and accuracy of the available data it was apparent that statistically meaningful estimates of the parameters could not be obtained. Instead the model in its original form was used to simulate the monitored casts and it was found that, with only minor adjustments, the original model could simulate very accurately those casts during which no abrupt changes in operation occurred.

### 6.2 Further plant studies

#### 6.2.1 General study of the modes of furnace operation

In terms of increasing difficulty to simulate, the following is a classification of the various modes of furnace operation.

- (a) Stagnant closed furnace - no power or oxygen input
- (b) Closed furnace - constant power and/or oxygen input

bulk additions to be made or  
slagging-off. (With or without  
power and/or oxygen input.)

- (d) Open furnace - roof swung back to allow large  
additions of slag-making materials  
to be made.

The model, as developed so far, is capable of simulating the  
chemistry of the process, ignoring the effects of heat loss and  
power input. To extend the simulation to cover the complete  
range of operating modes is the long term aim, but in the interim  
only modes (a) and (b) will be considered. The thermal dynamics  
of the process when operated in these modes may be described by  
the following general equation

$$\dot{S} = f_1(T) + f_2(E) + f_3(X,U) \quad 6.1$$

where  $S$  = heat content, J,

$f_i(\cdot), i=1,2,3$  = function describing the heat flow  
due to  $(\cdot), W$

$T$  = process temperature,  $^{\circ}K$

$E$  = electric power input, W

$X$  = state vector

$U$  = oxygen input, kmol/tonne/s.

To simplify the development of this thermal balance it was  
assumed that the contribution due to chemical reactions,  $f_3(\cdot)$ ,  
is negligible when the oxygen input is zero. This assumption  
permits the components  $f_1(\cdot)$  and  $f_2(\cdot)$  to be identified by  
statistical analysis of data pertaining to operation in modes  
(a) and (b) without oxygen injection. The component,  $f_3(\cdot)$ ,  
has already been formulated, (see section 3.12) and cannot be  
studied in isolation from the mathematical model of the process  
chemistry.

A three-week period of plant studies was conducted and in addition to the production data recorded by the furnace operators the following details were also noted:

- (i) The injection rate and the duration of the periods of oxygen lancing
- (ii) The times of transformer tap changes and the transformer tap settings.

### 6.2.3 Slag sampling

During the refining period a number of samples are taken from the furnace. These samples are obtained by inserting a long shafted sampling spoon into the furnace. Upon removal from the furnace a coating of slag is normally to be found adhered to the shaft of the spoon. By ensuring that the shaft was clean prior to use, a sample from the slag was obtained simultaneous to the standard sample from the bath. These samples were collected and subsequently analysed in the Department of Metallurgy at Sheffield City Polytechnic. Although many of these samples proved to be satisfactory a number were discarded. In particular, it was found that some samples contained an unrealistically high concentration of a single oxide. Such unrepresentative samples may be anticipated since the slag is rarely homogeneous and it is quite possible for the sample to contain undissolved lime or excessive amounts of a particular oxide. A typical record is presented in Table 6.1 and the complete set of records are presented in Appendix 6.

### 6.2.4 Further data

In addition to these data, recorded during this series of plant studies, further thermal and chemical data were made

CAST NO. \*\*\*

QUALITY 0.3 CARBON

TIME HR. MIN.	OBSERVATIONS	TRANSFORMER TAP
0 . 0	Melt-out, Sample 1, Power On, Temperature = 1560°C	7
0 . 13	Power, Off, Oxygen On,	
0 . 17	Power On, Carbon "Boil"	9
0 . 20	Oxygen Off (Lance Change)	
0 . 23	Oxygen On	
0 . 25	Sample 2, Power Off Temperature = 1630°C, Oxygen Off	
0 . 30	Oxygen On, Door Open, Slagging Off	
0 . 35	Sample 3	
0 . 36	Temperature = 1645°C	
0 . 45	Boil Ebbing	
0 . 47	Sample 4, Oxygen Off Temperature = 1660°C	
0 . 49	Power On	12
0 . 55	Temperature = 1660	
0 . 56	Power Off, Furnace Tapped	

## NOTES:

Weight of metallic charge = 145 tonnes  
 Weight of lime charge = 2 tonnes  
 Oxygen injection rate = 42.48 m<sup>3</sup>/min

TABLE 6.1 Typical Cast Record

available by the works Quality Control Department. These included a log of the thermal behaviour of the furnace made over a number of weeks of operation and twenty sets of slag analyses obtained for samples taken at 'meltout' and at 'tapping'.

### 6.3 Investigation of the thermal behaviour of the process during refining

A study of the available sets of thermal data, which covered forty casts, revealed that only a limited number of these sets could be usefully employed in statistical studies. Many of the sets were rejected because of corruption of the data by the effects of interruptions in the standard operating practice, such as, swinging the roof of the furnace back to permit bulk additions to be made. From the remaining data those presented in Table 6.2 relate to periods during which the furnace was operated without oxygen lancing. The following linear regression equation was obtained from these data

$$\frac{d}{dt} (T) = 2.18 \times 10^{-6} E + 0.166 \quad 6.2$$

where  $E$  = the power input, W. The apparent anomaly of the constant increase in temperature for  $E = 0$  will be resolved later when this term is incorporated in an overall constant heat loss term for the process.

It is of interest to note the following interpretation of equation 6.2

$$\frac{d}{dt} (T) = (\eta E + \alpha) / C_p \quad 6.2(a)$$

where  $\eta$  is the efficiency of the energy transfer and  $C_p$  is the heat capacity of the system. It will be shown later that (see eqn 7.1)  $\alpha_T = (1/C_p) = 4 \times 10^{-6} \text{ } ^\circ\text{K.J}^{-1}$  hence from eqns. 6.2 and 6.2(a)

$$\eta = 2.18 \times 10^{-6} / 4 \times 10^{-6}$$

$$\eta = 0.55$$

This estimate of the efficiency compares favourably with the results of Wheeler et al<sup>23</sup> who obtained an estimate of 0.588 for  $\eta$  from data gathered on 73 production heats.

Power Input E (W)	Time Interval $\Delta t$ (min)	Approx. $\dot{T}$ °C/min	$\dot{T}$ (from Eqn. 6.2) °C/min
1.8 $10^6$	11.0	4.09	3.13
1.32 $10^6$	15.0	1.0	2.7
6.6 $10^5$	22.0	1.59	1.73
1.32 $10^6$	10.0	4.0	2.7
1.178 $10^6$	7.0	0.71	2.5
2.0 $10^5$	9.0	-0.55	0.79
9.9 $10^5$	14.0	2.5	2.27
9.9 $10^5$	14.0	2.14	2.27
9.9 $10^5$	5.0	5.0	2.27
6.0 $10^5$	5.0	3.0	1.622
1.2375 $10^6$	1.25	1.25	2.6
9.9 $10^5$	1.42	1.42	2.27
9.9 $10^5$	1.66	1.66	2.27
6.0 $10^5$	3.0	3.0	1.622

LEAST SQUARES FIT TO GIVE

$$\dot{T} = \alpha_1 E + \alpha_2$$

RESULTS  $\alpha_1 = 2.17788 \cdot 10^{-6}$

$\alpha_2 = 0.16576$

Correlation Coefficient = 0.52

TABLE 6.2 Thermal Data

the process a number of attempts were made to obtain a more complete description of the energy transfer in the furnace. A variety of nonlinear and linear dynamic and static model structures were considered. Statistical analyses of the significance of these models were conducted using the available parameter estimation program. No significant improvement on the results presented in Table 6.2 obtained using eqn. 6.2 was, however, achieved. In particular the best results obtained, from analysis of data for periods of operation when bulk furnace additions were made, gave an error on the temperature prediction<sub>from the model</sub> of standard deviation 50°C. Such an estimate is considerably less accurate than the 'educated guess' of the furnace operator who can estimate the temperature of the process to a standard deviation of 20°C.

#### 6.4 Parameter Optimization

In theory, optimum estimates of the unknown parameters in the model might be obtained by employing an optimization technique to systematically vary the parameter values until the minimum deviation between the predicted and measured values of the process variables is obtained. For the present model the use of this technique is denied by the lack of sufficient accurate process measurements and the variety of modes of furnace operation. Instead the sensitivity of the model response to parameter variations was studied by conducting simulations on an interactive computer terminal. This approach enabled manual adjustments of the parameter values to be made and the monitored casts were simulated. To facilitate these studies it was assumed that the time variation of the slag species can be determined solely in terms of their initial concentrations and a mass balance on the bath species. In addition this assumption implies that the time

same mass balance. Hence, the number of state equations (see Appendix 3) was reduced from twelve to four with retention only of those describing the dynamics of the following process variables.

$x_1$  = concentration of carbon in molten bath, kmol/tonne

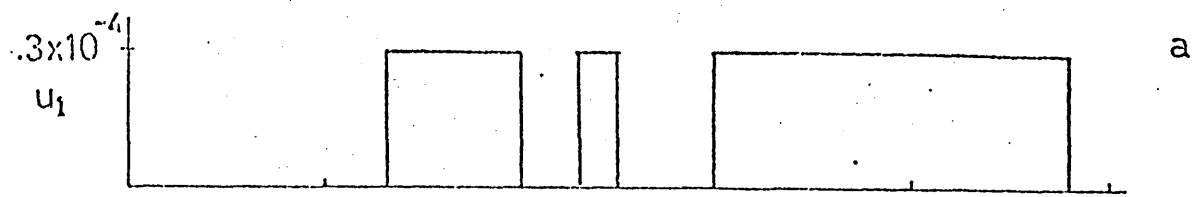
$x_2$  = concentration of manganese in molten bath, kmol/tonne

$x_3$  = concentration of iron-oxide in slag, kmol/tonne

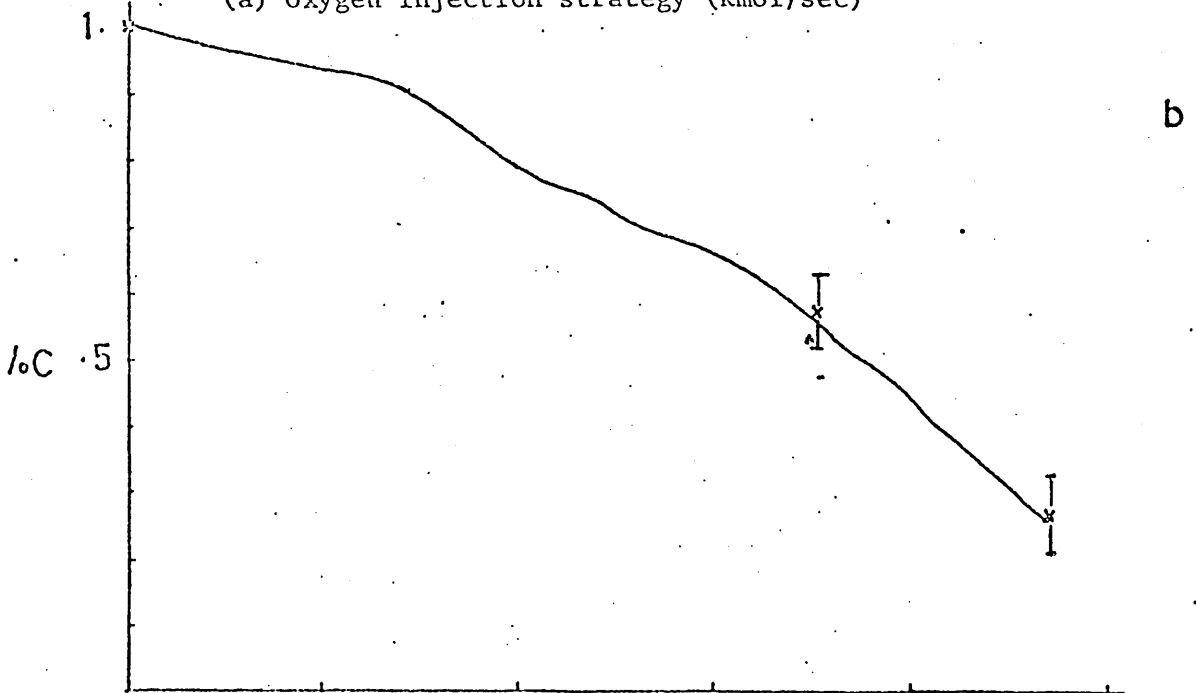
$x_4$  = temperature of molten bath, °K.

This simplified model is presented in section 7.3.1.

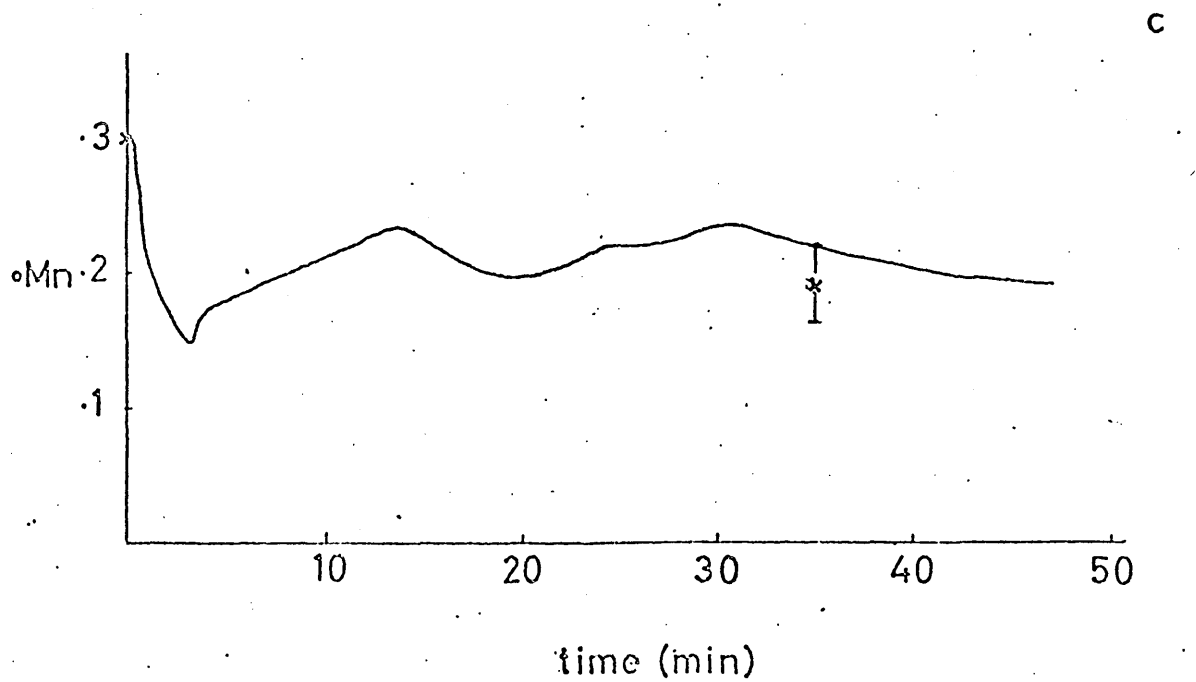
These studies exposed that the model responses were especially sensitive to the choice of values for the parameters  $\Delta_1$  = the mass transfer coefficient for the reaction  $\underline{C} + \frac{1}{2}O_2 = CO$  and  $\Delta_7$  = the reciprocal of the heat capacity of the system. The investigation of the accuracy with which the model simulated the monitored casts revealed a strong dependence between the operating mode of the furnace and the accuracy. In particular, it was observed that with only minor adjustments of the parameters  $\Delta_1$  and  $\Delta_7$  the model was accurate for those during which the furnace was operated in modes (a) and (b) of section 6.2.1. The results of a simulation of such a cast are shown in Fig. 6.1 and the accuracy these demonstrate is especially noticeable from the responses of the states  $x_1$  and  $x_2$  which are the industrially most important variables. The results presented in Fig. 6.2 are, however, more typical and these demonstrate the inaccuracy of the responses obtained when the furnace operating practice includes all the modes (a) to (d). The final form of the model of the process arrived at from these simulation studies is presented in the next chapter and this represents the limit of the development of the model on a deterministic structure.



(a) Oxygen injection strategy (kmol/sec)



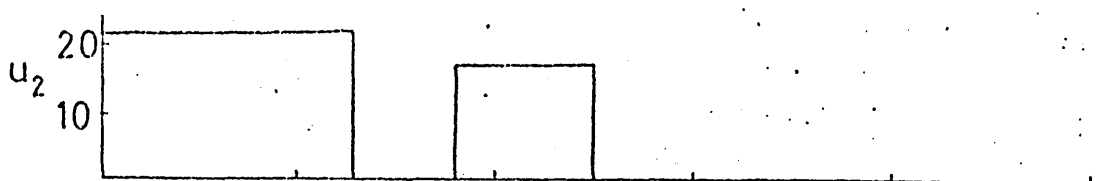
(b) Carbon response



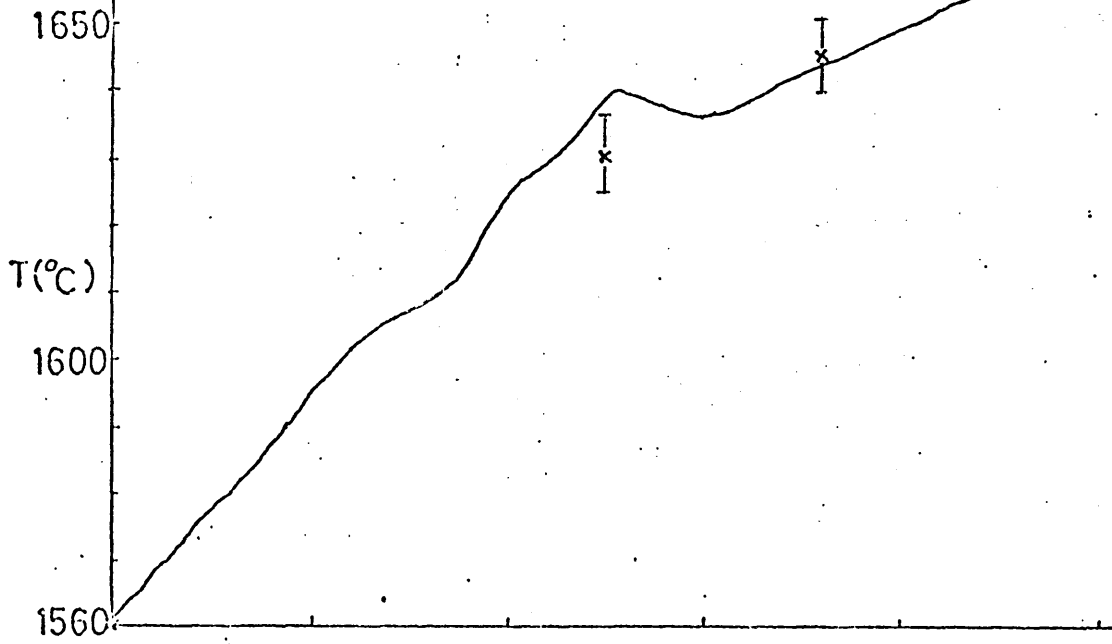
(c) Manganese response

FIG 6.1 Result of Simulation Study

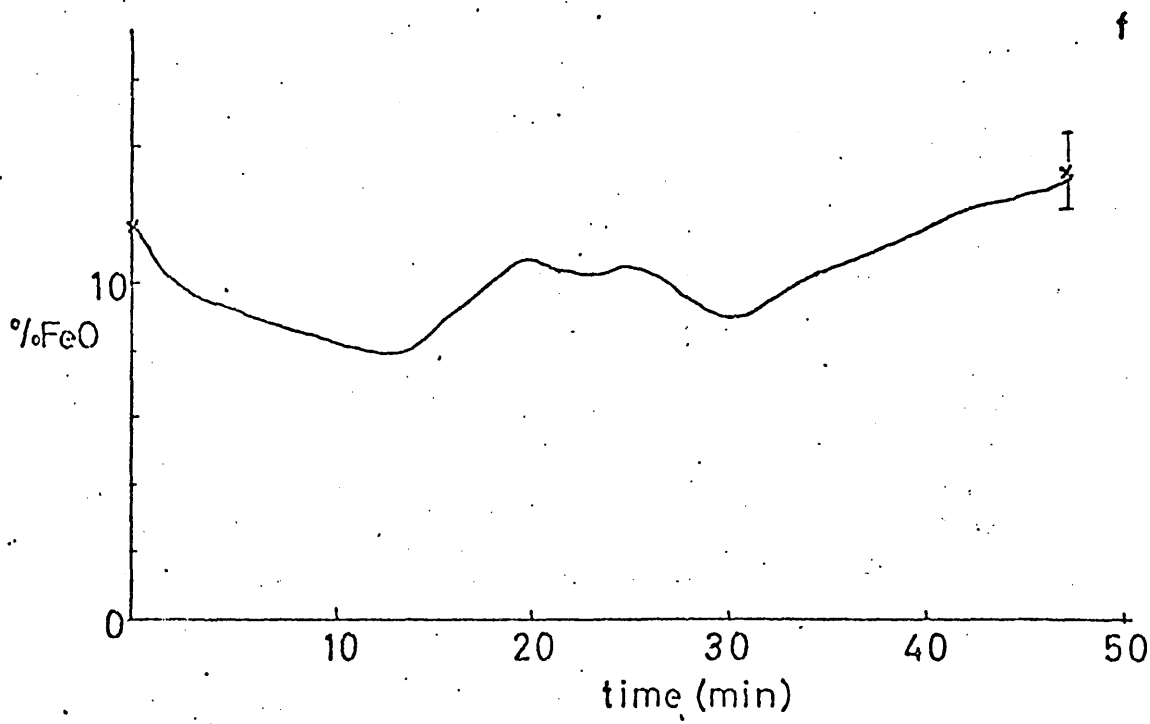
x = Measurement    | maximum error bounds



(d) Power input strategy (MW)



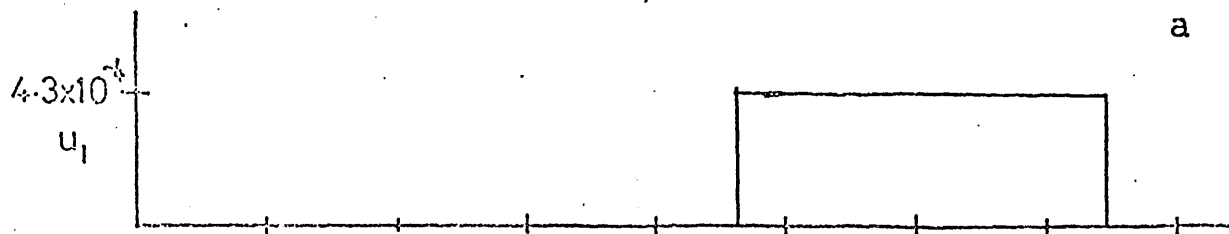
(e) Temperature response



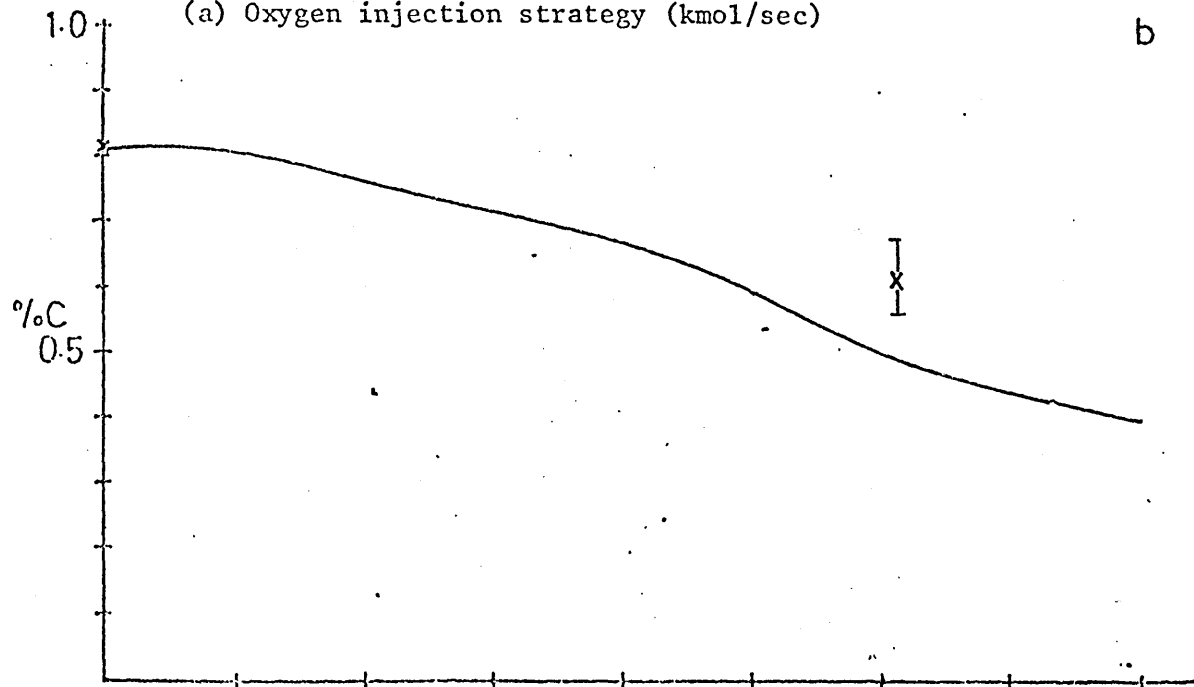
(f) Iron oxide response

FIG 6.1 Result of Simulation Study

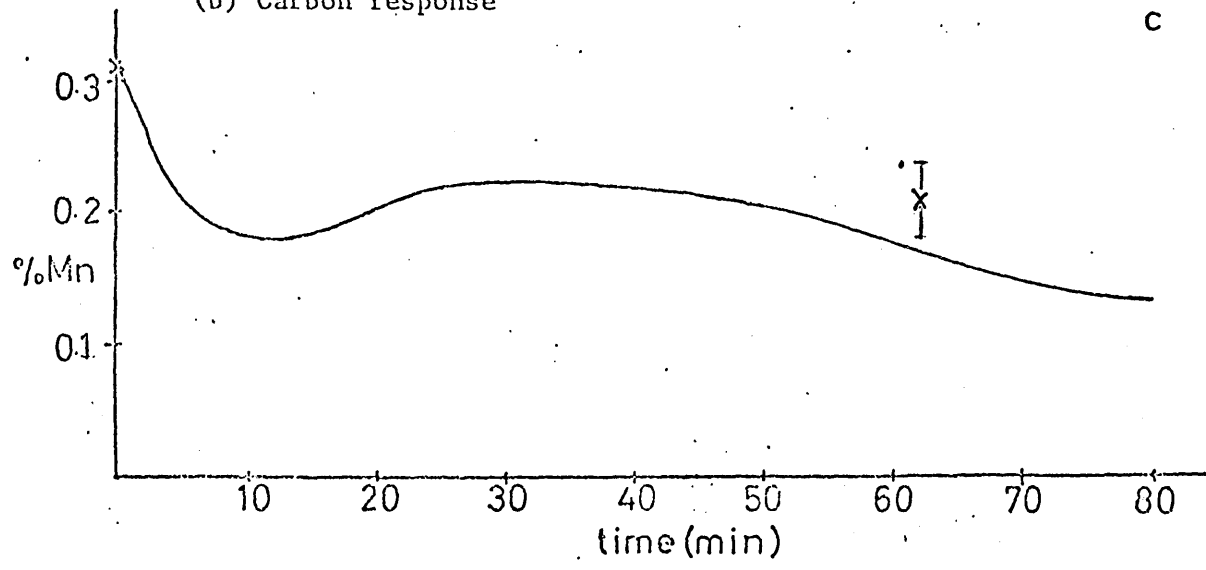
x = Measurement    I maximum error bounds



(a) Oxygen injection strategy (kmol/sec)



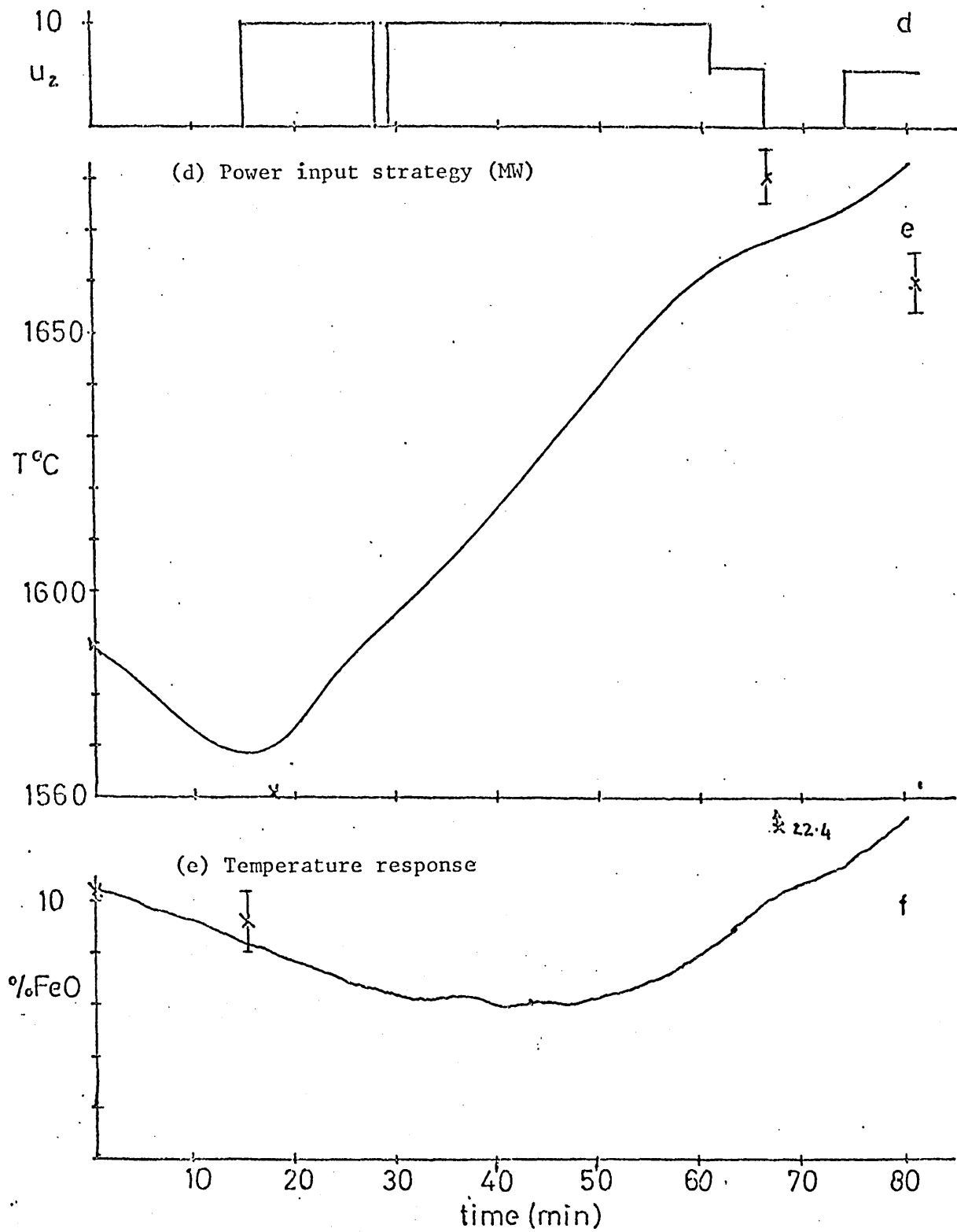
(b) Carbon response



(c) Manganese response

FIG 6.2 Result of Simulation Study

x = Measurement I maximum error bounds



(f) Iron oxide response

FIG 6.2 Result of Simulation Study

x = Measurement | maximum error bounds

## 6.5 Discussion

The ability of the theoretically evolved model to simulate a limited class of operating practice has been demonstrated. Its failure to be accurate over the complete range of operating modes had been anticipated from the results of on-plant studies and the difficulties encountered when collecting process data. The shortcomings in the model exposed by these simulation studies can be interpreted as an indication of a lack of sufficient a priori information about the process for accurate deterministic predictions of its behaviour to be made. It was therefore decided that the inherent uncertainty in the model should be studied and that the possibility of combining the limited information in the model with that available from indirect process measurements, to give best estimates of the process states, should be investigated.

Estimation of the states during refining in  
the electric arc furnace

7.1 Introduction

The results presented in Chapter 6 demonstrate that, given sufficient process data the model of the refining process can accurately simulate a limited class of operating practices. The need for a complete and accurate analysis of the slag at meltout is, however, very restrictive. The additional effort required to obtain this analysis could make any control system based on this model uneconomical to implement, especially since it seems probable that the simulation must be re-initialized after any variation from the standard operating practice. In addition, although the weight of slag at meltout can be estimated from the known charge weight of lime and the CaO concentration, it is not possible to model the changes that occur during 'slagging-off'.

In this chapter the effects of forcing with a stochastic process are introduced to resolve these sources of indeterminism and to account for the uncertainty due to estimated parameter values and the hypotheses on which the model has been formulated.

7.2 Reduced dimension model

7.2.1 Stochastic variables

To reduce the complexity of the model and to remove its dependence on the non-measurable chemical states associated with the slag phase the following stochastic variables were introduced.

$\xi_1 = \beta$  , the slag basicity ratio

$\xi_2 = \sum_i N_i$  , where  $N_i$  = the total number of kmols of the slag specie,  $i$ , per tonne of slag

per tonne of slag at meltout

$\xi_4 = (\text{FeO})^0$ , the number of kmols of iron oxide per tonne of slag at meltout.

The mean values and variances of these variables were determined from the following data obtained during plant studies.

(a)  $\xi_1 = \beta$  the basicity ratio

Data

$\xi_1 = \beta$			$\xi_1 = \beta$			$\xi_1 = \beta$		
Cast No.	Start	End	Cast No.	Start	End	Cast No.	Start	End
1	3.956	--	11	3.124	6.52	21	4.914	5.256
2	4.01	--	12	6.299	5.736	22	4.631	5.042
3	3.028	--	13	3.372	4.114	23	4.096	5.143
4	4.023	--	14	3.041	5.3	24	--	4.95
5	5.06	--	15	4.049	3.544		5.693	6.158
6	3.013	--	16	5.837	5.494		3.963	
7	3.027	4.438	17	3.385	5.678		4.730	
8	3.887	4.887	18	3.954	4.491		5.997	
9	4.747	5.137	19	2.626	3.407			
10	3.982	4.155	20	--	3.819			

Mean values,  $\bar{\xi}_1 = 202/45 = 4.5$

Variance  $\sigma_{\xi_1}^2 = 1$

(b)  $\xi_2$ , the total oxide content

Data

$\xi_2 = \sum N_i$			$\xi_2 = \sum N_i$			$\xi_2 = \sum N_i$		
Cast No.	Start	End	Cast No.	Start	End	Cast No.	Start	End
1	15.8	--	11	15.66	15.5	21	15.31	--
2	15.1	--	12	15.1	14.7	22	15.62	--
3	15.43	--	13	15.73	16.01			
4	16.55	--	14	15.41	15.73			
5	15.57	--	15	15.16	14.51			
6	17.07	--	16	14.39	15.09			
7	15.44	--	17	15.29	15.27			
8	15.67	16.3	18	14.57	--			
9	15.62	15.69	19	15.06	15.94			
10	14.73	14.2	20	14.18	15.72			

Mean value,  $\bar{\xi}_2 = 15.4$  kmol/tonne

Variance,  $\sigma_{\xi_2}^2 = 0.35$  (kmol/tonne)

(c)  $\xi_3$  and  $\xi_4$ , initial MnO and FeO respectively

Data

Cast	%MnO	%FeO
1	4.8	14.3
2	3.87	13.63
3	4.73	12.73
4	3.85	18.17
5	5.64	14.22
6	5.54	12.32
7	5.06	19.57
8	4.24	16.1
9	4.94	15.2
10	8.21	13.8

Cast	%MnO	%FeO
11	4.23	18.32
12	6.02	15.9
13	4.86	20.02
14	5.19	13.84
15	2.94	15.39
16	3.77	22.95
17	5.07	21.7
18	5.2	17.74
19	7.03	15.53
20	4.16	20.18

$$\text{Mean values } \bar{\xi}_3 = 5\% \text{ MnO} \quad \equiv 0.7 \text{ kmol/tonne}$$

$$\bar{\xi}_4 = 15.86\% \text{ FeO} \quad \equiv 2.3 \text{ kmol/tonne}$$

$$\text{Variances } \sigma_{\xi_3}^2 = 0.03 \text{ (kmol/tonne)}^2$$

$$\sigma_{\xi_4}^2 = 0.18 \text{ (kmol/tonne)}^2$$

### 7.2.2 Stochastic process model

Combining the stochastic variables  $\xi_i$ , ( $i = 1, \dots, 4$ ) with the results presented in Chapter 6 permits the following reduced dimension model describing the dynamics of  $x_1$  = the carbon content,  $x_2$  = manganese content,  $x_3$  = iron oxide content,  $x_4$  = process temperature, to be formulated. (See Appendix 3)

$$\dot{x}_1 = a_1 \left( \frac{K_1}{1.2x_1} + a_2 \right) + s_1(x, u) s_2(x, u) / K_2 - 1.6a_3 x_1^a$$

$$\dot{x}_2 = s_1(x, u) (5.49x_2 - s_3(x, u) / Y_3 x_3) \quad 7.1$$

$$\dot{x}_3 = a_5 (u_1 + \dot{x}_1 (1 - s_4(x, u)) + \dot{x}_2)$$

$$\dot{x}_4 = a_6 + a_7 \left( \sum_{i=1}^3 \Delta H_i \dot{x}_i + \Delta H_4 \dot{x}_1 s_4(x, u) + \Delta H_5 u_1 \right) + a_9 u_2$$

where the functions  $s_i(\cdot)$ , ( $i = 1, \dots, 4$ ) are as follows:

$i = 1$ , see Eqn. 4.8

$$s_1(x, u) = 0.00263 + 6.15 u_1$$

$$s_2(x, u) = 0.555 - 0.112\xi_1 + 2.24x_3/\xi_2$$

$i = 3$ , see Eqns. 3.12 and 4.9

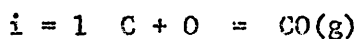
$$s_3(x, u) = (1 - 3.27 \exp(-0.95\xi_1))(\xi_3 + a_5(x_2^0 - x_2))$$

$i = 4$ , see Eqns. 3.15 and 4.1

$$s_4(x, u) = a_3 a_4 x_1^{a_4 - 1}$$

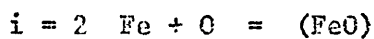
The coefficients  $K_i$ ,  $i = 1, 2, 3$ , are the equilibrium constants of the following reactions:

$K_1$



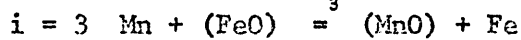
$$\text{at equilibrium } \frac{P_{CO}}{a_C a_O} = K_1 = \exp(-4.77 - 2690/x_4)$$

$K_2$



$$\text{at equilibrium } \frac{a_{FeO}}{a_{Fe} a_O} = K_2 = \exp(-6.3 + 14564/x_4)$$

$K_3$



$$\text{at equilibrium } \frac{a_{MnO} a_{Fe}}{a_{Fe} a_{Mn}} = K_3 = \exp(-8.0 + 17053/x_4)$$

The parameter set  $a_i$  ( $i = 1, \dots, 9$ ) has values

$$a_1 = \begin{cases} -0.00635 & \text{if } u_1 > 0 \\ 0 & \text{if } u_1 = 0 \end{cases}$$

$$a_i (i = 2, \dots, 9) = 0.0146, 0.00524, -0.633, 7.0, -0.01, \\ -4.0 \cdot 10^{-6}, 140., 0.8$$

The thermochemical coefficients,  $\Delta H_i$  ( $i = 1, \dots, 5$ ), have values<sup>47</sup>

$$\Delta H_i (i = 1, \dots, 5) = -0.138 \cdot 10^6, -0.36 \cdot 10^6, -0.353 \cdot 10^5, \\ 10.12 \cdot 10^6, -0.27 \cdot 10^5$$

The values of the process parameters given in the previous section are the mean values of a vector of random variables which is assumed to be time-invariant. Combining the uncertainty associated with these parameters with that arising from the hypotheses on which the model has been evolved results in a stochastic representation of the general non-linear form,  $\dot{x} = f(x,u,w)$ , where  $w$  is a Gaussian process. The assumption, that the sum effect of these many sources of uncertainty is equivalent to forcing by a Gaussian process, follows from the central limit theorem.

Using the simple Euler integration formula and assuming that the model is separable into stochastic and deterministic parts permits the following vector difference equation description of the process to be obtained.

$$x_{k+1} = F(x_k, u_k) + G_k w_k \quad 7.2$$

The statistics of the noise process  $w_k$  are given by

$$E(w_k) = 0 \quad E(w_k w_j^T) = Q_k \delta_{kj} \quad 7.3$$

The 4x4 diagonal covariance matrix  $Q_k$  has elements  $q_{ii}$  ( $i = 1, \dots, 4$ ) which represent a measure of the uncertainty associated with the parameter set. The values of these elements were approximated by considering the maximum error, for each of the difference equations, to be given by

$$(\text{Error}_i)^2 = \sum_{j=1}^N \left( \frac{\partial F_i}{\partial \beta_j} \delta \beta_j \right)^2 \quad i = 1, \dots, 4 \quad 7.4$$

where  $\beta_j \pm \delta \beta_j$  ( $j = 1, \dots, N$ ) are the elements of the parameter vector. Since the sum effect of this uncertainty is Gaussian distributed it is reasonable to assume that  $\text{Error}_i$  is equivalent to the 3-Standard Deviation bound on component  $w_i$ . The value of  $\text{Error}_i$  is obviously dependent upon the value of the state,  $x$ , and controls,  $u$ , but the general form for the covariance matrix  $Q$  is given by

Equation 7.4 was evaluated over the normal operating range of the process, see Appendix 4, and it was found that the covariance matrix could be reasonably approximated by

$$Q_k = 0.0625 \text{ diag. } [F_1(x_k, u_k)^2, \dots, F_4(x_k, u_k)^2] \quad 7.6$$

The evaluation of a suitable noise matrix,  $G_k$ , is a matter for engineering judgement. The simplest solution is to assume that  $G_k = I_{4 \times 4}$ . There are, however, readily apparent objections to this choice. In particular, this choice is equivalent to assuming that the uncertainties associated with the components of  $F$  are uncorrelated.

The evaluation of these cross-correlation effects is not easy, but the following approach proved satisfactory, in the present case.

(a) Determine the dominant parameter or relationship common to two components  $F_i$  and  $F_j$

(b) Isolate this common variable,  $\theta$ , in component  $F_j$  to give

$$\theta = g(F_j), \text{ where } g(F_j) \text{ is a function relating } \theta \text{ to } F_j.$$

(c) Replace  $\theta$  in  $F_i$  by  $g(F_j)$  and set  $F_{ij} = \frac{\partial F_i}{\partial F_j}$ .

For example, in the continuous-time case considering  $f_1(x, u)$  and  $f_2(x, u)$ , the dominant variable common to both functions was found to be  $s_1(x, u)$ . Writing  $s_1(x, u)$  as a function of  $f_2(x, u)$  gives

$$s_1(x, u) = -f_2(x, u) / (5.49x_2 - s_3(x, u)/k_3x_3) \quad 7.7$$

Substituting this expression into  $f_1(x, u)$  and differentiating with respect to  $f_2(x, u)$  gives

$$\begin{aligned} G_{12}(t) &= \partial f_1(x, u) / \partial f_2(x, u) \quad 7.8 \\ &= (s_2(x, u)/k_2 - 1.6a_3x_1^4) / (5.49x_2 - s_3(x, u)/k_3x_3) \end{aligned}$$

$$G_k = \{g_{ij}\}_k \quad i, j = 1, \dots, 4$$

7.9

where  $g_{ii} = 1$  and  $g_{ij} = 1/g_{ji}$

#### 7.4 Measurements

Indirect measurement of the carbon concentration,  $x_1$ , by measuring the flow rate and composition of the waste gases forms the basis for a number of control and estimation systems<sup>10,63,64</sup> in use in the BOF sector of the steelmaking industry. So far as the author is aware no such systems are at present in use in the arc furnace section of the industry. The following analysis, which employs conservative estimates of the achievable accuracy using this technique, demonstrates that the uncertainty associated with this measurement of the carbon concentration is too large for it to be used in lieu of the standard discrete sampling technique.

At time  $t$ , the measurement of the carbon concentration,  $C(t)$ , obtained from the gas analyser is given by

$$C(t) = \{C(0)W(0) - \int_0^t V(\tau) (b_1 CO(\tau) + b_2 CO_2(\tau)) d\tau\} / W(t) \quad 7.10$$

where  $W(t)$  is the weight of hot metal,  $V(t)$  is the gas flow rate and  $b_1, b_2$  are coefficients relating the volumetric carbon monoxide  $CO$ , and dioxide  $CO_2$ , to equivalent weights. If it is assumed that  $W(t) = m(t)W(0)$ , where  $m(t)$  is a known function of time, then the percentage accuracy of the measurement,  $C(t)$  is given by

$$\begin{aligned} \delta C(t) = & \{W(0)C(0) (\delta W + \delta C) + (\delta V + \delta CO) \int_0^t b_1 V(\tau) CO(\tau) d\tau \\ & + (\delta V + \delta CO) \int_0^t b_2 V(\tau) CO_2(\tau) d\tau\} / \{C(0)W(0) \\ & - \int_0^t V(\tau) (b_1 CO(\tau) + b_2 CO_2(\tau)) d\tau\} + \delta m(t) + \delta W \quad 7.11 \end{aligned}$$

$\delta W = \pm 3.5\%$ ,  $\delta C = \pm 4\%$  and it is assumed that  $\delta m(t) = 0$ .

For a typical cast

$$\text{at } t = 0 \quad W(0) = 140 \times 10^3 \text{ kg}; \quad C(0) = 1\% \equiv 140 \text{ kg}$$

$$\text{at } t = 25 \text{ min} \quad C(25) = 0.57\% \equiv 798 \text{ kg}$$

Therefore,  $\int_0^{25} V(\tau)(b_1 CO(\tau) + b_2 CO_2(\tau)) d\tau = 602 \text{ kg}$ , and substitution into equation 7.11 gives

$$\delta C(25) = \{1400(7.5) + 22(602)\}/798 + 3.5 = 33.25\%$$

Hence, the error on the final carbon measurement is

$$\Delta C(25) = \pm 0.57 \times 0.3325 = \pm 0.19$$

If this maximum error bound is associated with the Three-standard-Deviation,  $3\sigma_c$ , levels, then the probability that the measured value is within the required range of  $\pm 0.04$  is given by

$$\text{Pr} = (2\pi)^{-\frac{1}{2}} \int_{-\alpha}^{+\alpha} (\exp(-y^2)/2) dy = 0.47$$

where  $\alpha = 0.63 = 3(0.04/0.19)$ . It is thus apparent that in its present form the waste gas analysis technique is not sufficiently accurate to provide a consistent measurement of the carbon concentration. It is, however, possible to obtain the following stochastic measurement procedure for the carbon state  $x_1$ .

$$y_1(t) = x_1(t) + v_1(t) \quad 7.12$$

where  $v_1(t)$  is a zero mean Gaussian process with variance

$$\begin{aligned} E(v_1^2(t)) &= \{((x_1(0)\delta_1 - x_1(t)\delta_2)/x_1(t) + \delta W)x_1(t)/300\}^2 \\ &= \sigma_c^2(t) \end{aligned} \quad 7.13$$

where  $\delta_1 = \delta W + \delta C + \delta CO + \delta V$  and  $\delta_2 = \delta V + \delta CO$ .

direct measurement of the temperature of the molten bath can only be obtained by the use of a disposable thermocouple. A variety of techniques for obtaining an indirect measurement of the temperature are at present under investigation in the industry. To date none of these techniques are capable of providing the required measurement accuracy of  $\pm 10^{\circ}\text{K}$  but it is reasonable to assume that a continuous measurement of the temperature to an accuracy of standard deviation  $10^{\circ}\text{K}$  is achievable. For example, one technique<sup>65</sup> using thermocouples embedded in the lining of the furnace gives a reported accuracy of standard deviation  $7.7^{\circ}\text{K}$ . Hence the temperature of the process can be observed by the following stochastic measurement procedure

$$y_2(t) = x_4(t) + v_2(t) \quad 7.14$$

where  $v_2(t)$  is a zero mean Gaussian variable with variance

$$E(v_2^2(t)) = \sigma_T^2 = 100 \quad 7.15$$

### 7.5 Filter algorithm

The discrete-time form of the extended Kalman Filter, as described by the following equations, was implemented

$$x_{k+1}^k = F(x_k^k, u_k) \quad 7.16(a)$$

$$P_{k+1}^k = \phi_k^k P_k^k \phi_k^{kT} + G_k Q_k G_k^T \quad 7.16(b)$$

$$K_{k+1}^k = P_{k+1}^k H_{k+1}^{kT} (H_{k+1}^k P_{k+1}^k H_{k+1}^{kT} + R_{k+1})^{-1} \quad 7.16(c)$$

$$x_{k+1}^{k=1} = x_{k+1}^k + K_{k+1}^k (y_{k+1} - H_{k+1}^k x_{k+1}^k) \quad 7.16(d)$$

$$P_{k+1}^{k+1} = (I - K_{k+1}^k H_{k+1}^k) P_{k+1}^k (I - K_{k+1}^k H_{k+1}^k)^T + K_{k+1}^k R_{k+1} K_{k+1}^{kT} \quad 7.16(e)$$

where  $\phi$  is the linear approximation to the process equations obtained in terms of the Jacobian matrix of  $f$ , see Appendix 4,  $P$  is a  $4 \times 4$  real, symmetric, positive semi-definite matrix which approximates to the

matrices H and R are the observation and observation noise covariance matrices respectively, given by

$$H_k = H = \begin{bmatrix} 1 & 0 & 0 & 0 \\ 0 & 0 & 0 & 1 \end{bmatrix} \text{ and } R_k = \begin{bmatrix} \sigma_c^2 & 0 \\ 0 & \sigma_T^2 \end{bmatrix}$$

## 7. Implementation of the Filter Algorithm

### 7.6.1 Process-noise decoupling

The<sup>67</sup> has shown that it is necessary that certain elements in the transition matrix  $\Phi$  are not simultaneously zero, if the filter is not to diverge due to partial decoupling of the process noise covariance. Applying this technique to the case when only the carbon state is measured, that is for  $H = (1 \ 0 \ 0 \ 0)$ , it is found that the elements of interest are  $\Phi_{12}, \Phi_{13}, \Phi_{14}$ . If any or all of these elements,  $\Phi_{1j}$  ( $j = 2, 3, 4$ ), are zero then it is seen from the filter equations that, in the case of  $G = I_{4 \times 4}$ , the gain  $K$  is independent of the effects of the autocorrelation  $q_{jj}$ . This is apparent from the following simple analysis.

Let  $t = t_k$ , then

- (i) from eqn. 7.16(b) it follows that only  $(p_{jj})_k^{k-1}$  contains  $(q_{jj})_{k-1}$
- (ii) the gain  $K_k = (k_1, k_2, k_3, k_4)^T = \{(p_{11}, p_{12}, p_{13}, p_{14})\}^T / (p_{11} + r_{11})$ , hence the gain on this pass through the filter is independent of  $(q_{jj})_{k-1}$
- (iii) evaluating eqn. 7.16(e) shows that only element  $(p_{jj})_k^k$  contains  $(q_{jj})_{k-1}$
- (iv) on the next pass through the filter, at  $t = t_{k+1}$ , it is seen from eqn. 7.16(b) that if  $(\Phi_{1j})_k = 0$  then  $(p_{1j})_{k+1}^k$  will not contain  $(q_{jj})_{k-1}$ , and from (i), will not contain  $(q_{jj})_k$ .

is no uncertainty associated with the dynamics of  $x_j$  and the gain  $k_j$  will approach zero thus decoupling the state  $x_j$  from the estimation procedure. The analysis in the present case, where  $G_k \neq I_{4 \times 4}$ , is not so straight forward since now the autocorrelation  $(q_{jj})_k$  affects all the elements in  $P_{k+1}^k$ . It is, however, reasonable to assume that such decoupling will occur since  $\Phi_{12} = 0$  and  $\Phi_{14}$  is 'small' due to the effects of terms in  $1/x^2$  and  $(GQG^T)_{jj}$  contains the dominance of  $q_{jj}$ . This assumption is validated by the results shown in Fig 7.1 from which it may be concluded that the process temperature may not be observable if only the carbon content of the waste gases is measured.

#### 7.6.2 Divergence control

As developed so far, the state-estimation procedure is based on the assumption that the deterministic part of the process model is an accurate representation of the process dynamics and that any uncertainty, due to the parameter estimates and hypotheses on which it is formulated, is accounted for by the Gaussian noise process  $w$ . Unfortunately this is not true, since even a cursory inspection of standard furnace operating practice discloses that a number of significant, and often abrupt, changes in the thermal and chemical behaviour of the process occur. Unless some means of accounting for these changes is included in the estimation procedure the filter will tend to track the erroneous process model and divergence from the true states will result. A variety of methods<sup>68,69</sup> has been suggested for the control of divergence arising from modelling errors. However, all but two of these schemes<sup>70,71</sup> were found to be either too complex or dependent on engineering judgement to be applicable to the present problem. These two schemes

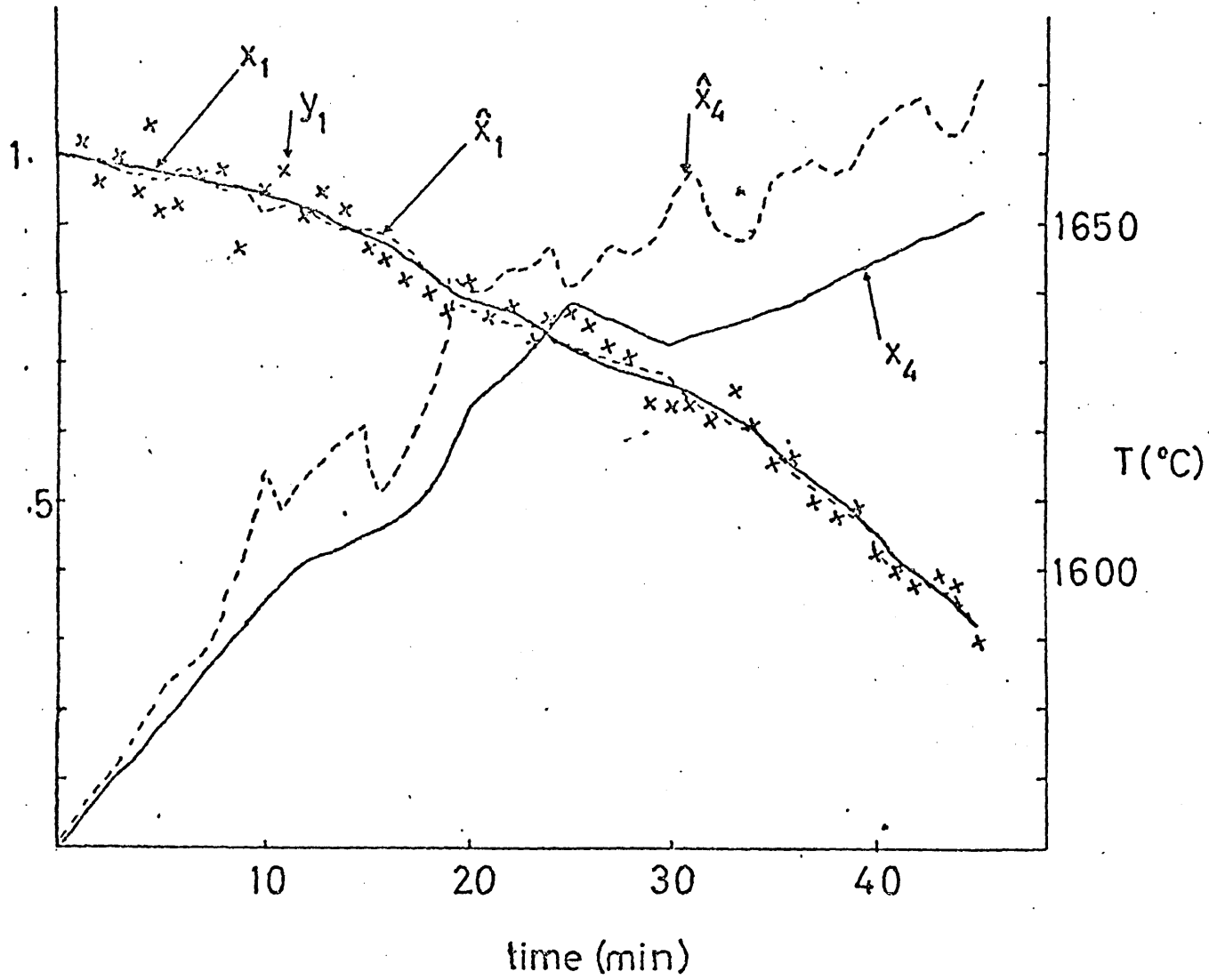


FIG 7.1 Process Noise Decoupling : H = (1 0 0 0)

$x_1$  = Actual %C

$\hat{x}_1$  = Estimated %C

$x_4$  = Actual temperature

$\hat{x}_4$  = Estimated temperature

defined as  $z_k \stackrel{\Delta}{=} y_k - Hx_k^{k-1}$  is a non-stationary Gaussian process with statistics

$$E(z_k) = 0; \quad E(z_k z_j^T) = (HP_k^{k-1} H^T + R_k) \delta_{kj} \quad 7.17$$

A study, see Appendix 5, of the applicability of these schemes to the present problem was conducted and a modified form of one<sup>71</sup> of these is the basis of the implemented scheme.

Following extensive simulations of the performance of the filter under a variety of modelling error levels it was concluded that divergence of the filter response from that of the industrial process, due to unknown changes in the furnace behaviour, could be best detected and controlled by the following algorithm which is initialised at  $t = t_0$  with the operation index  $\lambda = 0$  and the normalised variances

$$\beta_{-1} = \beta_{-2} = \beta_{-3} = 0.$$

- (i) At  $t = t_k$ ,  $E((z_k z_k^T)) = (HP_k^{k-1} H^T + R_k) = \alpha_k$
- (ii) Set  $\beta_k = ((z_k)_k)^2 / \alpha_k$
- (iii) Set  $\zeta_k = (\beta_k + \beta_{k-1} + \beta_{k-2} + \beta_{k-3}) / 4$
- (iv) If  $\lambda = 0$  to to (v)  
           = 1 go to (vi)
- (v) If  $\zeta_k < 1$  go to (vii), otherwise  
       set  $(q_{44})_j = 2.25 ((F_4(x,u))_j)^2$ , for  $j > k$ , and  
        $\lambda = 1$ , go to (vii)
- (vi) If  $\zeta_k > 0.5$  go to (vii), otherwise  
       set  $(q_{44})_j = 0.0625 ((F_4(x,u))_j)^2$ , for  $j > k$ , and  $\lambda = 0$
- (vii) Continue

Briefly, this procedure tests the consistency of the statistics of the smoothed innovation associated with the temperature measurement. The measure  $\zeta_k$  will be less than unity with

Q and R are correct. Divergence is suspected to occur when this measure exceeds unity and control is effected by increasing the uncertainty associated with the thermal dynamics. This increase in  $q_{44}$  is maintained until the measure falls below 0.5 when the variance  $q_{44}$  is restored to its original value.

## 7.7 Results

### 7.7.1 General

A FORTRAN program for implementing the extended Kalman filter was written. The program consists of the following sections as indicated in the flow chart in Fig. 7.2.

- (i) MAINLINE - a preliminary section which sets the number of states and observations, the discrete time interval and the observation interval. This section calls the subroutine EXKAF.
- (ii) EXKAF - a subroutine which has overall control of the filter and the simulation. In this subroutine the filter and the process model are initialised and the process model and filter model are solved using the Euler integration formula. This subroutine calls subroutines AUX and PREDI at each integration step and subroutine UPIAT when an observation is made.
- (iii) PREDI - a subroutine for evaluating the equation
 
$$P_{k+1}^k = \Phi_k P_k^k \Phi_k^T + G_k Q_k G_k^T$$
- (iv) AUX - a subroutine for evaluating the state equations and the elements of the Jacobian and noise matrices.

$K_{k+1}$ , and estimating the states  $x_{k+1}^{k+1}$ , and the covariance matrix,  $P_{k+1}^{k+1}$ . This subroutine also contains the divergence control algorithm.

- (v) OUTP - a subroutine called by EXKAF at 1 min intervals to output the states, the estimated states and the observations. At 5 min intervals the covariance and gain matrices are also printed.

This program implements the filter as described by equations 7.16. The equation for updating the covariance matrix, eqn. 7.16(e) is used in preference to the simpler equivalent expression

$$P_{k+1}^{k+1} = (I - K_{k+1} H_{k+1}) P_{k+1}^k \quad 7.16(f)$$

for the following reasons :

- (a) The right-hand side of 7.16(e) is the sum of two symmetric, positive definite matrices, and, when these are added, the sum will be positive definite. On the other hand, eqn. 7.16(f) is, at best, the difference of two positive definite matrices. As a consequence, eqn. 7.16(e), is better conditioned for numerical computations, and will tend to retain more faithfully the positive definiteness and symmetry of  $P_{k+1}^{k+1}$ .
- (b) If a small error  $\delta K_{k+1}$  is made in the computation of the filter gain  $K_{k+1}$ , then, to first order, eqn. 7.16(f) gives

$$\delta P_{k+1}^{k+1} = -\delta K_{k+1} H_{k+1} P_{k+1}^k$$

whereas eqn. 7.16(e), to first order, gives

$$\delta P_{k+1}^{k+1} = 0$$

Thus, to first order, eqn. 7.16(e) is insensitive to errors in the filter gain and is to be preferred in numerical computations.

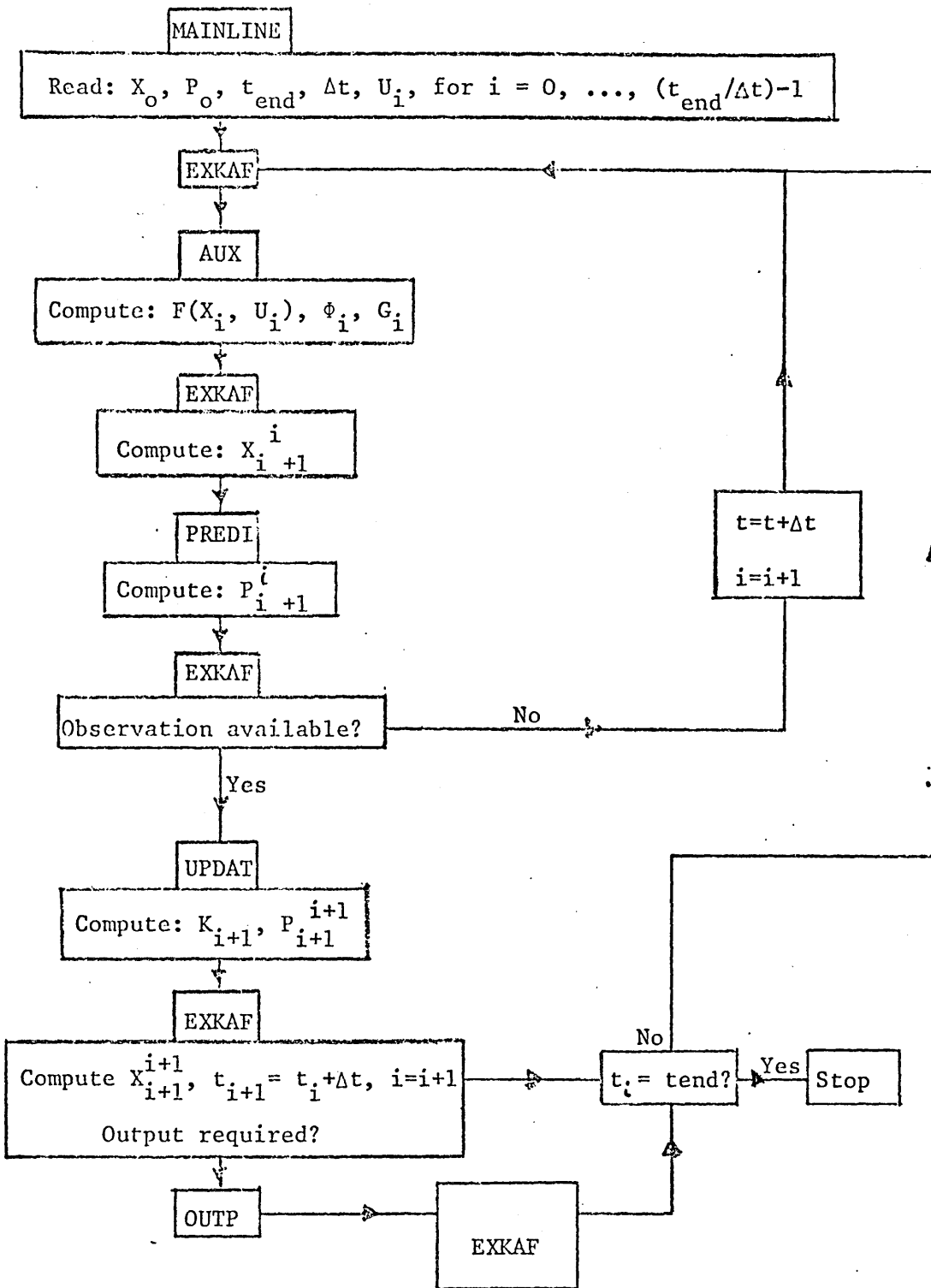


FIG 7.2 Flow Chart of Kalman Filter Program

The filter was initialised with the following values which are typical of normal operating practice.

$$x_0^0 = (0.233, 0.0546, 1.63, 1833)$$

$$P_0^0 = \text{diag} (0.0017, 0.83 \times 10^{-4}, 0.175, 6.25)$$

The initial process states,  $x(o)$  were obtained by perturbing the filter state vector,  $x_0^0$ , using a Gaussian random number generator to give for  $i = 1, \dots, 4$

$$E(x_i(o)) = (x_0^0)_i, \quad E((x_i(o) - (x_0^0)_i)^2) = (P_0^0)_{ii}$$

where  $E(\cdot)$  is the expectation operator. As determined in section 7.2.1,  $E(x_3(o)) = \xi_4$  and typically  $x(o) = (0.78675, 0.07107, 2.09, 1832)$ .

The effect of non-modelled perturbations to the process were introduced by assuming that, unknown to the filter, the process undergoes two abrupt changes in temperature of  $-10^\circ\text{C}$  at  $t = 10$  min and  $t = 25$  min. The rate of heat loss,  $a_6$ , was assumed to double over the interval  $33 \text{ min} < t < 43 \text{ min}$ .

The process was forced by the following oxygen injection,  $u_1(t)$ , and power input,  $u_2(t)$ , strategies which are typical of normal operating practice.

$$\begin{aligned} u_1(t) &= 0 && 0 \leq t \leq 13 \text{ min} \\ &= 4.3 \times 10^{-4} \text{ kmol/tonne.s} && 13 \text{ min} \leq t < 20 \text{ min} \\ &= 0 && 20 \text{ min} \leq t < 23 \text{ min} \\ &= 4.3 \times 10^{-4} \text{ kmol/tonne.s} && 23 \text{ min} \leq t < 25 \text{ min} \\ &= 0 && 25 \text{ min} \leq t < 30 \text{ min} \\ &= 4.3 \times 10^{-4} \text{ kmol/tonne.s} && 30 \text{ min} \leq t < 47 \text{ min} \\ u_2(t) &= 22 \text{ MW} && 0 \leq t < 13 \text{ min} \\ &= 0 && 13 \text{ min} \leq t < 18 \text{ min} \\ &= 17 \text{ MW} && 18 \text{ min} \leq t < 25 \text{ min} \end{aligned}$$

Subject to these initial conditions, process perturbations and control strategies the performance of the filter under varied conditions of uncertainty was examined. The range of these studies is covered by the following simulations.

Run 1: The process and filter models are identical, i.e. the parameter set  $a_i (i = 1, \dots, 9)$  of the process model have the same values as the parameter set  $a_i^* (i = 1, \dots, 9)$  of the filter model. The observation interval and the discrete time interval are equal with  $\Delta t = 10$  sec and the variance of the observation noise on the measurement of  $x_1(t)$  is given by, see eqn. 7.13

$$E(v^2(t_i)) = \{((x_1(t_{i-1})\delta_1 - x_1(t_i)\delta_2)/x_1(t_i) + \delta W)x_1(t_i) / 300\}^2 \quad 7.18(a)$$

The divergence control algorithm is not employed during this simulation.

Run 2: The process model differs from the filter model by perturbing the parameter set,  $a_i (i = 1, \dots, 9)$  using a Gaussian random number generator to give

$$E(a_i^*) = a_i, \quad E((a_i^* - a_i)^2) = 0.25 a_i^2$$

All other operating conditions for this simulation are the same as those given for Run 1.

Run 3: The variance of  $v_1(t)$  evaluated using eqn. 7.18(a) is not the actual variance of the noise that occurs in practice on the measurement,  $y_1$ . The actual variance at  $t = t_i$  is given by, see eqn. 7.13

$$E(v_1^2(t_i)) = \{((x_1(t_k)\delta_1 - x_1(t_i)\delta_2)/x_1(t_i) + \delta W)x_1(t_i) / 300\}^2 \quad 7.18(b)$$

where  $t_k$ , the time at which the last chemical analysis of the molten steel was obtained, satisfies  $t_k \leq t_i$ . During this and subsequent simulations  $k = 0$ ; that is, only the meltout

analysis is assumed to be available. In addition to the process disturbances considered in the previous simulations here the effects of a 1 min computation interval are introduced. Hence the filter output is  $x_k^j$  with  $t_k - t_j = 1$  min. This one minute lag is a conservative estimate of the time required to process the measurement from the waste gases and also allows for the transportation delay between the furnace and the gas take-off flue. It also takes into account the thermal lag associated with the embedded thermcouple measurements.

Run 4: This simulation has the same operating conditions as Run 3 but here the divergence control algorithm is employed.

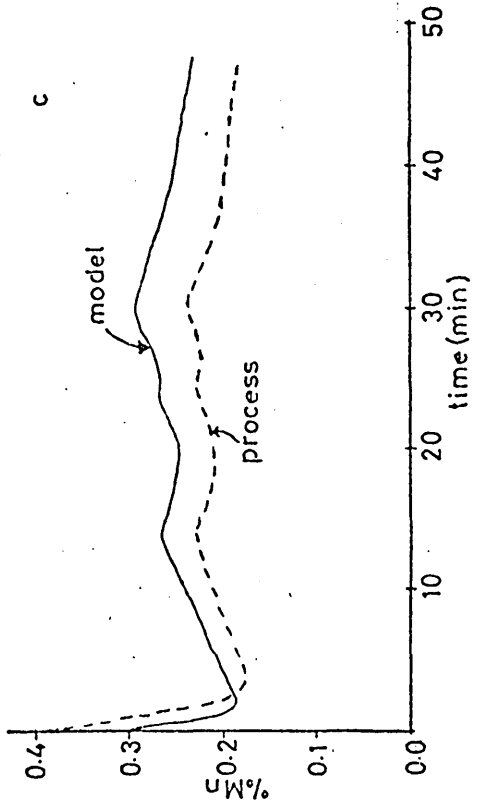
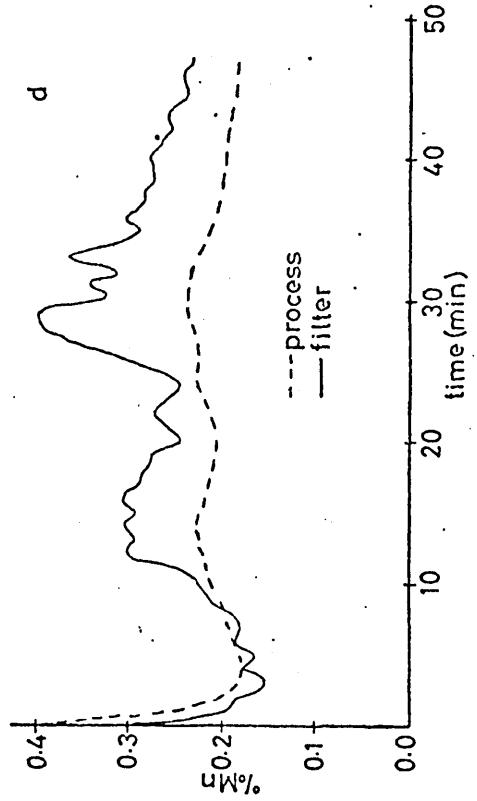
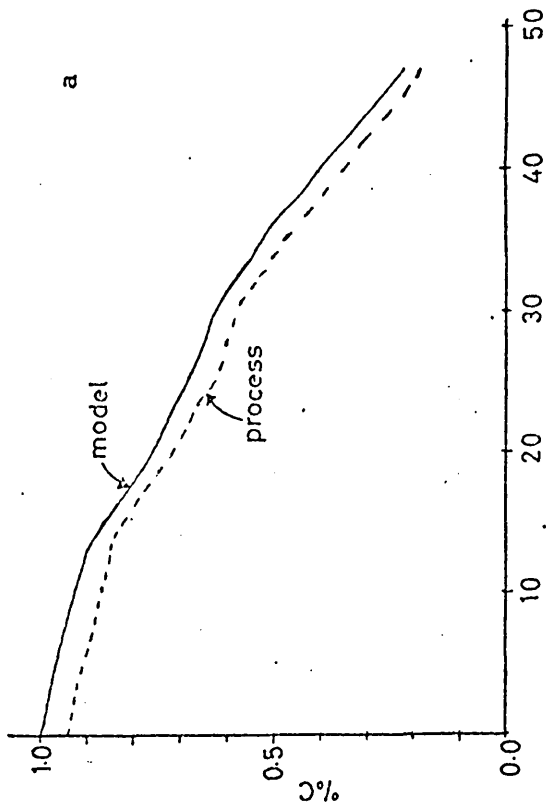
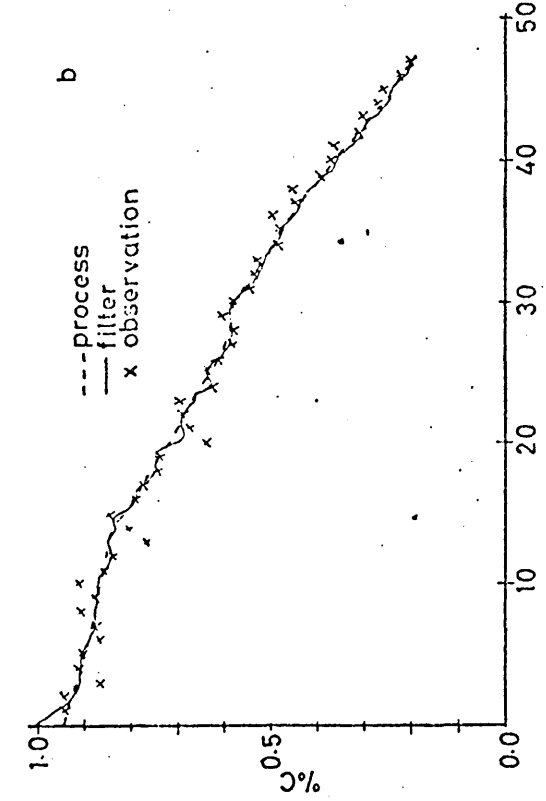
### 7.7.3 Discussion

The results of the simulations described in the previous section are presented in Figs. 7.3 to 7.6. The responses of the states shown in these figures are indicated as Model, Process or Filter. Those responses indicated as Model are the results obtained from the model employed in the filter. Those indicated as Process are the results of the process model and those indicated as Filter are the state trajectories as estimated by the filter.

The results of the simulation, Run 1, are presented in Fig. 7.3(a)-(h). The responses in Fig. 7.3(a), (c), (e) and (g) show that the carbon and iron oxide dynamics are not significantly effected by the perturbed initial conditions and that for  $i = 1$  and 3

$$x_i(t)_{\text{model}} - x_i(t)_{\text{process}} \dot{=} x_i(0)_{\text{model}} - x_i(0)_{\text{process}}$$

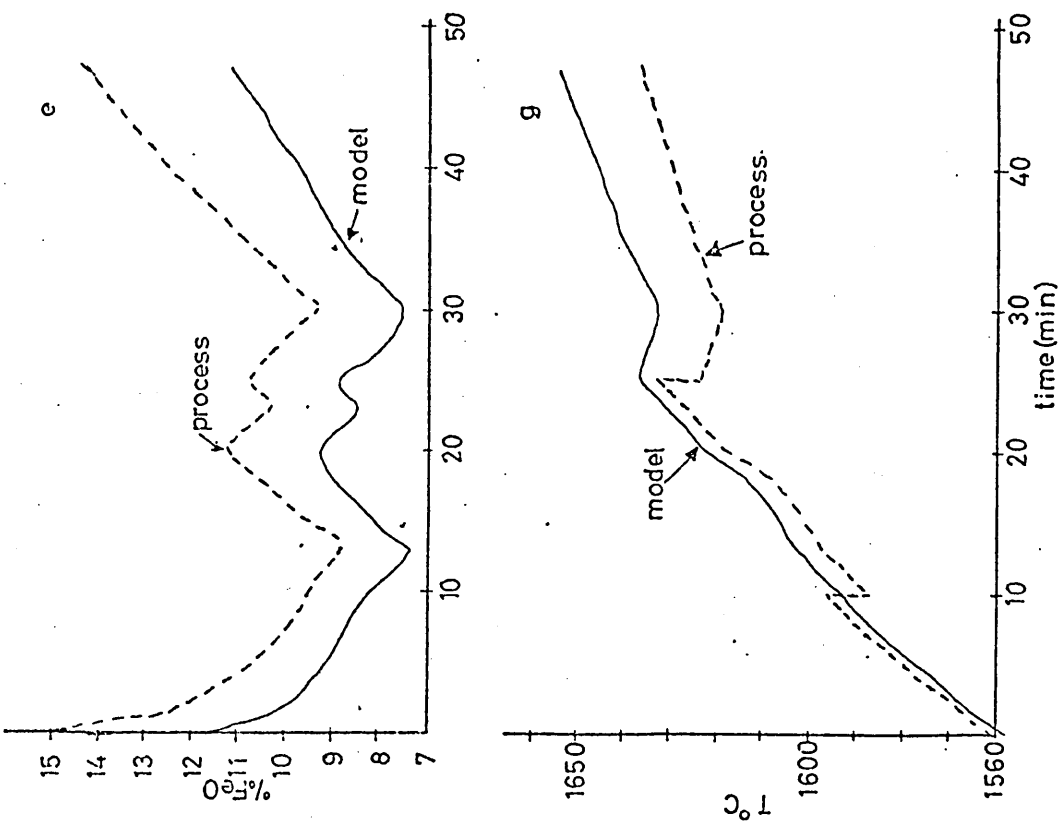
This perturbation of the initial conditions is, however, seen to effect significantly the manganese dynamics but the effect on the thermal dynamics is not clear due to the influence of the abrupt changes in the process response.



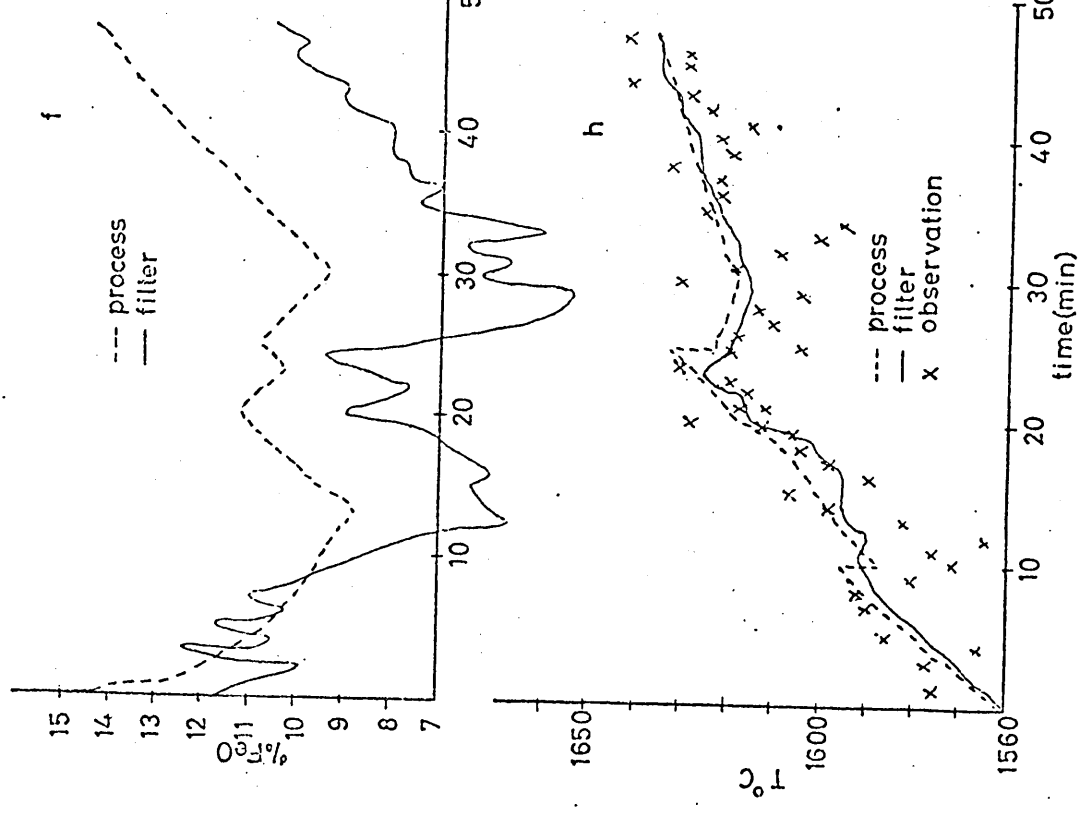
a, c The process and filter model responses

b, d The process and filter responses

FIG 7.3 Results of Simulation Run 1



e,g The process and filter model responses



f,h The process and filter responses

FIG 7.3 Results of Simulation Run 1

simulation explains the rapid alignment of the filter with the process as shown in Fig. 7.3(b). This low level of measurement noise gives rise to significantly large values of gain for elements  $k_{21}$  and  $k_{31}$ ; that is the emphasis within the filter tends towards tracking the observations and the apparent randomness of the filter estimates of states  $x_2$  and  $x_3$  as shown in Fig. 7.3(d) and (f) demonstrates the influence of the innovations process  $z_1(t_i)$ . The effects of the abrupt changes in process temperature and the doubling of the rate of heat loss are shown in Fig. 7.3(g) and it is apparent from the responses shown in Fig. 7.3(h) that the filter can operate effectively even in the presence of these discontinuities.

The variances of the estimates at  $t = 47$  min are

$$\text{diag. } P_{47}^{47} = (0.95 \cdot 10^{-5}, 0.76 \cdot 10^{-5}, 0.02, 9.)$$

In terms of weight percentages and  $^{\circ}\text{C}$  these correspond to the following standard deviations

$$\sigma_C = 0.005\%, \quad \sigma_{\text{Mn}} = 0.02\%, \quad \sigma_{\text{FeO}} = 1.0\%, \quad \sigma_T = 3^{\circ}\text{C}$$

Hence, subject to the simulation conditions of Run 1 the filter can accurately track the carbon and temperature trajectories.

The results for the manganese and iron-oxide trajectories demonstrate the 'weak' observability of these states, a feature which becomes more apparent in the subsequent simulations.

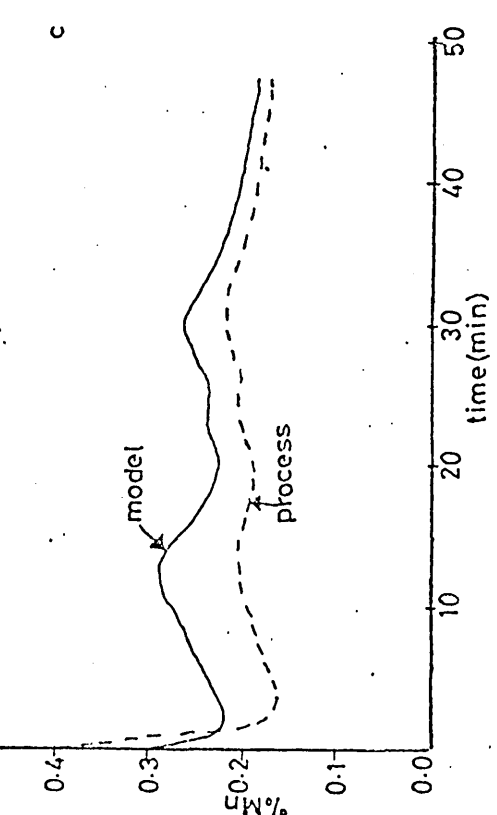
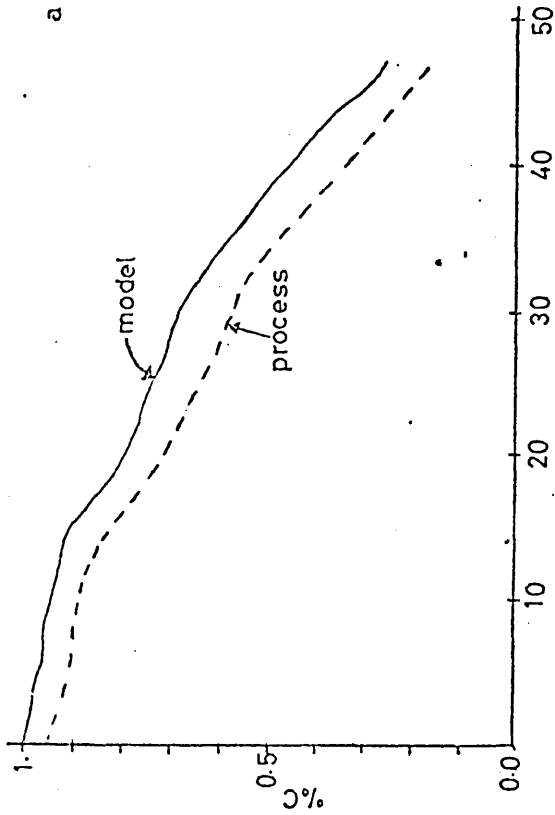
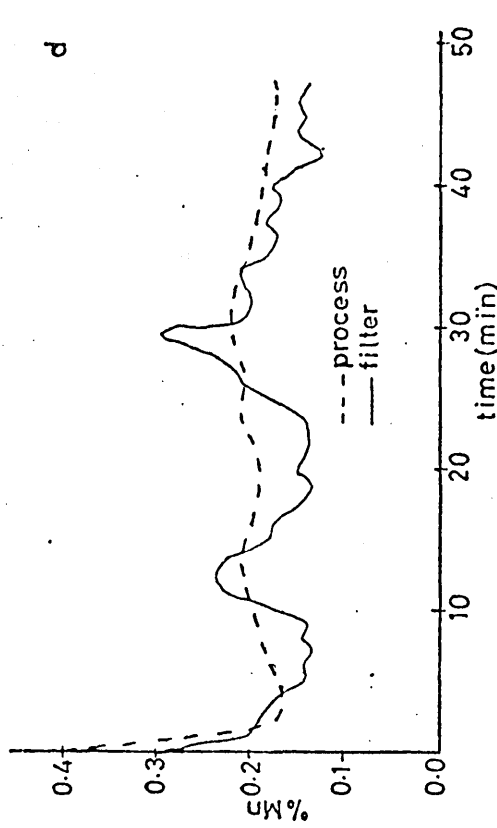
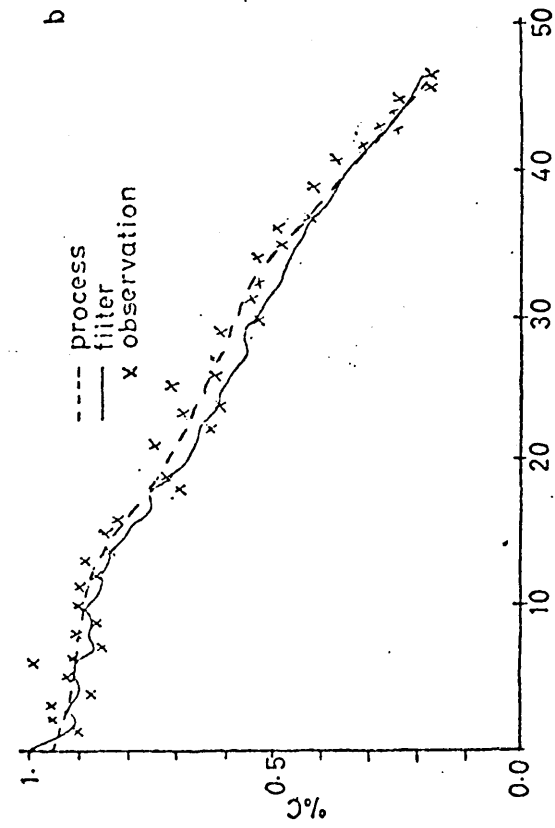
The use of identical process and filter models in Run 1 makes the results of that simulation have little practical significance.

As a first approach towards considering the level of uncertainty associated with the actual process the random parameters,  $a^*$ , were employed in the filter model. The variance of the measurement noise on  $y_1$  is again given by eqn. 7.18(a).

Simulation studies were conducted under the conditions

in Fig. 7.4 (a) - (h). Comparison of the responses in Figs. 7.3 and 7.4 (a), (c), (e) and (g) shows the increased divergence between the plant and filter models that results from introduction of the random parameters. It is apparent from the responses shown in Figs. 7.4(b), (d), (f) and (g) that although there is some degradation in the ability of the filter to track the state  $x_3$ , the introduction of the random parameters does not have a significant effect on the accuracy of the estimation of the other states. It is, however, important to remember that in both Run 1 and Run 2 the variance of the uncertainty on  $y_1$  is given by eqn. 7.18(a). This variance was found to be almost constant with  $E(v_1^2(t_i)) \approx 6.25 \times 10^{-4}$ , that is, the standard deviation on the carbon measurement is of the order of 0.03%, an accuracy that is attainable using a direct measurement technique for determining the carbon content. Hence, although the results of the simulation Run 2 are not representative of a practical waste gas analysis system, the results do demonstrate the sort of performance that could be obtained from the filter if the engineering problems, at present preventing the use of an in-furnace measurement device, were overcome.

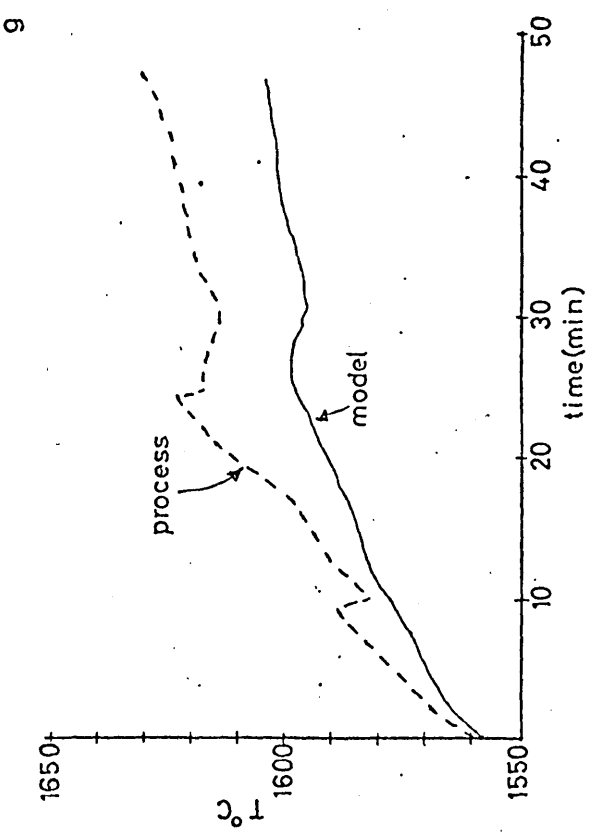
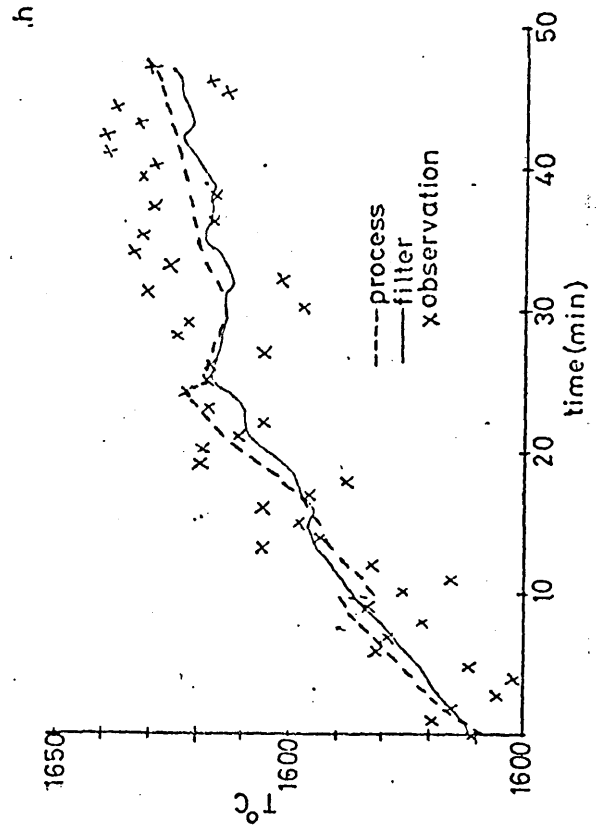
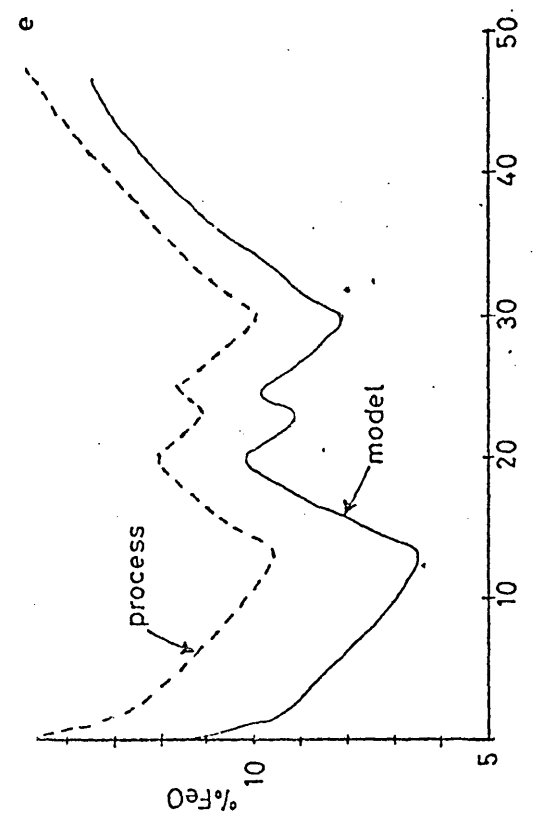
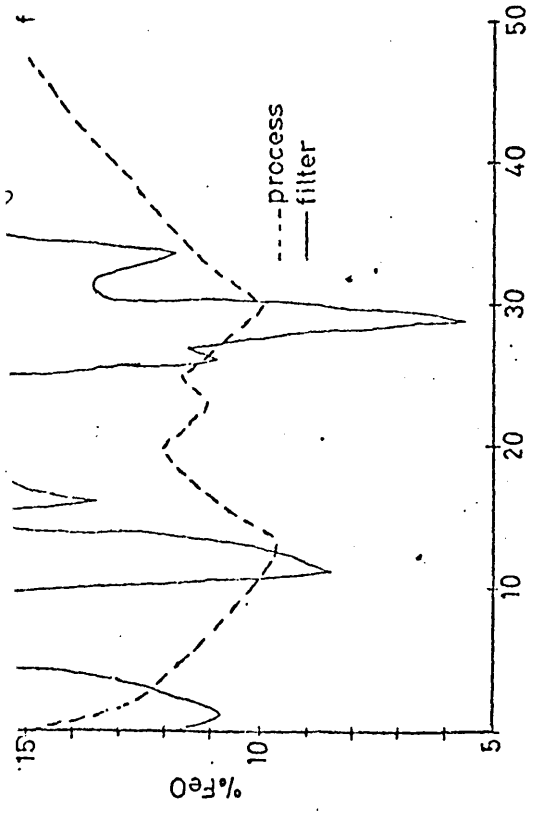
In 7.4 the variance of the uncertainty on the carbon measurement was shown to be dependent on the time elapsed since the last chemical analysis of the molten steel was obtained. If it is assumed that only the melt-out analysis is available then, from eqn. 7.18(b) it is apparent that the variance is a non-decreasing function of time since  $x_1(t_i) \leq x_1(t_k)$  for all  $t_i \geq t_k$ . Simulation studies were conducted under the conditions described in Runs 3 and 4. The process and filter models responses for these simulations are the same as those obtained from Run 2. and shown in Figs. 7.4(a), (c), (e) and (g).



b,d The process and filter responses

a,c The process and filter model responses

FIG 7.4 Results of Simulation Run 2



e,g The process and filter model responses

f,h The process and filter responses

FIG 7.4 Results of Simulation Run 2

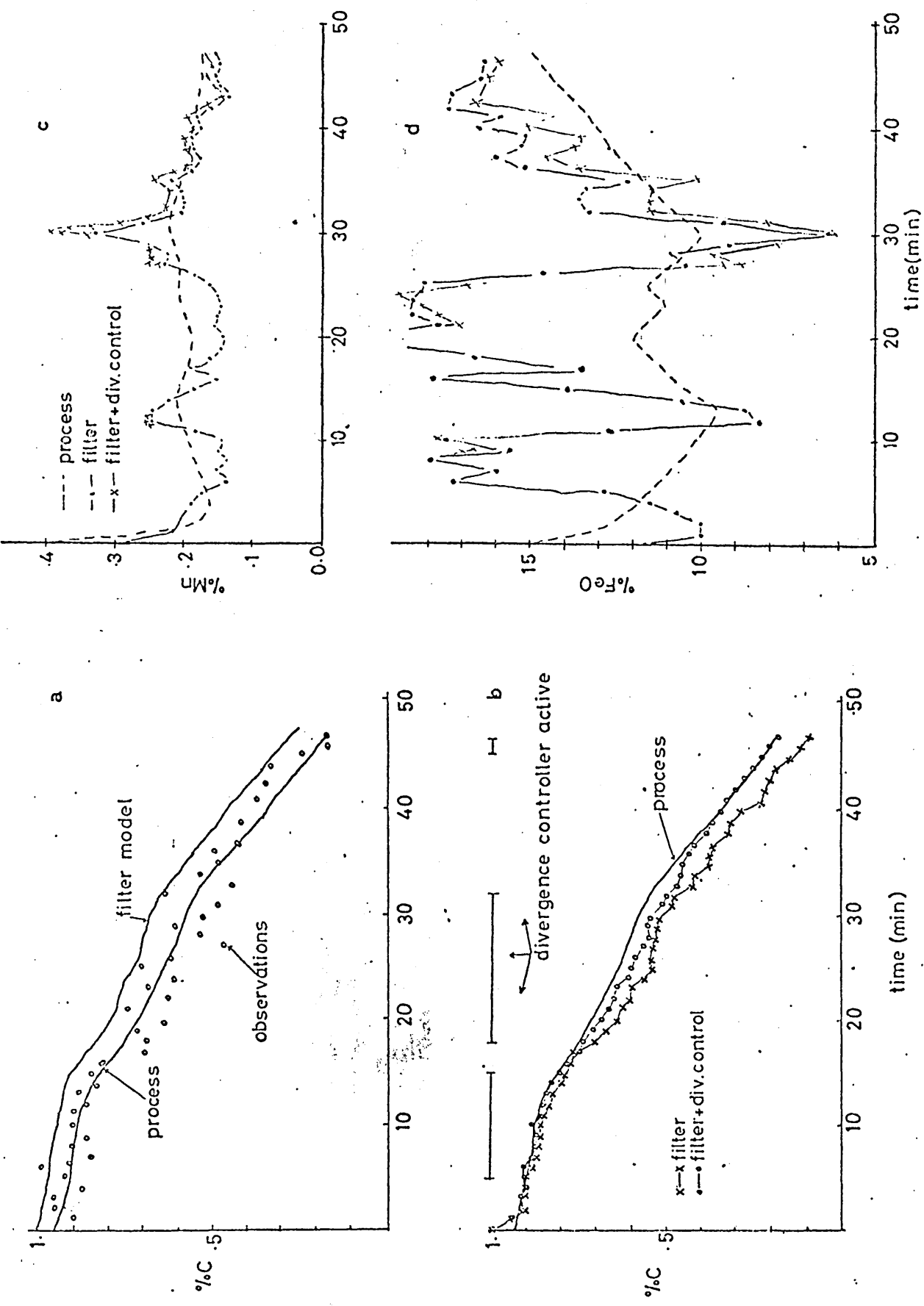
with 7.3(a) reveals the effect of the increasing variance of  $v_1(t_i)$ . The trajectories of the estimated state-variables as calculated with and without the divergence-control algorithm are shown in Figs. 7.5(b)-(f). The periods during which the control algorithm was active are shown in Fig. 7.5(b). The effect of the divergence controller on the filter gain matrix and on the variances of the state estimates is shown in Figs. 7.6(a)-(h) and Figs. 7.7(a)-(d). It is apparent from these results that the controller has a significantly greater influence on the gains  $k_{i1}$  ( $i = 1, \dots, 4$ ) than on the gains  $k_{i2}$  ( $i = 1, \dots, 4$ ). This is especially the case for the gains  $k_{11}$ ,  $k_{21}$  with  $k_{11}^D = 2k_{11}$  and  $k_{21}^D = 2k_{21}$ , where  $k_{ij}^D$  is the value of the gain in the 'controlled filter' during a period when the controller is active. The apparent anomaly that the controller, by increasing the magnitude of element  $q_{44}$  in the process noise covariance matrix, exerts greater influence on the gains associated with the carbon measurement,  $y_1$ , than on the gains associated with the temperature measurement,  $y_2$ , may be explained by the following analysis of the conditional variances  $p_{k+1}^k$  and measurement noise variances  $r_{11}$  and  $r_{22}$ .

At  $t_k = 25$ , (the superscript D denotes values from the 'controlled filter').

$$\begin{aligned}
 p_{25}^{24}{}_{11} &= 0.24 \times 10^{-3}; & p_{25}^{24}{}_{11}^D &= 0.3 \times 10^{-2} \\
 p_{25}^{24}{}_{44} &= 6; & p_{25}^{24}{}_{44}^D &= 10
 \end{aligned}$$

For both filters the measurement noise variances are

$r_{11} = 0.25 \times 10^{-2}$  and  $r_{22} = 100$ . Now if the sequential filter was employed and the carbon measurement was processed first then the gain vector  $k = (k_1, k_2, k_3, k_4)$  would have values



a, The process and filter model responses  
 b,c,d, The process and filter responses with and without divergence control

FIG 7.5 Results of Simulation Run 3 and 4

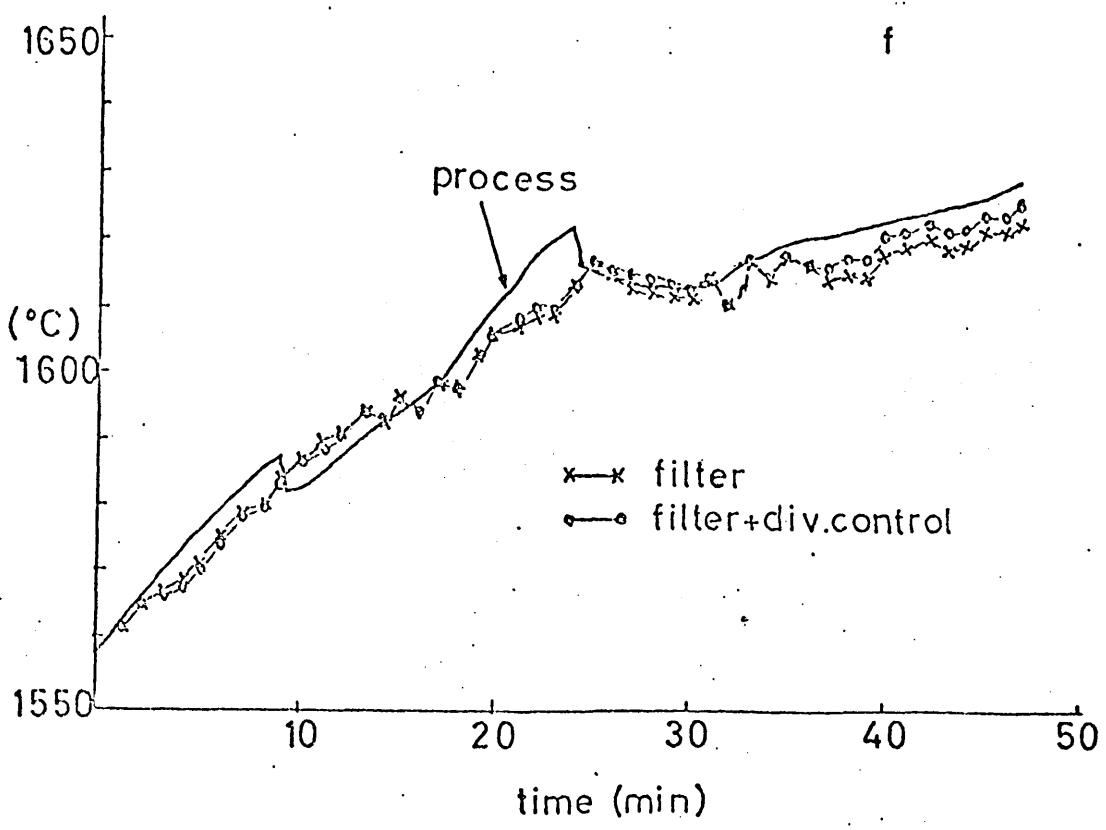
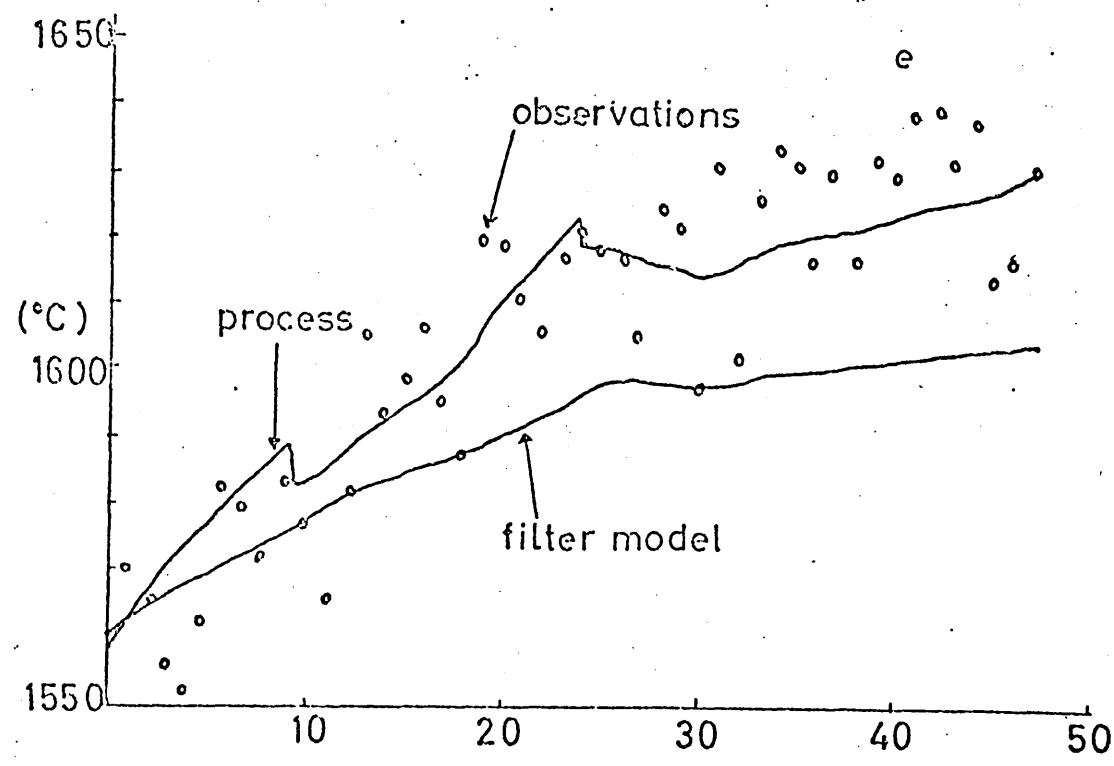


FIG 7.5 Results of Simulation Runs 3 and 4

- e The process and filter model responses
- f The process and filter responses with and without divergence control

For  $i = 1$

$$\begin{aligned}k_1 &= 0.24 \times 10^{-3} / 2.74 \times 10^{-3} \\ &= 0.087\end{aligned}$$

With divergence control

$$\begin{aligned}k_1^D &= 0.3 \times 10^{-2} / 0.55 \times 10^{-2} \\ &= 0.55\end{aligned}$$

These values of gain are approximately equal to the actual values for  $k_{11}$ , as shown in Fig. 7.6(a). Alternatively if the temperature measurement was processed first similar calculations give  $k_4 = 0.06$  and  $k_4^D = 0.1$ . The actual variation in the gain for the temperature measurement,  $k_{42}$ , see Fig. 7.6(h), is even less than obtained by this approximation. Thus what appears to be happening, while the divergence controller is in operation, is that both conditional variances,  $(p_{k+1}^k)_{11}$  and  $(p_{k+1}^k)_{44}$  are increased but due to the fact that the variance  $r_{22}$  is large in comparison to  $(p_{k+1}^k)_{44}$  only a small variation in the gain  $k_{42}$  is obtained. This analysis may be extended to explain the variation in the elements  $k_{ij}$  ( $i = 2, 3$ ) and  $k_{i2}$  ( $i = 2, 3$ ) when the divergence control algorithm is employed.

The importance of the relative magnitudes of the conditional and measurement noise variances in determining the filter gains may be seen from the results shown in Fig. 7.6(a)-(d). It is apparent from these that in the absence of the control algorithm that the gains  $k_{ij}$  ( $i = 1, \dots, 4$ ) decrease with increasing time due to the continuous growth of the variance of  $v_1(t_k)$ . The increase in gain which the controller introduces over the interval  $20 \leq t \leq 30$  of the refining period has the noticeable effect of correcting the tendency of the estimate of  $x_1$  to diverge from the process trajectory. This may be seen in the responses

Figs. 7.5(c) and (d) that even with the use of the control algorithm no significant improvement in the estimates of the states  $x_2$  and  $x_3$  can be obtained. The close alignment of the trajectories of the estimated temperature,  $x_4$ , see Fig. 7.5(e), obtained with and without the divergence controller may be explained by the approximate equality of the gains  $k_{42}$  and  $k_{42}^D$ .

The results shown in Fig. 7.7(a)-(d) demonstrate that the increase in the variances  $p_{ii}$  ( $i = 1, \dots, 4$ ), which occurs over the intervals of divergence control action, does not have a long term effect. That is, the perturbation introduced by the divergence controller decays quickly when the control action is removed. It is therefore reasonable to conclude that the filter is not particularly sensitive to the choice of the initial covariance  $p_0^0$ . That is, the prior data contains little information compared with the observations. Without divergence control the approximate final variances at  $t_k = 47$  are

$$\begin{aligned} \sigma_i^2 (i = 1, \dots, 4) &= (0.58 \times 10^{-3}, 0.9 \times 10^{-5}, 0.16, 6.55) \\ &= \text{diag. } p_{47}^{47} \end{aligned}$$

with divergence control

$$\begin{aligned} \sigma_i^2 (i = 1, \dots, 4) &= (0.65 \times 10^{-3}, 0.2 \times 10^{-4}, 0.25, 8.4) \\ &= \text{diag. } p_{47}^{47} \end{aligned}$$

In terms of weight percentages this means that with divergence control the final carbon and manganese estimates have standard deviations of 0.03 and 0.02 respectively. This implies that the estimation procedure can give results which have a better than 80% probability of satisfying the industrial accuracy requirement.

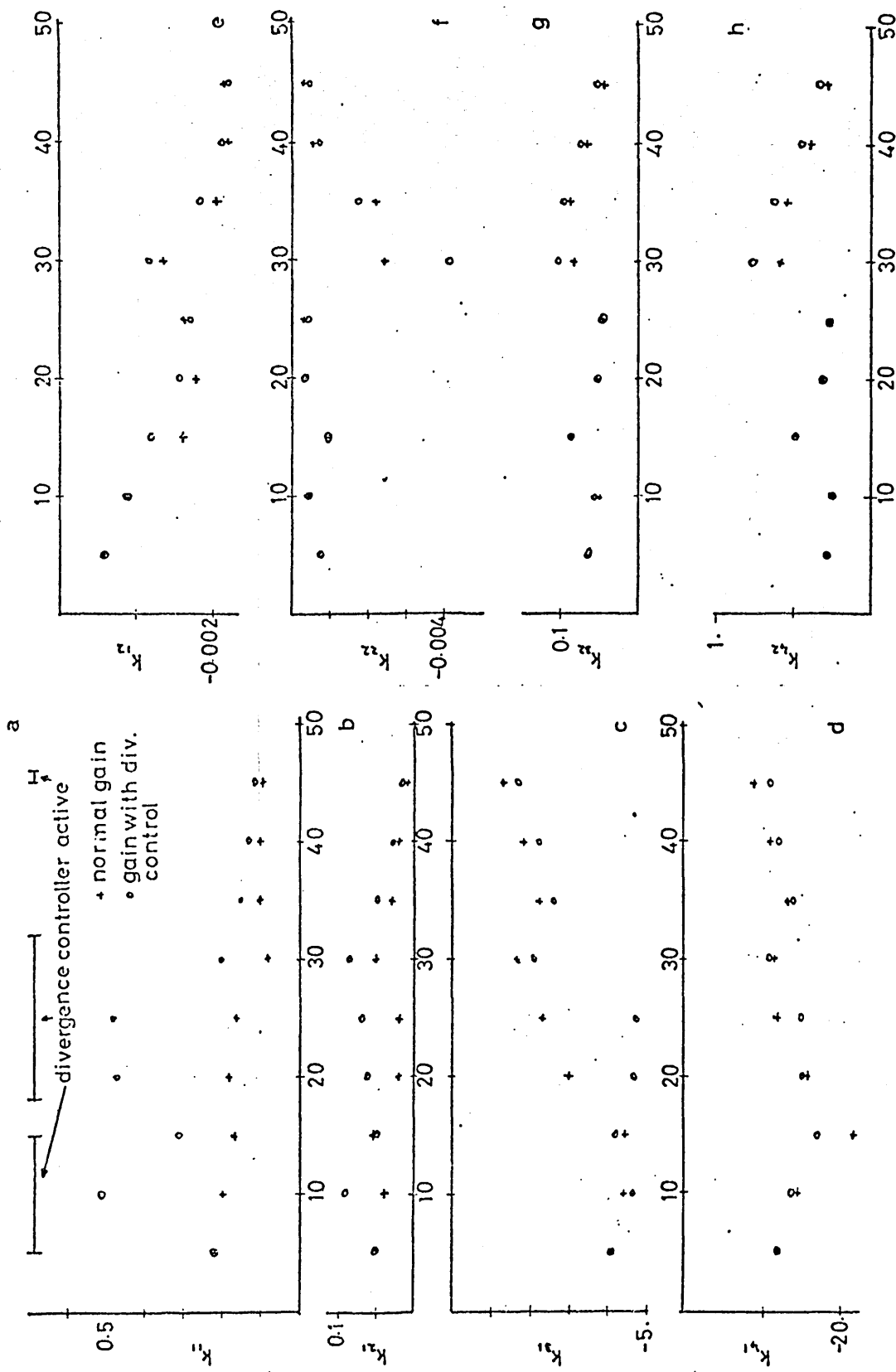


FIG 7.6 Effect of Divergence Controller on Kalman Gain

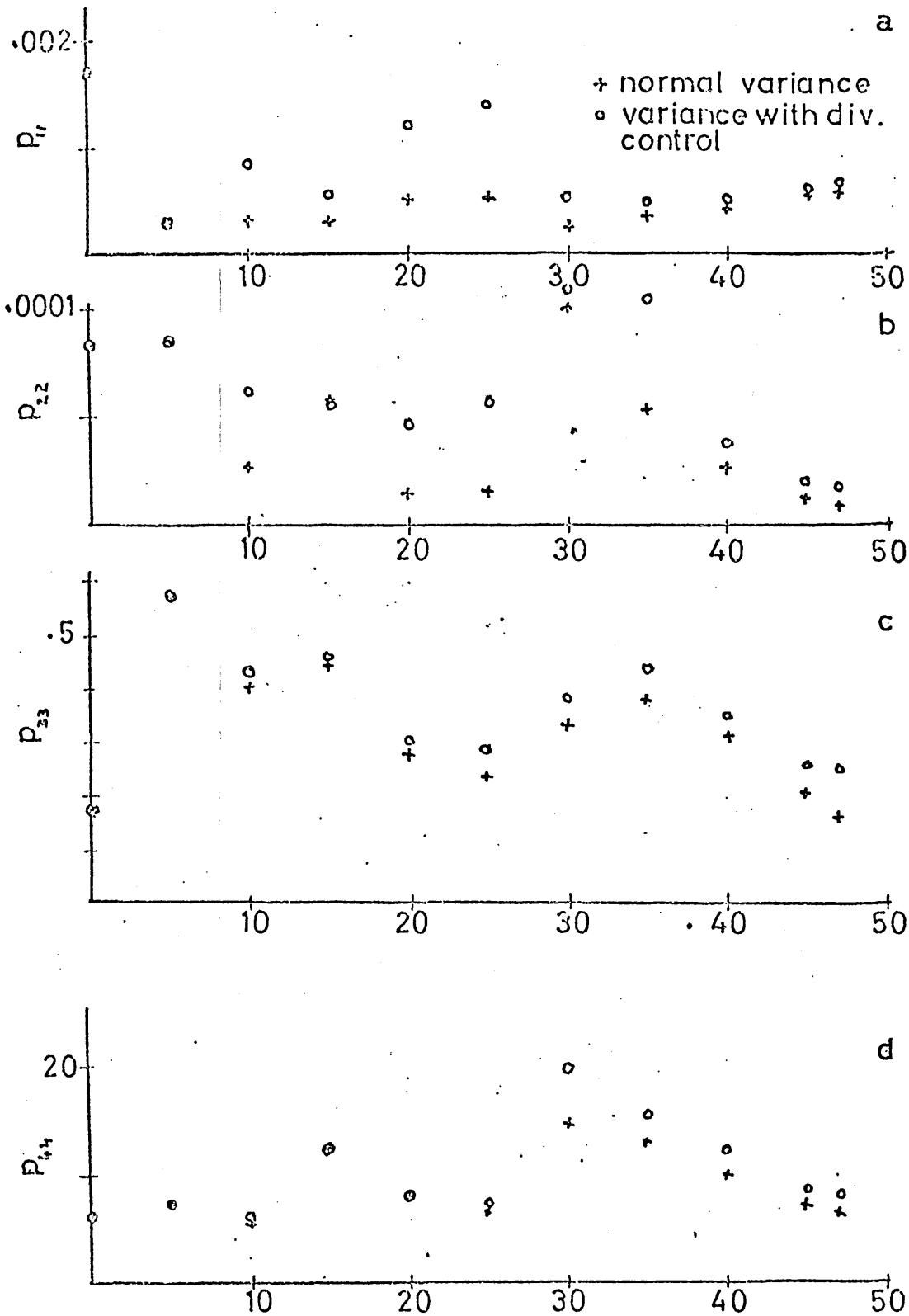


FIG 7.7 Effect of Divergence Controller on Variances of State Estimates

In view of the limited accuracy of the detailed mathematical model of process, as developed in the previous chapters, the need for a compromise between complexity and implied certainty of the model has been discussed. Subsequent to the reduction in the dimension of the process state vector, effected by treating some of the process states as random variables with statistics known a priori from the process data, the extended Kalman filter has been presented as an efficient method of combining the a priori information about the process in the form of a dynamical model with incomplete error-corrupted measurements. The implementation of the extended Kalman filter for on-line state estimation has been considered and the operation of the filter under varied conditions of uncertainty has been discussed. A technique for controlling divergence of the filter has been presented and the results of simulations indicate that estimates of the states can be obtained to the accuracy required for the design of a refining control strategy.

A number of alternative techniques for controlling divergence of the filter algorithm are presented in Appendix 5. Simulations were made under the conditions described in Run 3 to investigate the feasibility of employing these alternative techniques. These simulations failed due to effects of the large increases in the filter gain which these techniques introduced. In particular, it was found that freezing the gain and allowing the covariance matrix  $P$  to increase, as is recommended in method a<sup>70</sup>, resulted in an estimate of the state  $x_2$  which was negative and caused the simulation to be terminated due to overflow errors. Attempts to increase the complete process noise covariance matrix  $Q$  when divergence was suspected, as in recommended in method b<sup>71</sup> and method c<sup>78</sup>, had a similar effect on the gain matrix and a number of unsuccessful attempts were made to tune the controller. The technique for controlling divergence that has been employed successfully in this

study is a modified form of the methods a and b and its success may be attributed to the use that has been made of the available knowledge of the source of the divergence. In particular, in the present application of the filter it is known that the estimate of the states may diverge due to  $\frac{h_0}{h}$  effect of unknown but significant changes in the process temperature. Hence the divergence control algorithm has been based on a test of the statistical consistency of the innovation associated with the temperature measurement and action of the controller is limited to increasing the variance of the uncertainty associated with the thermal dynamics.

CONCLUSIONS

The motivation for obtaining improved control of the batch production of steel in the electric arc furnace has been highlighted. A survey of the literature has exposed that, to date, progress made towards obtaining computer control of the steelmaking process has been confined primarily to the problems of scrap selection for the initial charge and power allocation between furnaces. A study of conventional furnace operating practice has demonstrated the complexity of the process and the considerable skill required from the operator for its control. Justified by the common chemical principles and similarity in engineering environment of all steel-making processes a review of modelling of the Basic Oxygen Process has been presented. In this review both analytical and statistical techniques for model development have been considered. The former technique has been found to give non-linear models of large dimension which are unlikely to be practical for on-line applications. The latter technique, however, has been found to encounter difficulties due to the poor accuracy of the available furnace instrumentation.

The objectives of the present investigation have been shown to dictate that the analytical modelling technique be employed to develop a model of the steelmaking process in the electric arc furnace. Based on a study of the metallurgical theory of the steelmaking process and the range of variation of the constituent chemical species a set of chemical reactions describing the process has been determined. The evaluation of the equilibrium state for the chemical system has been shown to require the solution of a constrained non-linear programming problem. Although techniques for solving such problems are available the shortcomings in both the range and the accuracy of the necessary thermo-chemical data have been shown to make this approach unpractical.

A study of the sequence of steps contributory to the bulk reaction rates has been conducted and the rates of the major reactions have been shown to be determined by the effects of mass transport. A lumped parameter representation of Fick's first diffusion law has been employed to describe mathematically these mass transport effects. This approach has been based on the accepted assumption that the driving forces for diffusion may be approximated by the differences between the average chemical potentials in the various phases. The rates of mass transfer have been given as the product of these driving forces and system conductances. These conductances have been shown to be functions of a number of the process states and that an exact formulation of the rates of reaction gives a set of highly non-linear differential equations.

Subsequent to this study of the metallurgical theory of the process a set of system variables, necessary to describe the process, has been determined. The structure of a set of equations describing the dynamics of these variables has been developed. This development has made use of the results of the many recent studies on the chemistry of steelmaking. That the structure of some of the equations is determined wholly by regression techniques has been shown to be an inevitable consequence of the fact that much of the information on the process, available from the literature, is presented in graphical form. The validity of these statistically derived components of the model has been assessed by comparison with the results from independent studies.

To determine the accuracy with which this model described the dynamics of the major process phenomena, simulation studies have been conducted. Initial conditions for the process states and control strategies typical of the industrial process have been employed in these studies. The results obtained have demonstrated good agreement between the simulated and observed behaviour of the carbon, iron oxide and temperature state

trajectories. In the absence of adequate plant data little could be concluded about the accuracy with which the model simulated the dynamics of the manganese oxidation reaction. The oxygen efficiency of the process, as predicted by the model, has been compared with published data. The results obtained from the model have been shown to be in close proximity to these data indicating the validity of the structure of the model. A comparison of the total decarburization time as estimated by the model with that observed in practice exposes a discrepancy which has been assumed to be due to the losses inherent in the normal practice of stopping and starting the process. It has been concluded from these simulation studies that the techniques employed to develop the model have proved successful but that a significant amount of plant data would be required to facilitate the tuning of the model necessary to make it suitable for use in a practical control system.

A further study of plant operating practice has been reported and the difficulties encountered when monitoring the process for the collection of data have been described. The variety of modes of furnace operation have been considered and the collected data have been employed to extend the model to include the effects of the power input from the electrodes. However, because of the large and often abrupt perturbations in the trajectories of the process states that can result from either additions made to the furnace or de-slugging, only the simple operating modes have been considered. A proposal to employ a numerical technique for parameter estimation has been rejected because of the difficulties attendant to obtaining sufficient process data for statistically meaningful studies to be conducted. Instead minor manual adjustments made to a number of parameters when simulating the monitored casts have been shown to be sufficient to ensure that the model is accurate for a limited class of operating practice.

The inherent complexity of the mathematical model, evolved from theoretical considerations, has been examined. A reduction in the dimension of the model state vector has been effected by the introduction of stochastic parameters to account for the non-measurable states associated with the slag phase and the hypotheses on which the model has been developed. Techniques recently developed for obtaining noise corrupted measurements of the carbon content and temperature of the process have been investigated and the statistics of the uncertainty on these measurements has been determined. The implementation of the extended Kalman filter for on-line state estimation has been considered. Divergence of the estimation procedure has been shown to result from partial noise decoupling, when only the carbon state was measured. A simple scheme for ensuring that the filter does not diverge, due to modelling errors, has been incorporated in the filter and the performance of the state estimation procedure under varied conditions of uncertainty has been studied. It has been shown that even under extreme conditions the filter is capable of estimating the chemical and temperature states with the accuracy required for control of the industrial process.

This investigation of the refining of steel in the electric arc furnace<sup>82</sup> has exposed the feasibility of employing the following philosophy in the development of a model of the process suitable for use in an on-line control system.

- (i) A deterministic model of the process is evolved making full use of the available metallurgical theory of the process but also ensuring that its structure does not imply an unwarranted degree of certainty.
- (ii) From a consideration of plant data and an investigation of the attainable accuracy of the plant instrumentation, the nature and statistics of the uncertainty associated with the model and the measurements is determined.
- (iii) The extended Kalman filter is employed as an efficient method of combining the a priori information about the process contained in

the dynamical model with the incomplete error-corrupted process measurements.

The success with which similar techniques have been employed in the aerospace industry have been reported extensively (a compendium of applications is to be found in the NATO publication AGARDograph No. 139). Many general principles and techniques for a very broad range of applications of Kalman filtering are available but to date these have not had a significant impact on the steelmaking industry. The inertia of the industry is probably in part due to the fact that present control of the process is quite successful. Hence a high probability of a significant economic benefit would be required before any major changes would be made to the conventional operating practice. There is, however, an increasing interest in the use of computers to assist in the control of recently developed steelmaking processes such as the argon-oxygen process for stainless steelmaking. These processes offer facilities for control hitherto unavailable and it is to these and the continuous steelmaking processes of the future that the results of the present investigation are most likely to have a practical application. Further areas of application for these results may be found in the development of new process instrumentation, wherein the following questions might be answered:

- (a) If the statistics of the uncertainty associated with a model of the process are available then what measurements are necessary to ensure that the estimates of the endpoint states satisfy the process requirements?
- (b) There is a measureable cost associated with sampling the furnace to obtain an accurate estimate of the process state, hence does a least cost measurement policy satisfying the endpoint accuracy requirements exist?

## REFERENCES

1. U.S. Patent 1,512,735.
2. HARRIS, T. H. and BRANDT, D. J. O.: "The use of the oxygen lance in British electric furnace practice", J.I.S.I., August, 1950, pp.399-413.
3. PHILBROOK, W. O.: "The problem of mathematical simulation of Basic Oxygen Steelmaking", in ELLIOT, J. F., and MEADOWCROFT, T. R. (Eds.): "Steelmaking: The Chipman Conference" (M.I.T. Press, 1965), pp.223-238.
4. MIDDLETON, J. R. and ROLLS, R.: "A dynamic mathematical model of the LD steelmaking process". Proceedings of the I.S.I. Conference on Mathematical Process Models in Iron and Steelmaking, Amsterdam, 1973.
5. WEEKS, R.: "Dynamic model of the B.O.S. process", *ibid.*
6. ASAI, S., and MUCHI, I.: "Theoretical analysis by the use of mathematical model in LD converter operation", ISIJ Trans., 1970, pp.250-263.
7. NILLES, P. and DENIS, E. M.: "Problems of oxygen transfer in BOF steelmaking", J. of Metals, July 1969, pp.74-79.
8. WELLS, C. H.: "Optimum estimation of carbon and temperature in a simulated BOF". Proceedings of the 11th Joint Automatic Control Conference of the American Control Council, Atlanta Georgia, 1970, Session Paper 1-B, pp.7-18.
9. GREENFIELD, A. A.: "A statistical approach to oxygen steelmaking", British Steel Corporation Open Report, MG/45/72.
10. MEYER, H. W., AUKRUST, E. and PORTER, W. F.: "Process analysis and control of Basic Oxygen Furnaces" in Hills, A. W. D. (Ed.) "Heat and Mass Transfer in Process Metallurgy" (Institution of Mining and Metallurgy, 1967), pp.173-205.
11. GALANOG, E., and GEIGER, G. H.: "Optimization of stainless steel melting practice by means of dynamic programming", J. of Metals, July, 1967, pp.96-104.
12. LIPSZYC, N.: "Computer control of the electric arc furnace". Proceedings of the third IFAC Congress, London 1966, Paper 11A.
13. KATSURA, K., ISOBE, K. and ITACKA, T.: "Computer control of the Basic Oxygen Process", J. of Metals, April, 1964, pp.340-345.
14. KAWASAKI, R.: "Computer control of the Basic Oxygen Furnace", J. of the Australian Institute of Metals, 1973, 18, No. 1, pp.37-46.
15. CESSSELIN, P. and WESTERCAMP, P.: "One-line computers installed in Basic Oxygen steelmaking plants". Proceedings of the third IFAC Congress, London, 1966, Paper 11C.
16. KALMAN, R. E.: "A new approach to linear filtering and prediction theory", Trans. ASME, Series D, J. of Basic Eng., 1960, 82, pp35-45.

17. KALMAN, E. E. and BUCY, R. S.: "New results in linear filtering and prediction theory", *ibid.*, 1961, 83, pp.95-107.
18. WAGNER, J. T.: "Estimation of the BOF Steelmaking process" Proceedings of the 4th Hawaii International Conference on Systems Sciences, Honolulu, 1971, pp.269-271.
19. KORNBLUM, R. J., and TRIBUS, M.: "The use of Bayesian Inference in the design of an endpoint control system for the Basic Oxygen steel furnace", *IEEE Trans.*, 1970, SSC-6, No. 4, pp339-348.
20. U.S. Patent 3377158 (April 9, 1968)
21. SOLIMAN, M. A., RAY, W. H. and SZEKELY, J.: "Applications of non-linear filtering to the stainless-steel decarbonization process", *Int. J. Control*, 1974, 20, No. 4, pp.641-653.
22. GOSIEWSKI, A. and WIERSBICKI, A.: "Dynamic optimization of a steel-making process in electric arc furnace", *Automatica*, 1970, 6, pp.7671778.
23. WHEELER, F. M., BUZEK, Z., and HLINENY, J.: "Dynamic power control during the refining period on electric arc furnaces". Proceedings of the I.S.I. Conference on Mathematical Process Models in Iron and Steelmaking, Amsterdam, 1973.
24. HENN, H. J., SHIMKETS, J. D. and JOHN, T. G.: "Development and operation of a refining control system for stainless steels". *Electric Furnace Proceedings*, 1969, Gas-Metal Reactions Session, pp.14-19.
25. WOODSIDE, C. M., PAGUREK, B., PAUKSENS, J. and OGALE, A. N.: "Singular arcs occurring in optimal electric steel refining", *IEEE Trans.*, 1970, AG-15, pp.549-556.
26. ZADEH, L. A.: "From circuit theory to system theory", *Proc. IRE*, 1962, 50, pp.8561865.
27. DANTZIG, G. B., JOHNSON, S. M. and WHITE, W. B.: "A linear programming approach to the chemical equilibrium problem", *Management Science*, 1958, 5, pp.38-43.
28. BRACKEN, J. and McCORMICK, G. P.: "Selected applications of non-linear programming", (John Wiley, 1968), pp.46-49.
29. JORGENSEN, C. and THORNGEN, I.: "Thermodynamic tables for process metallurgists", (Almqvist and Wiksell, Stockholm 1969).
30. FLOOD, H. and GRJOTHEIM, "Thermodynamic calculation of slag equilibria", *JISI*, May, 1952, pp.64-70.
31. ELLIOTT, J. F. and GLEISER, M.: "Thermochemistry for steelmaking" (Addison-Wesley, Mass., 1962).
32. WARD, E. G.: "An introduction to the physical chemistry of iron and steelmaking", (Edward Arnold, London, 1962).
33. GAUREAU, P. and GAUTIER, J. J.: "Practical advantage of oxygen determination in steel", *C.D.S. Circ.*, 1968, 10, pp.2217-2240.
34. COHEUR, J. P. and NILLES, P.: "Physico-chemical comparison of four steelmaking processes", *CNRM*, Sept., 1967, pp.43-56.

35. PEARSON, T. F., VENKATADRI, A. S., and O'HANLON, J.: "Critical comparison of slag/ metal reactions in L.D. and Kaldo processes at Consett", JISI, Oct., 1966, pp.997-1006.
36. HILL, G. and KNAGGS, K.: "Oxygen analysis as a non-aid to riming steel production", Iron and Steel, Dec., 1966, pp.552-562.
37. FUJII, T., and ARAKI, T.: "A kinetic study on decarburization in molten steel", Tetsu-to-Hagane Overseas, 1965, 5, No. 4, pp.290-302.
38. SAHOO, K. C., and GHOSH, D. N.: "Mechanism of carbon oxidation reaction in Iron-Carbon-Sulphur melts", JISI, June, 1972, pp.406-411.
39. GHOSH, D. N.: "Kinetics of the decarburization of Fe-C melts (Parts 1 and 2)", Ironmaking and Steelmaking (Quarterly), 1975, 1, pp.36-48.
40. KNAGGS, K.: "Control of oxygen injection in foundry steelmaking", JISI, 1961, May, pp.14-21.
41. NILLES, P.: Steel Coal, 1962, 20, pp.763-768.
42. BARNSELY, B. P., and THORNTON, D. S.: "The efficiency of carbon removal by oxygen in electric arc furnaces", JISI, 1964, September, pp.82-86.
43. BISHOP, H. L., LANDER, H. N., GRANT, N. J., and CHIPMAN, J.: "Equilibria of Sulphur and Oxygen between liquid iron and open hearth slags", AIME, 1956, 206, pp862-868.
44. PEHLKE, R. D.: "Open Hearth Proceedings", AIME, 1964, 47, pp.77-85.
45. BARDENHEUER, F., vom ENDE, H., and SPEITH, K. G.: "Contribution to the metallurgy of the LD process", Blast Furnace and Steel Plant, 1970, June, pp.401-407.
46. "The making, shaping and treating of steel", McGannon, H. E. (Ed), (United States Steel, USA, 1964).
47. PEARSON, J.: "Heat balances in steelmaking heats of reaction and heat contents", British Iron and Steel Research Association, SM/AE/12/65 and SM/AE/12/65 Addendum 1.
48. GATTELIER, C.: "Determination of the oxygen dissolved in liquid iron and steel using electrochemical cells", Rev. Met. 1969, Oct., pp.673-693.
49. Anon. "Determination of gasses in steel and application of the results", JISI, 1972, March.
50. SCHOLES, P. H.: "Internal progress in the determination of nitrogen and oxygen in steel" British Steel Corporation Open Report, BSc MG/CC/S28/72.
51. THEMLIS, I. J., TARASOFF, P. and SZEKELY, J.: "Gas-liquid momentum transfer in a copper converter", Trans. Met. Soc. of AIME, 1969, 245, pp.2425-2433.
52. SZEKELY, J., and THEMLIS, N. J.: "Rate phenomena in process metallurgy", (Wiley, New York, 1971).

53. IGWE, B. U. N., RAMACHANRAN, S., and FULTON, J. C.: "Jet penetration and liquid splash in submerged gas injection" *Met. Trans.*, 1973, 4, pp.1887-1894.
54. HOLDEN, C., and HOGG, A.: "The Physics of oxygen steelmaking", *JISI*, 1960, Nov., pp.318-332.
55. SOLAR, M. Y., and GUTHERIE, R. I. L.: "Kinetics of the carbon-oxygen reaction in molten iron", *Met. Trans.*, 1972, 3, pp.713-722.
56. STPIERRE, G. R.: "Kinetics of gas evolution from molten alloys", *Elec. Furnace Proc.*, 1969, pp.2-13.
57. LEIBSON, I., HOLCOMBE E. G., CACOSO, A. G., and JACMIC, J. J.: "A.I.Ch.E.J.", 1956, 2, pp.296-300.
58. "Electric Furnace Steelmaking", SIMS, C.E., (Ed), (Interscience, New York, 1963).
59. HEALY, G. W.: "Simplified calculation of effects of oxygen blowing rates", *Elec. Furnace Proc.*, 1958, pp.217-223.
60. JEMELJANOV, S. W., KAGANOV, W. J., SURGUITSCHOV, G. D., MOSSALOV, G. I., and DERKATSCHOY, E. N.: "Establishing a dynamic model of the oxygen converter process with the aid of computers", *Inter. Conf. on Automation in Iron and Steelmaking, Luxembourg/Dusseldorf*, 1970, Paper C-8.
61. MEYER, H. W., PORTER, W. F., SMITH, G. C., and SZEKELY, J.: "Slag-metal emulsions and their importance in BOF steelmaking", *J. of Metals*, 1968, pp.35-42.
62. NIWA, K.: Kinetics of the carbon-oxygen reaction in liquid iron" in "Physical chemistry of process metallurgy Pt. 2". (Interscience, 1959).
63. WELLS, G. H.: "Optimum estimation of carbon and temperature in a simulated BOF", *Proceedings of the 11th Joint Automatic Control Conference of the American Control Council, Atlanta, Georgia*, 1970, 1-B, pp.7-18.
64. GAVRYUSHIN, V. N., and SABIRZYANOV, T. F.: "Control of basic oxygen steelmaking", *Steel in the USSR*, March 1974, pp.190-191.
65. KOCHO, V. S.: "Continuous monitoring of the metal temperature in the basic oxygen converter", *Steel in the USSR*, March 1973, pp.186-187.
66. JAZWINSKI, A. H.: "Stochastic Processes and Filtering Theory", (Academic Press 1970).
67. THE, G.: "Kalman filtering divergence due to process-noise decoupling", *Proc.IEE*, 1974, 121, 6, pp.525-528
68. SAGE, A. P., and MELSA, J. L.: "Estimation theory with applications in communications and control", (McGraw-Hill 1971), p.412.
69. JAZWINSKI, A. H.: "Adaptive filtering", *Automatica*, 1969, 5, 4, pp.475-485.
70. SRIYAMANDA, H.: "A simple method for the control of divergence in Kalman-filter algorithms", *Int. J. Control*, 1972, 16, 6, pp.1101-1106.

- Kalman filter algorithms", Int. J. Control, 1973, 17, 4, pp.741-184.
72. MEHRA, R. K.: "On the identification of variances and adaptive Kalman filtering", IEEE Trans., 1970, AC-15, 2, pp.175-184.
  73. BOLAND, F. M., and NICHOLSON, H.: "Control divergence in Kalman filters", Electronic Letters, 1976, 12, No. 5, pp.367-369.
  74. LEONDES, C. T., and PEARSON, J. O.: "Kalman filtering of systems with parameter uncertainties - a survey", Int. J. Control, 1973, 17, 4, pp.785-801.
  75. MEHRA, R. K.: "Approaches to adaptive filtering", IEEE Trans, 1972, AC-17, pp. 693-698.
  76. MARTIN, W. C., and STUBBERUD, A. R.: "Uncoupled optimal identification of plant and noise parameters for linear dynamic systems", Proceedings of the 5th Symposium on nonlinear estimation theory, San Diego, California, Sept. 1974, pp.169-176.
  77. JAZWINSKI, A. H.: "Limited memory optimal filtering," IEEE Trans., 1968, AC-13, pp.558-563.
  78. NAHI, N. E., and SCHAEFER, B. M.: "Decision-directed adaptive recursive estimators: Divergence prevention", IEEE Trans, 1972, AC-17, 1, pp.61-68.
  79. SORENSON, H.: "Kalman filtering techniques", in LEONDES, C. T. (Ed): "Advances in control systems", Academic Press, New York, 1966, Vol. 3.
  80. DEUTSCH, R.: "Estimation Theory", Prentice-Hall Inc., 1965, pp.162-169.
  81. TURKDOGEN, E.T., and PEARSON, J.: "Activities of constituents of iron and steelmaking slags", J.I.S.I., 1953, March, pp.217-223.
  82. BOLAND, F.M., and NICHOLSON, H.: "Estimation of the states during refining in electric-arc-steelmaking", Proc. IEE, 1977, 124, 2, pp. 161-166.

Al.1 Introduction

Prior to commencing the investigation reported in the body of this thesis the author undertook a study of the industrial process. The purpose of this study was to gain some familiarity with the complex nature of the process. To this end the terms of reference under which the study was conducted were drawn up by the author's industrial supervisor and were approved by the manager of the melting-shop in which the study was conducted. This appendix is a synopsis of a report made on this study and is intended to expose the difficult engineering environment of the industrial process, the problems encountered when collecting plant data and the great skill required of the furnace operators to effect control of the process.

The types of steel produced in the melting-shop at which this study was conducted are described by in excess of ten thousand codes, some of which have additional sub-codes. All of these codes are part of the general classification of low and medium alloy steels. The approximate range of these steels is as follows:

- (a) Plain carbon steels -  $0.1 \leq \%C \leq 1.3$
- (b) Nickel steels -  $\text{max.}(\%Ni) = 4.0$
- (c) Chrome steels -  $\text{max.}(\%Cr) = 3.5$
- (d) Molybdenum steels -  $\text{max.}(\%Mo) = 0.5$

Al.2 Event sequence for a typical cast

Since the melting-shop at which this study was conducted only supplies steel billets for the plant's own rolling-mill the programme of casts for the shop's two furnaces is determined by

drawn up in the offices at the melting shop and this programme is passed to the scrap office and also to the shift-managers office in the melting-shop, to which it is accompanied by specification and instruction cards for each of the casts to be made.

At the scrap office the scrap-foreman decides the make-up of the initial charges for each cast on the programme. This decision is made with knowledge of the available scrap and the final specifications to be met by each cast. In making this decision the foreman uses the 'Least Cost Mix' method in a crude form, as the decision is made knowing the approximate alloy content of the available scrap and whether it was obtained internally, for example as waste from the rolling-shop or purchased from an external supplier. Scrap is stored in railway wagons and the scrap-foreman sends an order to the traffic controller giving the location of the desired loads and the sequence in which they are to be tipped into the charging-baskets. This sequence is important because no heavy scrap should be charged high in the furnace since its collapse during melting could cause electrode breakages. The scrap-foreman then enters the charge ordered on a charge-card giving an estimate of its nickel, chrome and molybdenum content. From an estimate of the carbon content of the charge the foreman orders any additional carbon required to be added in the form of graphite. Lime and scale, that is the iron-oxide removed from the surface of the billets in the rolling-shop, to give a basic slag are ordered and the quantity required is determined by the expected acidity of the charge. Finally a prediction is made of the meltout carbon, nickel and chrome and molybdenum content, the predicted carbon content should be sufficient to allow a minimum of a twenty point carbon boil, that

is the meltout carbon should be at least 0.2% greater than the desired end-point concentration. The charge-card is then passed to the traffic-controller who ensures that the loads ordered are tipped into the charging-baskets in the correct sequence.

The charge-card is then passed to the furnace operator who decides on the rate of charging, that is on the times during the melting period at which the baskets should be emptied to ensure a minimum melt down time. A record is kept of the time of charging of each basket and the weight of its contents. When the final basket has been emptied into the furnace the charge card is passed to the steel-maker who is responsible for ensuring that the finished steel satisfies the order specifications. The steel-maker is already aware, from the programme, of the type of cast being produced and has been informed of the weight of the total charge. On the basis of this information the steel-maker places provisional orders for any additions which may be required. At meltout, that is when the furnace temperature reaches about 1560°C, a sample of the hot metal is sent to the laboratory for analysis. When the result of this analysis is available the steel-maker, in conjunction with the furnace operator, decides on the actual additions required and when these should be made. The steel-maker then informs the furnace operator of the end-point carbon content and temperature required. The steel is then refined using oxygen injection to burn out the surplus carbon and electric energy to raise the temperature of the molten metal. During the refining period the furnace operator has a number of checks made on the carbon content using a discrete measurement device known as a Tect Tip and on the temperature of the steel using disposable thermocouples. When

the carbon content reaches the required level a sample of the hot metal is sent to the laboratory for analysis. The slag is then poured off and a de-oxidising slag known as Blocking Slag is put on. If the order specification is for a final sulphur content of less than 0.025% a reducing slag is then made up, this is known as Double Slag Practice. If a low sulphur content is not required the furnace is tapped, this is known as Single Slag Practice, and further alloy additions, decided on the results of the pre-Block sample, are made in the ladle. The extent of these additions will depend in part on whether or not the cast is to be de-gassed. If the cast is not to be de-gassed it should now satisfy the order specifications as further refining would be very costly and to re-grade the cast would upset the programme. If the cast is to be degassed it is then brought to the de-gasser unit. This unit extracts dissolved gases from the cast by drawing steel into an evacuated vessel. Vigorous stirring occurs when this metal flows back into the ladle. This stirring ensures that any additions made via the evacuated vessel are distributed homogeneously in the cast. After de-gassing the finished steel is poured into ingot moulds.

### A1.3 Sources of production data

#### A1.3.1 Data record on the charge-card

- (i) The charge: The origin, weight and types of scrap that make up the charge are recorded. An estimate is sometimes given of the nickel, chrome and molybdenum weights per load, but the accuracy of this estimate is limited by the heterogeneity of the scrap. Also recorded are the weights of any lime, graphite or iron oxide which are included in the charge.

- (ii) **Aim points:** Normally only a prediction of the carbon concentration at meltout is recorded, but if a significant nickel, chrome or molybdenum concentration is expected then this also may be recorded.
- (iii) **Charging:** The weight of the contents, the identification number and the time at which it charged the furnace is recorded for each basket. The weight of the contents is probably subject to an error in the order of 3% since this weight is only an estimate based on the known weight of the loads tipped into the basket and no account is made for the material which misses the basket.
- (iv) **Power:** Meter readings taken at power-on, meltout and tap give the energy used during each stage measured in hundreds of kWhrs.
- (v) **Oxygen:** The initial and final readings of a quantity meter are recorded for each cast and the total oxygen used can be calculated in thousands of cubic feet.
- (vi) **Furnace additions:** The quantity and time of charging is recorded for all additions of slag-making materials and alloys.
- (vii) **Chemical and thermal data:** A record is kept both of the times at which the furnace is sampled and of the results of the chemical analysis of these samples. A record is also kept of the time and result of each temperature measurement made during the refining period.

#### A1.4.1 The furnace control room

Meters in the furnace control room measure the following: Furnace power factor, the supply current (A), the supply voltage (kV), the total furnace power (MW), the arc current per phase (kA), the arc reference voltage per phase (V). The tap setting on the transformer is also displayed.

#### A1.4.2 The melting shop floor

Two oxygen rate meters are located adjacent to each furnace. The ranges of these meters are 0 to 500 cu.ft. per min. and 0 to 2000 cu.ft. per min respectively. The narrower range meter is employed to measure the oxygen flow rate during the melt-down period when oxygen is injected to assist melting. The other meter is employed to measure the high rates of flow which are used during refining.

#### A1.5 Conclusions

This study of a typical arc furnace steelmaking practice exposes the extent to which present control of the process is dependent on the experience and skill of the operators. The existing instrumentation serves only to assist the furnace operators and the extent of the data records maintained is determined by the needs of the quality control and commercial sections of the industry. Hence, the information at present available from the process is neither sufficiently accurate nor extensive enough for a model of the process to be developed using only statistical techniques. This lack of well monitored plant data can only be alleviated by a change to a standard operating practice and an

improvement in the range and accuracy of the production data logged.  
It is of interest to note<sup>24</sup> that a significant contribution to the  
increased productivity that is obtained when computer-aided  
refining control is implemented is probably due to the standardised  
operating practice which such control introduces.

Formulation of a simple model of the kinetics of the  
steelmaking reactions

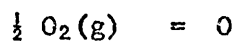
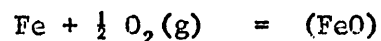
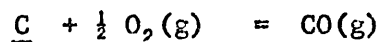
A2.1 Introduction

Prior to the development of the detailed process model described in this dissertation, a simple model of a possible reaction mechanism within the gas entrainment zone was investigated. This simple model was developed by employing some of the arguments presented in the reported work on the modelling of the BOF process<sup>4-7, 50</sup>. There are, however, some major differences between the arc furnace and the BOF processes, the important role of slag-metal emulsions<sup>61</sup> in the BOF is one example. The model of the BOF developed by Jemeljanov et al<sup>60</sup> not only ignores the effect of such emulsions but also the significant increase in the temperature of the hot metal during refining in the BOF. Consequently this rather restricted model of the steelmaking process in the BOF was considered to provide some basis for constructing a limited model of the electric arc furnace process.

A2.2 Assumptions

The following assumptions were made:

- (1) That all the injected oxygen takes part in reactions within the bath, i.e. none escapes with the flue gases.
- (2) That all the oxygen entering the reaction zone located at the lance end can be accounted for by the following reactions



- (3) That the specific rate constant for the carbon-oxygen reaction is given by the Arrhenius equation.
- (4) That the rate of oxidation of iron is dependent only on the rate at which oxygen is supplied to the process since a limitless supply of iron may be assumed.
- (5) The rate of diffusion of carbon into the reaction zone is a function of the excess of carbon above a critical value.
- (6) That the chemical activities of carbon and oxygen in the bath are equal to their respective concentrations expressed as weight percentages.

### A2.3 Development of model equations

#### A2.3.1 The oxidation of carbon

From assumption (3) the kinetics of the carbon oxidation reaction are described by

$$-\frac{dC}{dt} = A [C] [O] \exp (-E/RT) \quad A1$$

where A = the frequency factor for the reaction

E = the energy of activation for the reaction

#### A2.3.2 The oxidation of iron

From assumption (4) the dynamics of the iron oxidation reaction are described by the following second order equation

$$T_{Fe} \frac{d^2}{dt^2} (FeO) + \frac{d}{dt} (FeO) = K_1 U(t) \quad A2$$

where  $T_{Fe}$  = a time constant which is determined by thermodynamic and kinetic constants

$K_1$  = a stoichiometric coefficient

### A2.3.3 The dissolution of oxygen in the bath

The rate at which oxygen dissolves in the molten metal will be proportional to available iron oxide less that required for reaction with carbon. Hence the dynamics of the dissolution of oxygen may be described by the following equation

$$\frac{dO}{dt} = \alpha_1 \left( \frac{dFeO}{dt} \right) - K_2 \left( \frac{dC}{dt} \right) \quad A3$$

where  $K_2$  = a stoichiometric coefficient

$\alpha_1$  = a coefficient which characterizes the availability of oxygen

### A2.3.4 The diffusion of carbon into the reaction zone

Assumption (5) asserts that the limitation of the available supply of carbon begins to manifest itself at some critical concentration,  $C_k$ . Hence the dynamics of the entry of carbon into the reaction zone may be represented by the following equation

$$T_C \frac{d[C]}{dt} + [C] = \alpha_2 [C]_i \quad A4$$

with  $[C]_i = C^0$  at  $t = 0$

$$[C]_i = C^0 - C_k - \int_0^t \left( \frac{dC}{dt} \right) dt \quad t > 0$$

where  $T_C$  = a time constant which is determined by thermodynamic and kinetic constants

$\alpha_2$  = a coefficient which characterises the carbon concentration gradient

### A2.4 Estimation of process parameters

Three estimates of the value of activation energy,  $E$ , for the carbon-oxygen reaction obtained from the literature are given as

45171.	60
58080.	55
117230.	62

The largest of these estimates was ignored since the results of the most recent studies<sup>60,65</sup> were obtained using quite different experimental techniques and imply that Niwa's<sup>62</sup> estimate is excessive. The value of  $E$  given in Jemeljanov<sup>60</sup> was obtained from an analysis of BOF process data whereas Solar and Guthrie's<sup>55</sup> estimate was obtained in the laboratory. Since the arc furnace process is more alike the BOF, in mode and temperature of operation, than the laboratory vessel a value of  $-50000$  kJ/kmol was taken as an estimate for  $E$ .

Since no estimate of the value of the frequency factor,  $A$ , was to be found in the literature it was evaluated using the following empirical analysis.

- (i) For an oxygen injection rate of  $0.0135$  kmol/tonne/min at a process temperature of  $1873^{\circ}\text{K}$  the rate of decarburization is approximately  $0.0083$  kmol/tonne/min.
- (ii) The equilibrium  $[\text{C}][\text{O}]$  product is  $0.00105$  at  $1873^{\circ}\text{K}$  and  $1$  atm pressure.
- (iii) Assuming that  $E = -50000$  kJ/kmol and  $T = 8.32$  kJ/kmol/ $^{\circ}\text{K}$  then

$$A \doteq 0.0083 / (0.00105 \exp(-50000/16583))$$

$$A \doteq 160$$

In view of the larger  $[\text{C}][\text{O}]$  product expected during oxygen injection it was decided that a value of  $120$  be taken for  $A$ .

The critical carbon concentration  $C_k$  below which the effect of carbon shortage manifests was obtained from the results of Barnsely

and Thornton<sup>74</sup> (see 3.4.3) who found that the efficiency of decarburization decreased rapidly once the carbon concentration fell below 0.066 kmol/tonne.

For the remaining process parameters the following values were obtained from Jemeljanov et al.<sup>60</sup>

$$T_{Fe} = 0.539 \text{ min}, \quad K_1 = 2.0$$

$$\alpha_1 = 0.586 \quad K_2 = 1.05$$

$$T_C = 0.337 \text{ min} \quad \alpha_2 = 1.07$$

### A2.5 Solution of model equations

The system of equations A1-A4 was investigated on an analogue computer using the values of process parameters given in A2.4 and the following initial values for the process variables.

At  $t = 0$  for a bath weight of 140 tonne

$$[C] = 0.75\% \equiv 0.625 \text{ kmol/tonne}$$

$$[C] = \% O(\text{equilibrium}) \equiv 0.00105/0.625 = 0.00168 \\ \text{kmol/tonne}$$

$$T = 1873^{\circ}\text{K}$$

$$U = 1500 \text{ ft}^3/\text{min} \equiv 0.135 \text{ kmol/tonne/min}$$

The results of this computer study are shown in Figs A2.1, A2.2.

### A2.6 Discussion

The responses shown in Figs. A2.1 and A2.2 are in general agreement in shape and magnitude with plant data, but this does not necessarily imply that the model is validly constructed. Indeed analysis of the behaviour of the model from the chemical viewpoint exposes some fundamental theoretical weaknesses in the present formulation. These weaknesses are typified by the presence of equation A1 which is rate limiting for high carbon concentrations.

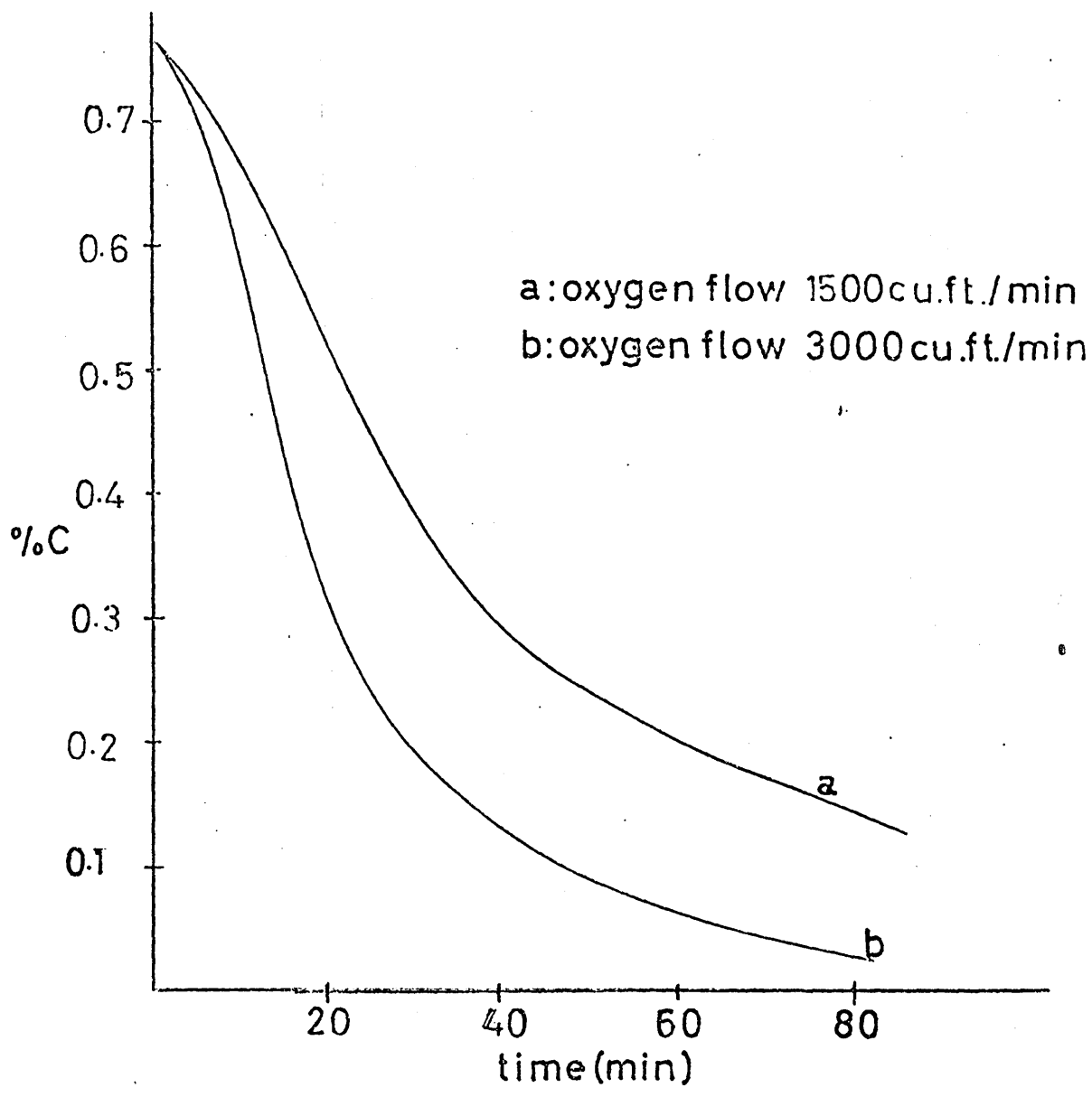


FIG A2.1 Effect of Oxygen Flow Rate on Carbon Response

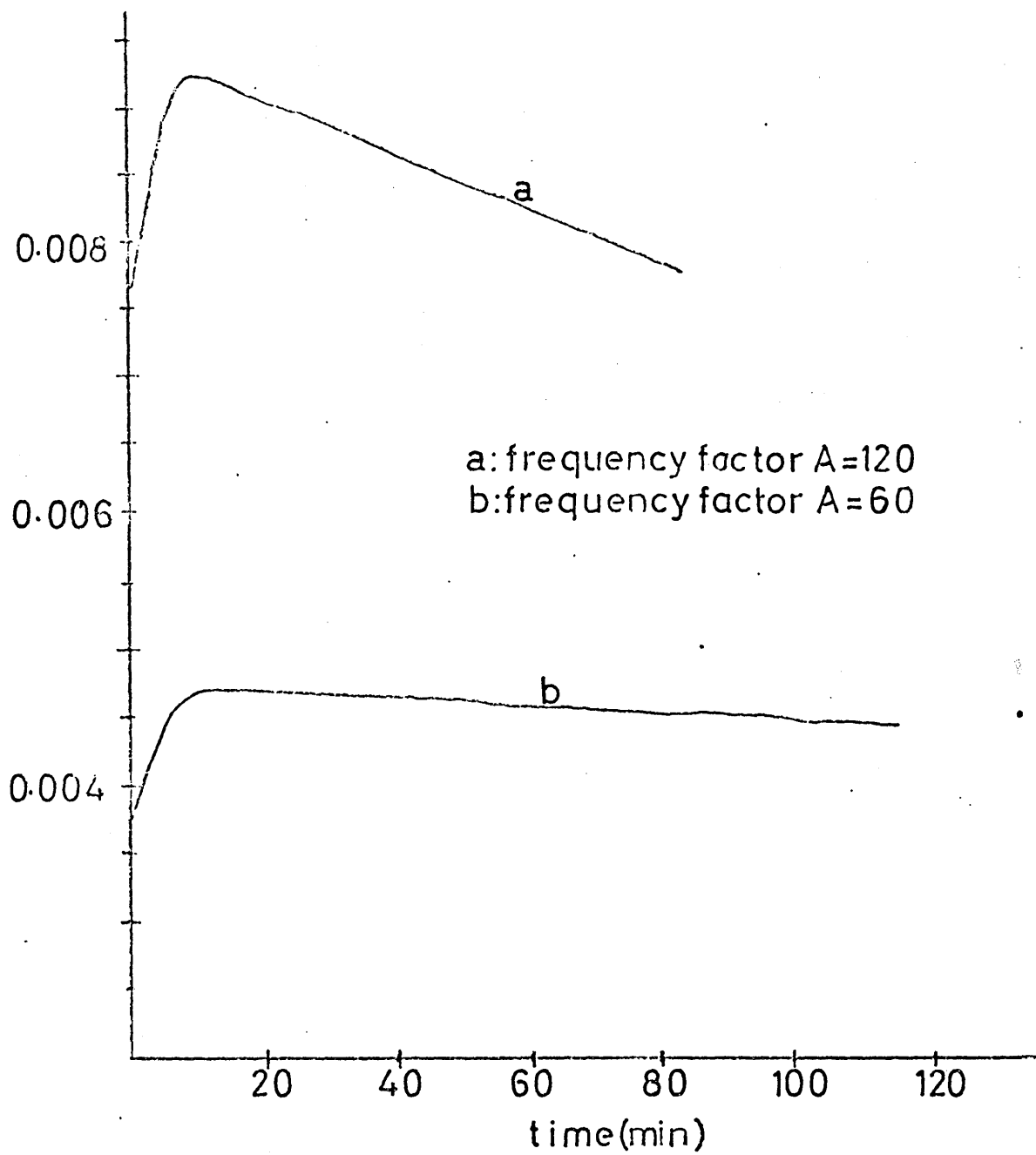


FIG A2.2 Effect of Frequency Factor on Decarburization Rate

Al describes the rate of the chemical reaction yet the accepted theory is that for such carbon concentrations it is the mass transfer of oxygen (see 2.2.3) that is rate limiting.

Since to pursue the development of a model along the present lines would probably lead to a model with very little theoretical validity it was decided that a detailed theoretical analysis of the process should be conducted (see Chapter 2).

A3.1 State variables

- $x_1$  = carbon concentration, kmol/tonne of hot metal
  - $x_2$  = manganese concentration, kmol/tonne of hot metal
  - $x_3$  = iron oxide concentration, kmol/tonne of slag
  - $x_4$  = weight of hot metal, tonne
  - $x_5$  = temperature of hot metal, °K
  - $x_6$  = weight of slag time, tonne
  - $x_7$  = manganese oxide concentration, kmol/tonne of slag
  - $x_8$  = magnesium oxide concentration, kmol/tonne of slag
  - $x_9$  = phosphorous pentoxide concentration, kmol/tonne of slag
  - $x_{10}$  = alumina concentration, kmol/tonne of slag
  - $x_{11}$  = silica concentration, kmol/tonne of slag
  - $x_{12}$  = calcium oxide concentration, kmole/tonne of slag
- Control input,  $u$  = oxygen injection rate, kmol/tonne of hot metal/sec

A3.2 Dependent variables

- $y_1$  = oxygen concentration, kmol/tonne of hot metal
- $y_2$  = slag basicity ratio
- $y_3$  = ratio of weight of slag to weight of hot metal

A3.3 State equations  $\dot{x}_i = f_i(x, u)$  ( $i = 1, \dots, 11$ )

$i = 1$ ,  $\dot{x}_1 = f_1(x, u)$ , see eqn. 3.8(a), it is assumed here that  $\xi_1 > \xi_2$ , i.e. that the rate of reaction is controlled by the rate of oxygen diffusion. This is reasonable in the present case since it is rare that the end-point carbon is less than 0.1%.

$$\dot{x}_1 = \frac{-[p_1(p_2 - K_1/1.2x_1) + p_3(g_1(x)/K_2 - 1.6y_1)]}{[1 - p_4p_3(g_1(x)/K_2 - 1.6y_1)]}$$

i = 2,  $\dot{x}_2 = f_2(x, u)$ , see eqn. 3.12

$$\dot{x}_2 = -p_5(1 + p_6 f_1(x, u))(5.5x_2 - g_2(x)/K_3)$$

i = 3,  $\dot{x}_3 = f_3(x, u)$ , see eqn. 3.15

$$\dot{x}_3 = (2u + f_1(x, u)(1 + p_7 y_1/x) + f_2(x, u))/y_3$$

i = 4,  $\dot{x}_4 = f_4(x, u)$  see eqn. 3.16

$$\dot{x}_4 = -55.85 x_4 y_3 f_3(x, u)$$

i = 5,  $\dot{x}_5 = f_5(x, u)$ , see eqn. 3.18

$$\begin{aligned} &= x_4(f_1(x, u)(\Delta H_1 + \Delta H_2 p_7 y_1/x) + f_2(x, u) \\ &\quad \Delta H_3 + f_3(x, u)y_3 \Delta H_4 + u \Delta H_5)(\Delta H_6 x_4 + \Delta H_7 x_6)^{-1} \end{aligned}$$

i = 6,  $\dot{x}_6 = f_6(x, u)$ , see eqn. 2.16

$$= 68x_4 y_3 f_3(x, u) + 56.08x_6 f_{12}(x, u)$$

i = 7,  $\dot{x}_7 = f_7(x, u)$  see eqn. 3.12

$$\dot{x}_7 = f_2(x, u)/y_3$$

i = 8, ..., 12

$$\dot{x}_i = f(x, u), \text{ see 3.6}$$

$$\dot{x}_i = 0$$

A3.4 The dependent variables  $y_i$  (i = 1, 2, 3) and the parameters

$p_j$  (j = 1, ..., 7)

i = 1, see eqn. 4.1(a)

$$y_1 = 1.6\alpha_0(1.2x_1)^{\alpha_1}$$

where  $\alpha_0 = 0.0094$

$$\alpha_1 = -0.633$$

i = 2, see eqn. 3.12

$$\begin{aligned} y_2 &= (x_{12}/56.08 + x_7/70.94 + x_8/40.32)/(x_{11}/60.09 \\ &\quad + x_{10}/101.96 + x_9/141.96) \end{aligned}$$

i = 3, see eqn. 3.16

$$y_3 = x_6/x_4$$

j = 1, see 4.3.5

$$\begin{aligned} p_1 &= A_1 D_0 \rho_i / \delta (\text{wt. bath}) \\ &= 0.007 \text{ s}^{-1} \end{aligned}$$

j = 2, see 4.3.6

$$\begin{aligned} p_2 &= a_0^1 \\ &= 0.06 \end{aligned}$$

j = 3, see 4.5.3 and 4.6

$$\begin{aligned} p_3 &= k_2 A_{\min} \\ p_3 &= 0.0035 \text{ m}^2/\text{s} \end{aligned}$$

j = 4, see eqn. 4.8

$$\begin{aligned} p_4 &= k_2 A_{\min} e \\ &= 5.95 \end{aligned}$$

j = 5, see eqn. 3.13 and 4.8

$$\begin{aligned} p_5 &= k_3 A_{\min} \\ &= 0.0098 \text{ m}^2/\text{s} \end{aligned}$$

j = 6, see eqn. 3.13

$$\begin{aligned} p_6 &= e \\ &= 1700 \end{aligned}$$

j = 7, see eqns. 3.15 and 4.1(a)

$$\begin{aligned} p_7 &= \alpha_1 \\ &= -0.633 \end{aligned}$$

#### A3.4 The functions $g_i(x)$ (i = 1, 2)

i = 1, see eqn. 4.7

$$\begin{aligned} g_1(x) &= a_{\text{FeO}}^{12} \\ &= 0.555 + 2.24x_3 / \left( \sum_{j=7}^{12} x_j + x_3 \right) - \\ &\quad - 0.117y_2 \end{aligned}$$

i = 2, see eqns. 3.11 and 4.9

$$\begin{aligned} g_2(x) &= \gamma_{\text{MnO}} N_{\text{MnO}} / (\gamma_{\text{FeO}} N_{\text{FeO}}) \\ &= (1 - 3.27 \exp(-0.95y_2)) x_7 / x_3 \end{aligned}$$

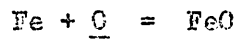
coefficients  $\Delta H_j$  ( $j = 1, \dots, 7$ )

$i = 1$   $K_1$  is the equilibrium constant for the reaction



$$K_1 = \exp(4.77 - 2.690/x_5)$$

$i = 2$   $K_2$  is the equilibrium constant for the reaction



$$K_2 = \exp(-6.3 + 14564/x_5)$$

$i = 3$   $K_3$  is the equilibrium constant for the reaction



$$K_3 = \exp(-8 + 17053/x_5)$$

$$j = 1 \quad \Delta H_1 = -0.1382 \cdot 10^6 \text{ kJ/kmol}$$

$$j = 2 \quad \Delta H_2 = 0.1172 \cdot 10^6 \text{ kJ/kmol}$$

$$j = 3 \quad \Delta H_3 = -0.3601 \cdot 10^6 \text{ kJ/kmol}$$

$$j = 4 \quad \Delta H_4 = 0.247 \cdot 10^6 \text{ kJ/mol}$$

$$j = 5 \quad \Delta H_5 = -0.2726 \cdot 10^5 \text{ kJ/kmol}$$

$$j = 6 \quad \Delta H_6 = 860 \text{ kJ/tonne/}^\circ\text{K}$$

$$j = 7 \quad \Delta H_7 = 2300 \text{ kJ/tonne/}^\circ\text{K}$$

### A3.6 Plant data and initial conditions

The initial conditions are determined by the values of the elements

of  $z_i$  ( $i = 1, \dots, 14$ ), the process data record. The values for  $z_i$

presented in Table A3.1 are those employed in the simulation study

reported in Chapter 5 and the initial values of  $x_i = x_i^0$  ( $i = 1, \dots, 14$ )

are related to  $z$  as follows

$$x_1^0 = z_1/1.2$$

$$x_2^0 = z_2/5.5$$

$$x_3^0 = z_4/6.3$$

$$x_4^0 = z_{12}$$

$$x_5^0 = z_{10} + 273$$

INPUT VARIABLE	DESCRIPTION	VALUE FROM PLANT DATA
z <sub>1</sub>	Initial C Concentration	.75%
z <sub>2</sub>	" Mn "	.3 %
z <sub>3</sub>	" CaO "	46.1 %
z <sub>4</sub>	" FeO "	11.3 %
z <sub>5</sub>	" MnO "	9.3 %
z <sub>6</sub>	" MgO "	7.3 %
z <sub>7</sub>	" P <sub>2</sub> O <sub>5</sub> "	1.6 %
z <sub>8</sub>	" SiO <sub>2</sub> "	13.5 %
z <sub>9</sub>	" Al <sub>2</sub> O <sub>3</sub> "	5.2 %
z <sub>10</sub>	Process Temperature	1600°C
z <sub>11</sub>	Approx. inner shell Diameter	6.7m
z <sub>12</sub>	Initial Bath Weight (approx.)	140 tonnes
z <sub>13</sub>	Oxygen Injection Rate	1500 cu.ft/min
z <sub>14</sub>	Weight of Charged Line	7.75 tonnes

TABLE A3.1 Input Data

$$x_6^0 = 100z_{14}/z_4$$

$$x_7^0 = z_5/7.094$$

$$x_8^0 = z_6/4.032$$

$$x_9^0 = z_7/14.196$$

$$x_{10}^0 = z_9/10.196$$

$$x_{11}^0 = z_8/6.009$$

$$x_{12}^0 = z_3/5.608$$

$$u = z_{13}/47462.912z_{12}$$

$$A_{\min} = \pi z_{11}^2/4$$

Elements of the stochastic process modelA4.1 Determination of the process noise covariance matrix

Let the maximum error on the state equation  $f_i(x,u)$  be given by

$$(\text{Error}_i)^2 = \sum_{j=1}^M \left( \frac{\partial f_i}{\partial \beta_j} \delta \beta_j \right)^2 \quad \text{A1}$$

where the vector  $\beta$  has elements

$$\beta_j = a_j \quad j = 1, \dots, 9$$

$$\beta_j = p_m \quad j = 10, \dots, 16. \quad m = 1, \dots, 7$$

$$\beta_j = \xi_n \quad j = 17, \dots, 20. \quad n = 1, \dots, 4$$

Here  $p_m$  ( $m = 1, \dots, 7$ ) are the parameters occurring in the functions  $s_k(x,u)$  ( $k = 1, \dots, 4$ ) as defined in section 7.2.2 and have values

$$p = (0.00263, 6.15, 0.555, 0.12, 2.24, 3.27, 0.95)$$

For convenience of notation let  $\phi_i = (\text{Error}_i)^2$ . It is apparent from the state equations, see eqn. 7.1, that only the following partial derivatives are required in the evaluation of  $\phi_1$ .

$$\frac{\partial f_1}{\partial \beta_1} = \frac{\partial f_1}{\partial a_1} = -K_1/1.2x_1 + a_2; \quad \frac{\partial f_1}{\partial \beta_2} = \frac{\partial f_1}{\partial a_2} = a_1$$

$$\begin{aligned} \frac{\partial f_1}{\partial \beta_3} &= \frac{\partial f_1}{\partial a_3} = -s_1(x,u) 1.6x_1 a_4 \\ \frac{\partial f_1}{\partial \beta_4} &= \frac{\partial f_1}{\partial a_4} \\ &= 1.6a_4 a_3 s_1(x,u) x_1 a_4^{-1} \end{aligned}$$

$$\frac{\partial f_1}{\partial \beta_{10}} = \frac{\partial f_1}{\partial p_1} = s_2(x,u)/K_2 - 1.6a_3 x_1 a_4$$

$$\frac{\partial f_1}{\partial \beta_{11}} = \frac{\partial f_1}{\partial p_2} = u_1 \frac{\partial f_1}{\partial p_1}$$

$$\frac{\partial f_1}{\partial \beta_{12}} = \frac{\partial f_1}{\partial p_3} = s_1(x,u)/K_2; \quad \frac{\partial f_1}{\partial \beta_{13}} = \frac{\partial f_1}{\partial p_4} = \frac{\partial f_1}{\partial p_3}$$

$$\frac{\partial f_1}{\partial \beta_{14}} = \frac{\partial f_1}{\partial p_5} = \frac{x_3}{\xi_2} \frac{\partial f_1}{\partial p_3} ; \frac{\partial f_1}{\partial \beta_{17}} = \frac{\partial f_1}{\partial \xi_1} = p_3 \frac{\partial f_1}{\partial p_3}$$

$$\frac{\partial f_1}{\partial \beta_{18}} = \frac{\partial f_1}{\partial \xi_2} = \frac{p_5}{\xi_2} \frac{\partial f_1}{\partial p_5}$$

To evaluate  $\phi_2$  the following partial derivatives are required

$$\frac{\partial f_2}{\partial \beta_5} = \frac{\partial f_2}{\partial a_5} = (1 - p_6 \exp(-p_7 \xi_1)) (x_2^0 - x_2) / K_3 x_3$$

$$\frac{\partial f_2}{\partial \beta_{10}} = \frac{\partial f_2}{\partial p_1} = 5.49 x_2 - s_3(x, u) / K_3 x_3$$

$$\frac{\partial f_2}{\partial \beta_{11}} = \frac{\partial f_2}{\partial p_2} = u_1 \frac{\partial f_2}{\partial p_1}$$

$$\frac{\partial f_2}{\partial \beta_{15}} = \frac{\partial f_2}{\partial p_6} = s_1(x, u) \exp(-p_7 \xi_1) (\xi_3 + a_5 (x_2^0 - x_2)) / K_3 x_3$$

$$\frac{\partial f_2}{\partial \beta_{16}} = \frac{\partial f_2}{\partial p_7} = -p_6 \xi_1 \frac{\partial f_2}{\partial p_6} ; \frac{\partial f_2}{\partial \beta_{17}} = \frac{\partial f_2}{\partial \xi_1} = p_6 p_7 \frac{\partial f_2}{\partial p_6}$$

$$\frac{\partial f_2}{\partial \beta_{19}} = \frac{\partial f_2}{\partial \xi_3} = s_1(x, u) (1 - p_6 \exp(p_7 \xi_1)) / K_3 x_3$$

Employing the linear dependence of  $f_3(x, u)$  on  $f_1(x, u)$  and  $f_2(x, u)$

permits  $\phi_3$  to be written as, (see eqn. 7.1)

$$\begin{aligned} \phi_3 = & a_5 (1 - s_4(x, u)) \phi_1 + a_5 \phi_2 + \left( \frac{\partial f_3}{\partial \beta_5} \right)^2 \delta \beta_5^2 \\ & + \left( \frac{\partial f_3}{\partial \beta_3} \right)^2 \delta \beta_3^2 + \left( \frac{\partial f_3}{\partial \beta_4} \right)^2 \delta \beta_4^2 \end{aligned}$$

where  $\frac{\partial f_3}{\partial \beta_3} = \frac{\partial f_3}{\partial a_3} = a_5 f_1(x, u) s_4(x, u) / a_3$

$$\frac{\partial f_3}{\partial \beta_4} = \frac{\partial f_3}{\partial a_4} = a_4 a_5 f_1(x, u) s_4(x, u) / x_1$$

$$\frac{\partial f_3}{\partial \beta_5} = \frac{\partial f_3}{\partial a_5} = f_3(x,u)/a_5$$

The simulation studies presented in Chapter 6 indicate that the model can accurately describe the thermal dynamics when the process is operated in an undisturbed manner. Consequently it is reasonable to confine the present error analysis to the chemical state equations and thereby avoid the need to evaluate the extremely complex components which the state equation  $f_4(x,u)$  would introduce.

An estimate of the process noise covariances may be obtained from the errors  $\phi_i$  ( $i = 1,2,3$ ) by setting

$$q_{ii} = \phi_i^2/9, \quad i = 1,2,3 \quad A2$$

The dependence of the errors  $\phi_i$  on the value of the state,  $x$ , and controls,  $u$ , is apparent from the expressions describing the partial derivatives of the state equations with respect to the vector  $\beta$ . On-line evaluation of these errors would significantly increase both the computation time and computer storage requirements for the state estimator. It was therefore decided that a study be made of the time variation of the ratio  $|\overline{\phi_i}/3|f_i(x,u)|$  over the refining interval. Estimates of the errors  $\delta\beta$  were made by setting

$$\delta\beta_j = \Delta\beta_j \quad \text{for } j = 1, \dots, 16$$

where  $\Delta$  is a constant. For  $j = 17, \dots, 20$   $\delta\beta_j$  is determined by the standard deviations presented in section 7.2.1.

For  $\Delta = 0.01, 0.1, 0.5$  a constant defined by

$$\epsilon = \left[ \sum_{i=1}^3 \int_0^T (|\overline{\phi_i}/3|f_i(x,u)|) dt \right] / 3T \quad A3$$

was evaluated using the data presented in Fig. 6.1, here  $T$  = the duration of the refining period. The following values were calculated:

$$\Delta = 0.01 \quad \epsilon = 0.06$$

$$\Delta = 0.1 \quad \epsilon = 0.25$$

$$\Delta = 0.5 \quad \epsilon = 1.2$$

Since 10% (that is  $\Delta = 0.1$ ) is a reasonable estimate of the average error on the elements of  $\beta$  a choice of 0.25 for  $\epsilon$  was made. It follows therefore from eqn. A3 that the state and control dependence of  $\phi_i$  may be approximated by setting

$$|\bar{\phi}_i| = 0.75 |f_i(x,u)| \quad A4$$

From eqn. A2 it follows that

$$q_{ii} = 0.0625 f_i^2(x,u) \quad i = 1,2,3 \quad A5$$

Since  $f_u(x,u)$  includes terms linear in  $f_1(x,u)$ ,  $f_2(x,u)$  and  $f_3(x,u)$  it was decided that this expression should be used to estimate  $q_{uu}$ .

#### Remarks

(a) The analysis, presented above, considers the continuous time process model. However, since the discrete time model has been obtained using the Euler integration formula, see section 7.3, the equivalent variances of the vector noise sequence are

$$q_{ii} = 0.0625 F_i^2(x,u)$$

(b) This analysis provides an initial estimate for the parameter  $\epsilon$  which may be employed as a tuning factor when implementing the filter on-line. Two possible extensions of this technique would be to consider  $\epsilon$  as an adaptive variable which might be updated at the end of each cast. Alternatively a different value of  $\epsilon$  might be associated with each component of the system model. Further comments on the problems of on-line implementation of the filter are to be found in Appendix 5.



Element G<sub>23</sub>:       $\theta = f_2(x, u)$

From eqn. 7.1       $\theta = f_3(x, u)/a_5 - u_1 \cdot (1 - s(x, u))f_2(x, u)$

$$G_{23} = \frac{\partial \theta}{\partial f_3} = 1/a_5$$

Element G<sub>24</sub>:       $\theta = f_2(x, u)$

From eqn. 7.1       $\theta = \left[ ((f_4(x, u) - a_6)/a_7 - a_9 u_2)/a_8 - (\Delta H_1 + \Delta H_4 s(x, u))f_1(x, u) - \Delta H_3 f_3(x, u) - \Delta H_5 u_1 \right] / \Delta H_2$

$$G_{24} = \frac{\partial \theta}{\partial f_4} = 1/a_7 a_8 \Delta H_2$$

Element G<sub>34</sub>:       $\theta = f_3(x, u)$

From eqn. 7.1       $\theta = \left[ ((f_4(x, u) - a_6)/a_7 - a_9 u_2)/a_8 - (\Delta H_1 + \Delta H_4 s(x, u))f_1(x, u) - \Delta H_2 f_2(x, u) - \Delta H_5 u_1 \right] / \Delta H_3$

$$G_{34} = \frac{\partial \theta}{\partial f_4} = 1/a_7 a_8 \Delta H$$

#### A4.3 The linearized process model

The implementation of the extended Kalman filter requires the evaluation of a linear approximation to the discrete-time process model, see eqn. 7.2. Let  $\Phi$  denote the transition matrix of the linearized model, see eqn. 7.15. The elements of  $\Phi$  are, in general,  $\Phi_{ij} \doteq (\Delta t \partial f_i / \partial x_j) + \delta_{ij}$ , where  $\Delta t$  is the discrete-time interval and it follows that the Jacobian matrix of  $f(x, u)$  must be evaluated. The Jacobian matrix has the following form, see eqn. 7.1.

$$\partial f_1 / \partial x_1 = a_1 K_1 / 1.2 x_1^2 + 1.6 a_3 a_4 s_1(x, u) x_1^{a_4 - 1}$$

$$\partial f_1 / \partial x_2 = 0$$

$$\partial f_1 / \partial x_3 = 2.24 s_1(x, u) / E_2 K_2$$

$$\partial f_1 / \partial x_4 = 2690. a_1 K / 1.2 x_1 x_4^2 + 14564 s_1(x, u) s_2(x, u) / K_1 x_4^2$$

$$\partial f_2 / \partial x_1 = 0$$

$$\partial f_2 / \partial x_2 = -5.49s_1(x,u) - a_5s_1(x,u)(1 - 3.27\exp(-.95\xi_3))/k_3x_3$$

$$\partial f_2 / \partial x_3 = -s_1(x,u)s_3(x,u)/K_3x_3^2$$

$$\partial f_2 / \partial x_4 = 17053s_1(x,u)s_3(x,u)/K_3x_3x_4^2$$

$$\partial f_3 / \partial x_1 = a_5(1 - s_4(x,u))\partial f_1 / \partial x_1 - a_5(a_4 - 1)s_4(x,u)f_1(x,u)/x_1$$

$$\partial f_3 / \partial x_2 = a_5\partial f_2 / \partial x_2$$

$$\partial f_3 / \partial x_4 = a_5(\partial f_2 / \partial x_4 + (1 - s_4(x,u))\partial f_1 / \partial x_4)$$

$$\partial f_4 / \partial x_1 = a_7a_8 \left[ (\Delta H_1 + s_4(x,u)\Delta H_4)\partial f_1 / \partial x_1 + \Delta H_4 f_1(x,u) \right. \\ \left. (a_4 - 1)s_4(x,u)/x_1 \right]$$

$$\partial f_4 / \partial x_2 = a_7a_8\Delta H_2\partial f_2 / \partial x_2$$

$$\partial f_4 / \partial x_3 = a_7a_8\Delta H_3\partial f_3 / \partial x_3$$

$$\partial f_4 / \partial x_4 = 0$$

## Control of Divergence in Kalman Filters

### A5.1 Introduction

In practice the information required to construct the Kalman filter is only approximately known. The noise parameters and models may be based on limited data and the system model may not be adequate. As a result of these errors, inconsistency between the error covariance, as calculated by the filter and the actual error covariance can arise. This phenomenon, known as divergence, is in effect the result of the filter placing undue confidence on the erroneous description of the system and ignoring subsequent measurements. A study of the literature exposes a variety of methods for the control of divergence. The range of these methods<sup>74</sup> extends from adaptive filters<sup>66,72,75,76</sup>, wherein parameters in the models and/or the noise covariance matrices are estimated, to filters<sup>68</sup> in which a fixed lower limit on the gain is set to ensure that adequate insensitivity to errors in the system description is obtained. Intermediate to these are the methods based on limited memory filtering<sup>77</sup> and decision directed<sup>70,71,78</sup> divergence prevention. Here, a number of methods of the latter type are considered and their application in practice is commented upon.

A5.2 Filter: We consider the linear discrete time filter, but the results can be readily applied in the non-linear case when the linearized extended filter is employed. The system model is

$$x_{k+1} = \phi_k x_k + G_k v_k \quad A1$$

$$y_{k+1} = H_{k+1} x_{k+1} + w_{k+1} \quad A2$$

where  $v_k \sim N(0, Q_k)$  and  $w_k \sim N(0, R_k)$  are white gaussian vector noise sequences. The filter equations are

$$x_{k+1}^k = \phi_k x_k^k \quad A3$$

$$P_{k+1}^k = \phi_k P_k^k \phi_k^T + G_k Q_k G_k^T \quad A4$$

$$K_{k+1}^k = P_{k+1}^k H_k^T (H_{k+1}^k P_{k+1}^k H_{k+1}^T + R_{k+1})^{-1} \quad A5$$

$$P_{k+1}^{k+1} = (I - K_{k+1}^k H_{k+1}^k) P_{k+1}^k \quad A6$$

$$z_{k+1}^k = y_{k+1} - H_{k+1}^k x_{k+1}^k \quad A7$$

$$x_{k+1}^{k+1} = x_{k+1}^k + K_{k+1}^k z_{k+1}^k \quad A8$$

where the notation  $(\cdot)_i^j$  denotes the estimate of  $(\cdot)$  at time  $t = i\Delta t$ , with measurements made on the interval  $t = [0, j\Delta t]$ . Useful information on the accuracy of the filter can be obtained from the innovations process,  $z_k$ , which is known<sup>72</sup>, in theory, to be a white gaussian noise sequence with covariance  $(H_k P_k^{k-1} H_k^T + R_k)$ .

Based on tests on the consistency of the statistics of  $z_k$  the following three methods have been proposed for detecting and controlling divergence.

Method a<sup>70</sup>:

Test: if  $z_k^T z_k > 3 \text{ trace}(H_k P_k^{k-1} H_k^T + R_k)$ , suspect divergence.

Action: freeze filter gain at present value and by-pass eqn 6.

Maintain this action until  $z_k^T z_k < \text{trace}(H_k P_k^{k-1} H_k^T + R_k)$ .

Method b<sup>71</sup>:

Test: if  $J = z_k^T (H_k P_k^{k-1} H_k^T + R_k)^{-1} z_k > J_{\max}$ , suspect divergence.

Action: set  $Q_k = Q_k + \delta Q_k$ . Maintain this action until  $J < J_{\min}$ .

The thresholds  $J_{\max}$  and  $J_{\min}$  are positive scalars.

Method c<sup>78</sup>: This method requires that the measurement is a scalar, hence in the case of multiple measurements it is assumed that the filter is implemented in its sequential form<sup>79</sup>.

Test: if  $\alpha_1 \leq z_k^2 \leq \alpha_2$ , choose hypothesis  $A_0$   
 if  $z_k^2 < \alpha_1$ , choose hypothesis  $A_1$   
 if  $z_k^2 > \alpha_2$ , choose hypothesis  $A_2$ .

where  $\alpha_1, \alpha_2$  represent positive scalar thresholds.

Action: if  $A_0$  is accepted, leave  $P_k^{k-1}$  unchanged,  
 if  $A_1$  is accepted, change  $P_k^{k-1}$  to  $P_k^-$ ,  
 if  $A_2$  is accepted, change  $P_k^{k-1}$  to  $P_k^+$ .

The modified covariance matrices  $P_k^-$  and  $P_k^+$  have values such that  
 $P_k^- \leq P_k^{k-1} \leq P_k^+$ .

The test proposed in method a is not statistically meaningful in the case of non-scalar  $z$ . The measure,  $3 \text{ trace}(H_k P_k^{k-1} H_k^T + R_k)$  will be influenced most by the largest variances, as in the following example obtained from the study of the steelmaking process. Consider the measurement  $y = (\% \text{ Carbon, Temperature } ^\circ\text{K})^T$  with typically  $z = (0.3, 6)^T$  and

$$(HPH^T + R) = \begin{pmatrix} .009 & -0.1 \\ -0.1 & 40 \end{pmatrix}$$

Also  $z^T z = 36.09 < 3 \text{ trace}(HPH^T + R) = 120.027$

Hence the test in method a does not imply divergence yet  $z_1^2 \gg \sigma_{z_1}^2$ , where  $\sigma_{z_1}$  = the standard deviation on  $z_1$ .

Writing eqn 6 in the equivalent form

$$P_k^k = [(P_k^{k-1})^{-1} + H_k^T R_k^{-1} H_k]^{-1} \quad A9$$

shows that the action proposed in method a, that is, that eqn A6 should be by-passed, is similar to setting  $R_k^{-1} = 0$ . This is intuitively undesirable since in effect we are saying that the filter is diverging and there is no information in the measurement, i.e.  $R_k = \infty$ .

The test presented in method b is statistically meaningful since the quadratic form  $J$  defines an  $m$ -dimensional ( $m = \dim y$ ) closed ellipsoid

centred at the origin. This ellipsoid is called the ellipsoid of probabilities associated with the quadratic form  $J$ . The values of threshold levels  $J_{\max} = 9$  and  $J_{\min} = 1$  suggested for their correspondence to the commonly used 3 and 1 - Standard Deviation tests, only have this meaning in the scalar,  $m = 1$ , case. It is, however, easily shown<sup>80</sup> that  $J$  is a chi-square variate with  $m$  degrees of freedom. Hence, values of  $J_{\max}$  and  $J_{\min}$  can be obtained to give any desired confidence interval. The action proposed in method b is intuitively agreeable if we assume that the divergence is due to errors in the process model or the estimate of its noise covariance. It is apparent that the extent to which the emphasis within the filter is shifted from the model to the measurements is determined by the choice of value of the 'control' variable  $\delta Q_k$ . This value must be precomputed and in the case when  $Q$  is time-varying a reasonable approach may be to consider  $\delta Q_k = \epsilon Q_k$  or  $\delta Q_k = \epsilon P_k^{k-1}$ , where  $\epsilon$  is a small positive constant. For invariant  $Q$ , useful information on the performance of the filter under different values of control may be obtained by conducting studies on the sensitivity<sup>65,68</sup> of the filter to changes in the description of the process.

The tests proposed in method c were derived from the Neyman-Pearson criterion for hypotheses selection. The thresholds  $\alpha_1$  and  $\alpha_2$  are determined as follows.

$$\text{Let } t_1 = [\alpha_1 / (\text{HPH}^T + R)]^{\frac{1}{2}}$$

$$\text{then } Pr_1 = (2/\pi)^{\frac{1}{2}} \int_0^{t_1} \exp(-\tau^2/2) d\tau \quad A10$$

$$\text{Similarly } t_2 = (\alpha_2 / (\text{HPH}^T + R))^{\frac{1}{2}}$$

$$\text{then } Pr_2 = 1 - (2/\pi)^{\frac{1}{2}} \int_0^{t_2} \exp(-\tau^2/2) d\tau \quad A11$$

where  $Pr_1$  and  $Pr_2$  represent the probability of choosing  $A_1$  and  $A_2$  respectively when  $A_0$  is true. If values of 0.68 and 0.002 are taken

for  $Pr_1$  and  $Pr_2$  respectively then the thresholds  $\alpha_1$  and  $\alpha_2$  will correspond to the respective 1 and 3-Standard Deviation levels. Other values of  $Pr_1$  and  $Pr_2$  may of course be selected. The action proposed in method c is obviously similar in effect to that in method b and the values of  $P_k^-$  and  $P_k^+$  may be associated with changes  $-\delta Q_k^-$  and  $+\delta Q_k^+$  in the process noise covariance matrix. Since the components of the measurement vector are processed sequentially, different control actions, that is different values of  $P_k^-$  and  $P_k^+$ , may be associated with each test. This increase in complexity compared with that proposed in method b may cause difficulties during tuning, but it has been found\* that the association of suspected divergence with an increase in uncertainty in one of the state equations can enable simple but effective control of the filter to be obtained.

### A5.3 Conclusions

Three decision directed methods for controlling divergence in the Kalman filter have been discussed. Two of these, methods b and c, have been shown to propose similar action when divergence is suspected. The latter of these methods has the appeal that it has been developed using the decision theory of Neyman and Pearson. In its present form this method is restricted to application with the sequential filter. An extension of the method to the standard filter, wherein all the observations are processed simultaneously, can be obtained by use of the test proposed in method b, which provides a measure of the filter quality which is a chi-square variate. The following method therefore suggests itself for application with the standard filter.

Test:    if  $\beta_1 < J < \beta_2$  , choose  $A_0$  ,  
           if  $J < \beta_1$          , choose  $A_1$  ,  
           if  $J > \beta_2$          , choose  $A_2$  ,

\* See section 7.6.2

Action: if  $A_0$  is accepted, leave  $Q_k$  unchanged

if  $A_1$  is accepted, set  $Q_k = Q_k - \delta Q_k$

if  $A_2$  is accepted, set  $Q_k = Q_k + \delta Q_k$

The thresholds  $\beta_1$  and  $\beta_2$ , relate to probabilities  $Pr_1$  and  $Pr_2$  as defined in method c. But here the values of these thresholds are obtained from the probability density function of the chi-square variate.

## Process Data

A6.1 Records of process operation

CAST NO. 1		
Time (min)	Action	Transformer Tap
0	Power-On, Sample - 1.1, T = 1560°C	7
13	Power-Off, Oxygen-On	
17	Power-On	9
20	Oxygen-Off	
23	Oxygen-On	
25	Power-Off, Oxygen-Off, T = 1630°C	
30	Oxygen-On, Slagging-off	
35	Sample 1.2	
36	T = 1645°C	
47	Oxygen-Off, Sample - 1.3	
49	Power-On	12
55	T = 1660°C	
56	Power-Off, Tapping	

Time (min)	Action	Transformer Tap
0	Power-On, Oxygen-On, Sample - 2.1	7
23	Power-Off, T = 1620°C	
24	Oxygen-Off	
25	Power-On	12
27	Power-Off, Lime addition of 3000 kg, Roof-off	
30	Power-On	12
33	Power-Off	
35	Oxygen-On	
42	Oxygen-Off, T = 1600°C	
45	Spar addition of 750 kg	
47	Oxygen-On, Power-On	12
50	Power-Off	
52	Oxygen-Off, Slagging-Off	
53	Oxygen-On	
58	Oxygen-Off, Sample - 2.2, T = 1590°C	
73	Sample - 2.3	
76	T = 1565°C	
78	Power-On	12
86	Power-Off, Spar addition of 500 kg	
87	Power-On	12
105	Oxygen-On, Slagging-Off	
110	Tap change	15
120	Sample - 2.4	
124	Power-Off, T = 1680°C	
130	Sample - 2.5	
132	Oxygen-Off, Power-On	15
140	T = 1660°C	
143	Power-Off, Tapping	

Time (min)	Action	Transformer Tap
0	Sample - 3.1, T = 1570°C	
3	Power-On, Slagging-off	5
12	T = 1615°C	
17	Power-Off, 170 kg of Mo added	
18	Power-On	
22	Tap change, T = 1660°C	9
25	Slagging-off	
29	Power-Off	
34	Sample - 3.2, Power-On	
38	Power-Off	
47	Blocking-Slag additions	
	Double-Slab Practice .	

CAST NO. 4

Time (Min)	Action	Transformer Tap
0	Sample - 4.1	
5	Power-On	5
13	T = 1530°C	
14	Oxygen-On, Slagging-off	
15	Tap change	11
25	Sample - 4.2, Power-Off	
26	Oxygen-Off	
28	T = 1530°C	
30	Power-On	9
38	Power-Off, T = 1575°C	
39	Power-On	
42	Power-Off, Blocking-Slag additions	
	Double-Slag Practice	

(Min)

Tap

0	Sample - 5.1, T = 1540°C	
15	Lime addition of 2250 kg and Spar addition of 750 kg	
21	Power-On	12
25	Oxygen-On	
37	Power-Off	
42	T = 1558°C	
44	Sample - 5.2, Oxygen-Off	
63	Power-On	14
71	T = 1575°C	
77	Slagging-off	
79	Oxygen-On	
83	Power-Off	
86	Oxygen-Off	
87	T = 1615°C, Sample - 5.3	
90	Blocking - Slag additions	
	Double-Slag Practice	

## CAST NO. 6

Time (Min)	Action	Transformer Tap
0	Sample - 6.1, Power-On	9
33	Slagging-Off	
20	T = 1540°C	
35	Power-Off, Additions of 230 kg Mo and 220 kg Ni	
38	Power-On	
49	Slagging-Off	
50	T = 1605°C	
58	Power-Off, T = 1640°C	
61	Additions of 1000 kg FeMn, 300 kg FeAl and 750 kg FeO	
66	Power-On	
70	Power-Off, Blocking - Slag additions Sample - 6.2, T = 1640°C	

Double-Slag Practice

## CAST NO. 7

Time (min)	Action	Transformer Tap
0	Sample - 7.1, T = 1580°C	
4	Power-On	7
15	Tap change	11
20	Power-Off, Addition to 80 kg Mo and 450 kg FeMn	
22	Sample - 7.2	
24	Power-On	9
28	T = 1630°C	
30	Power-Off, Sample - 7.2	
45	Sample - 7.3, T = 1625°C	
	Blocking-Slag additions	
	Double-Slag Practice	

A6.2 Slag and metal analyses

Weight Percentages

Sample No.	C	Mn	SiO	Total Fe	CaO	MgO	MnO	Al O	Cr O	P O
1.1	1.	.3	19.24	11.7	44.07	3.73	6.09	6.68	0.73	1.316
1.2	0.57	0.19	12.92	20.8	41.97	4.31	5.88	5.01	0.76	1.386
1.3	0.27	0.15	16.36	13.2	49.67	5.01	4.64	5.0	0.79	1.11
2.1	1.09	---	21.7	9.4	46.	2.61	5.42	5.44	0.86	2.03
2.2	0.81	0.31	12.0	10.4	59.	3.6	2.97	3.32	0.91	1.42
2.3	---	---	11.3	9.2	60.3	3.62	3.1	3.44	0.97	1.4
2.4	0.61	0.21	10.8	22.4	42.7	6.47	2.58	3.14	.364	1.06
3.1	0.09	0.12	---	---	---	---	---	---	---	---
3.2	0.05	0.1	---	---	---	---	---	---	---	---
4.1	0.62	0.13	15.34	15.15	46.5	3.28	4.9	4.88	2.42	2.1
4.2	0.46	0.76	---	---	---	---	---	---	---	---
5.1	0.51	0.17	12.2	14.2	42.6	4.51	4.32	4.19	0.54	1.01
5.2	0.65	0.2	16.66	19.2	46.2	5.33	3.1	3.86	0.57	1.3
5.3	0.57	0.14	13.7	14.73	48.66	6.2	2.2	3.62	0.62	1.41
6.1	0.09	0.12	10.33	21.1	48.72	3.10	3.73	3.54	0.91	1.61
6.2	0.11	0.6	10.11	15.44	45.16	7.32	4.56	4.13	0.78	1.55
7.1	0.08	0.08	13.04	15.12	45.84	5.42	7.05	4.26	0.53	0.95
7.2	.35	.47	---	---	---	---	---	---	---	---
7.3	.36	.47	10.85	16.48	43.32	7.66	5.01	4.53	1.02	1.13